



HAL
open science

New material of *Parabrychodus hypotamoides* from Samane Nala, Bugti Hills (Pakistan) and the origin of Merycopotamini (Mammalia: Hippopotamoidea)

Killian Gernelle, Fabrice Lihoreau, Jean-Renaud Boisserie, Laurent Marivaux, Grégoire Métais, Pierre-Olivier Antoine

► To cite this version:

Killian Gernelle, Fabrice Lihoreau, Jean-Renaud Boisserie, Laurent Marivaux, Grégoire Métais, et al.. New material of *Parabrychodus hypotamoides* from Samane Nala, Bugti Hills (Pakistan) and the origin of Merycopotamini (Mammalia: Hippopotamoidea). *Zoological Journal of the Linnean Society*, 2023, 198 (1), pp.278-309. 10.1093/zoolinnean/zlac111 . hal-04091159

HAL Id: hal-04091159

<https://hal.science/hal-04091159>

Submitted on 7 May 2023

HAL is a multi-disciplinary open access archive for the deposit and dissemination of scientific research documents, whether they are published or not. The documents may come from teaching and research institutions in France or abroad, or from public or private research centers.

L'archive ouverte pluridisciplinaire **HAL**, est destinée au dépôt et à la diffusion de documents scientifiques de niveau recherche, publiés ou non, émanant des établissements d'enseignement et de recherche français ou étrangers, des laboratoires publics ou privés.

Zoological Journal of the Linnean Society, 2023, **198**, 278-309. With 11 figures (DOI: <https://doi.org/10.1093/zoolinnea/zlac111>)

New material of *Parabrachyodus hyopotamoides* from Samane Nala, Bugti Hills (Pakistan), and the origin of Merycopotamini (Mammalia: Hippopotamoidea)

KILLIAN GERNELLE^{1*}, FABRICE LIHOREAU¹, JEAN-RENAUD BOISSERIE^{2,3},
LAURENT MARIVAUX¹, GRÉGOIRE MÉTAIS⁴, PIERRE-OLIVIER ANTOINE¹

¹*Institut des Sciences de l'Evolution de Montpellier (ISE-M, UMR 5554), Université de Montpellier, CNRS, IRD, EPHE, Place Eugène Bataillon, F-34095 Montpellier Cedex 5, France*

²*Laboratoire Paléontologie Evolution Paléocosystèmes Paléoprimatologie (PALEVOPRIM), UMR 7262, CNRS, Université de Poitiers, Bât. B35 - TSA 51106, F-86073 Poitiers Cedex 9, France*

³*Centre Français des Études Éthiopiennes (CFEE), CNRS, Ministère de l'Europe et des affaires étrangères – PO BOX 5554, Addis Abeba, Ethiopia*

⁴*Centre de Recherche en Paléontologie - Paris (CR2P), UMR 7207 CNRS, Muséum national d'Histoire naturelle, Sorbonne Université, CP38, 8 rue Buffon, F-75005 Paris, France*

*** Corresponding author:** Killian Gernelle

Email address: killian.gernelle@umontpellier.fr

ORCID identifier: <https://orcid.org/0000-0001-9698-0223>

ABSTRACT

The revision of the anthracothere *Parabrachyodus hyopotamoides*, endemic to the Lower Miocene of the Indian sub-continent, and thus far confused with *Brachyodus*, is made possible by the description of unpublished specimens from the Samane Nala fossil-bearing deposits of the Bugti Hills (Pakistan). This is the first biochronologically constrained occurrence for a comprehensive series of this species. The analysis of cranial and dental morphological variations based on all known specimens of *Parabrachyodus* allows us to provide the diagnostic characters for this monotypic genus. These include a four-crested upper molar protocone unique among artiodactyls, and several convergences with subfamily Anthracotheriinae, like the two puzzling distal cristae on the last upper premolar protocone. A phylogenetic analysis at the hippopotamoid level, including for the first time *Parabrachyodus* as well as the enigmatic genera *Telmatodon* and *Gonotelma* (both also endemic to the Bugti Hills), is performed for the first time. These phylogenetically related taxa turn out to be basal to the tribe Merycopotamini, leading us to propose a more inclusive definition of the diagnosis of this tribe. Our results formally establish *Elomeryx* as the sister-group of Merycopotamini within Bothriodontinae, and definitely locate the early evolutionary history of Merycopotamini on the Indian subcontinent.

KEYWORDS: *anthracotheres* – *Bothriodontinae* - *Early Miocene* - *dental morphology* – *polymorphism* – *cladistics*.

INTRODUCTION

The study of the famous fossil-bearing deposits of the Bugti Hills in Pakistan (Balochistan) is particularly critical for understanding the diversification of mammals during the Early Miocene on the Indian subcontinent (e.g. [Welcomme *et al.*, 1997, 2001](#); [Métais *et al.*, 2009](#); [Antoine *et al.*, 2013](#)), inasmuch as this subcontinent was then in contact with adjacent landmasses (e.g. [Barrier *et al.*, 2018](#)). Yet many emblematic Oligocene-Miocene taxa of this region are endemic (e.g. [Antoine & Welcomme, 2000](#); [Marivaux *et al.*, 2001, 2002, 2005](#); [Antoine *et al.*, 2004, 2010](#); [Crochet *et al.*, 2007](#); [Lihoreau *et al.*, 2016](#)). The Sulaiman Province is located in central Pakistan and includes the Bugti Hills and Zinda Pir Dome. This region has produced a rich fossil record of large mammals through two main waves of extensive survey, i.e. at the beginnings of the 20th and 21st centuries, respectively. This is especially important for anthracotheres of which the systematics and phylogenetic affinities are still poorly understood ([Antoine *et al.*, 2013](#)). Within this group, a recent work located the origin of the advanced tribe Merycopotamini on the Indian sub-continent, notably in what is now Pakistan ([Lihoreau *et al.*, 2016](#)), thereby underscoring the need for revising the fossil material in this context.

Early palaeontological surveys in the Bugti Hills have provided dental remains referred to as the ‘giant species’ of anthracotheres ([Lydekker, 1882](#)), *Hyopotamus giganteus* [Lydekker, 1883](#), and *Anthracotherium hyopotamoides* [Lydekker, 1883](#). Both taxa were soon after included in the genus *Brachyodus* [Depéret, 1895](#), by [Depéret \(1895\)](#). The increasing number of remains collected during the following field campaigns led to a multiplication of newly recognized species of *Brachyodus* in the Indian subcontinent, with up to ten distinct species in the Bugti Hills area alone ([Pilgrim, 1912](#); [Forster-Cooper, 1913, 1924](#)), and *Br. manchharensis* [Prasad, 1964](#), erected from the Kutch area, south of the Bugti Hills ([Prasad, 1964, 1967](#)). In parallel, [Forster-Cooper \(1915\)](#) coined the new genus *Parabrachyodus* for

two specimens displaying low crowns and strong wear (Fig. 1), considered sufficiently distinct from *Brachyodus* from the same localities. [Viret \(1961\)](#) was the first to propose uniting all *Brachyodus* material already described from this region under *Parabrachyodus hyopotamoides* ([Lydekker, 1883](#)), the only species of this endemic genus, because of strong morphological differences with the European and African *Brachyodus*. In addition to the confused systematics of these anthracotheres, no specimen from the Bugti Hills had formally been described since the beginning of the 20th century.

Although *Parabrachyodus* and *Brachyodus* were coeval during the Early Miocene, their respective spatial ranges in Asia appear mutually exclusive. *Brachyodus* is only known north of the Himalayan Range over this period ([Ducrocq et al., 2003](#)) concomitantly with the ‘*Brachyodus* event’ (mostly known as one of the ‘Proboscidean datum events’) occurring between Africa and Europe (e.g. [van der Made, 1999](#)). Consequently, the contemporary type species *Brachyodus onoideus* ([Gervais, 1859](#)) and *Brachyodus aequatorialis* ([MacInnes, 1951](#)) are known from Europe ([Dineur, 1981](#)) and Africa ([MacInnes, 1951](#)), respectively, while *Parabrachyodus* seems to be restricted to the Indian subcontinent ([Pickford, 1987](#); [Lihoreau & Ducrocq, 2007](#)). Hence, *Parabrachyodus* perhaps did not share with *Brachyodus* the dispersal abilities found in most anthracotheres (e.g. [Rasmussen et al., 1992](#); [Ducrocq, 1995](#); [Holroyd et al., 2010](#); [Lihoreau et al., 2019](#)), although authors have continued to closely relate the two genera, even viewing them as sister-taxa without any formal phylogenetic analysis (e.g. [Antunes & Ginsburg, 2003](#)). [Pickford \(1987\)](#) undertook a revision of *Par. hyopotamoides* and allied anthracotheres (i.e. *Gonotelma* [Pilgrim, 1908](#), *Hemimeryx* [Lydekker, 1878](#), *Sivameryx* [Lydekker, 1878](#) and *Telmatodon* [Pilgrim, 1907](#)), but he did not resolve these confusions, notably concerning the questionable subfamilial attribution of *Gonotelma*, *Parabrachyodus*, *Telmatodon*. The origin of the Merycopotamini was first questioned through the systematic revision of the genus *Hemimeryx* ([Lihoreau et al., 2016](#)).

Given that this tribe is seemingly deeply rooted in the Late Oligocene of the Indian subcontinent (Lihoreau *et al.*, 2016), and that *Parabrachyodus* displays a plesiomorphic dental morphology among Hippopotamoidea (e.g. supernumerary crests and styles on upper molars), the uncertainties related to this taxon need to be addressed. Its earliest occurrences remain notably poorly documented due to the lack of associated lithostratigraphic controls during the earliest surveys (e.g. Forster-Cooper, 1913).

We carried out a revision of the systematics of *Par. hyopotamoides*, incorporating recent data on dental nomenclature, hippopotamoid phylogeny (Boisserie *et al.*, 2010; Gomes Rodrigues *et al.*, 2020), and enamel microstructure (Alloing-Séguier *et al.*, 2014).

Unpublished fossils of this species discovered by the ‘Mission Paléontologique Française au Baloutchistan’ (MPFB) in the deposits of Samane Nala 4 (Bugti Hills; Welcomme *et al.*, 2001; Métais *et al.*, 2009, fig. 3) are here described, accounting for intraspecific variability, and by integrating all known dental remains of *Parabrachyodus*, to propose the most comprehensive systematic combination for this well-represented anthracothere. This is the first study gathering cranio-dental material of *Parabrachyodus* from a well-defined sample and in a stratigraphically constrained context, which is relevant to biochronological purposes and to understanding its morphological peculiarities. The phylogenetic position of this monospecific genus among Hippopotamoidea, and especially its relationships with *Brachyodus*, the Merycopotamini (*sensu* Lihoreau *et al.*, 2016) and the enigmatic genera *Telmatodon* and *Gonotelma* endemic to the Bugti Hills with which it could be confused (Pickford, 1987), was assessed via a phylogenetic analysis that included the entire Hippopotamoidea.

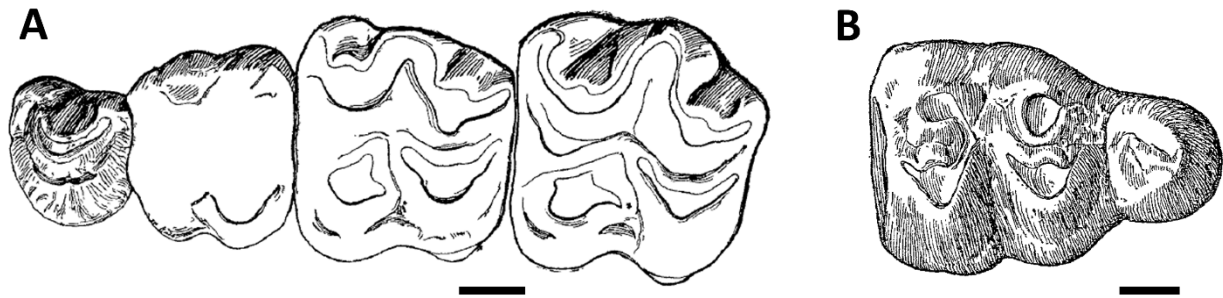


Figure 1. Drawings from [Forster-Cooper \(1915\)](#) of A, the first upper dental row (P4/-M3/, M12031) and B, lower molar (M/3, M12030) allocated to the anthracotheriid *Parabrachyodus*, from the Bugti Hills, Pakistan. Note the high degree of wear and the focus of the author on P4/'s morphology. Scale bars equal 10 mm.

ABBREVIATIONS

Institutions: GIZ, Deutsche Gesellschaft für internationale Zusammenarbeit; GSP, Geological Survey of Pakistan; HDIP, Hydrocarbon Development Institute of Pakistan, Islamabad; MPFB, Mission Paléontologique Française au Baloutchistan; NHM, Natural History Museum, London; UM, Université de Montpellier.

Localities and stratigraphy: DB, Dera Bugti area; FLA, first local appearance; LLA, last local appearance; SAM, Samane Nala; SFN, Safed Nala; TOB, Tobah.

Anatomy: dP/X, lower deciduous premolar; dPX/, upper deciduous premolar; EDJ, enamel-dentine junction; HSB, Hunter-Schreger bands; IPM, Interprismatic Matrix; MX/, Xth upper molar; M/X, Xth lower molar; OES, outer enamel surface; PX/, Xth upper premolar; P/X, Xth lower premolar.

MATERIAL AND METHODS

GEOLOGICAL SETTINGS AND ORIGIN OF THE FOSSIL MATERIAL

The unpublished material studied in this work was discovered by the MPFB from 1998 to 2004 in the Bugti Hills (Sulaiman Province, Balochistan, Pakistan) and is housed in the Palaeontological collections of the Université de Montpellier. The Samane Nala site is located on the northern flank of the Zin Anticline and the southern flank of the Dera Bugti syncline of Dera Bugti (Fig. 2A), and lies in an Oligo-Miocene sequence of terrestrial clastic sediments overlying Eocene marine limestones (Welcomme & Ginsburg, 1997; Welcomme *et al.*, 2001; Métais *et al.*, 2009). The Samane Nala 4 (SAM 4) fossil locality is stratigraphically located in the upper member of the Chitarwata Formation, which is considered as correlative to the

Early Miocene ([Welcomme et al., 2001](#)). Samane Nala 4 is a lateral equivalent of Kumbi 4 ([Welcomme et al., 2001](#); [Métais et al., 2009](#); [Orliac et al., 2009](#)) and Tobah (level Q = 4), which is in the south of the Zin anticline (see: [Métais et al., 2009](#); [Antoine et al., 2013](#): fig. 16.2). One isolated M3/ comes from Samane Nala 5 (SAM 5), a locality situated near the base of the Vihowa Formation, which directly overlies the Chitarwata Formation ([Antoine et al., 2013](#)). In addition to the material collected from the Bugti Hills, a M/3 from the Safed Nala locality, on the eastern flank of the central part of the Zinda Pir Anticline (GPS coordinates 30°13'54.2" N, 70°28'00.3" E) and discovered during a field campaign co-directed between the HDIP and GTZ in 1997 is also described. The fossils collected in the early 20th century and re-studied in this work are from Dera Bugti, Lundo Chur (= Chur Lando of early authors), Kumbi and Bugti Hills. The latter location corresponds to the flanks of the anticline with no exact stratigraphic position according to [Pickford \(1987](#): fig. 2).

Among the new specimens from SAM 4 and Tobah Q, there are six relatively small dental remains that we attributed with confidence to *Sivameryx palaeindicus* ([Lydekker, 1877](#)) and to the rare *Gonotelma shahbazi* [Pilgrim, 1908](#). Level 4 of the Chitarwata Formation provides the highest alpha diversity for both anthracotheres and rhinocerotids in this biochronologically constrained Oligocene-Miocene sequence of the Bugti Hills (Fig. 2B; [Antoine et al., 2010, 2013](#)). The mammalian assemblage of SAM 4 is species-rich (Table 1), and some large and meso-mammals, such as suoids ([Orliac et al., 2009](#); [Orliac et al., 2010](#)) and ruminants ([Ginsburg et al., 2001](#)), have already been studied, but carnivorans, creodonts, proboscideans, and rhinocerotids are yet to be described.

ENAMEL MICROSTRUCTURE

A lingual fragment of protocone of a right M3/ (UM-SAM4-007) and a labial fragment of hypoconid of left M/3 (UM-SAM4-017) were sectioned in horizontal, vertical, and tangential

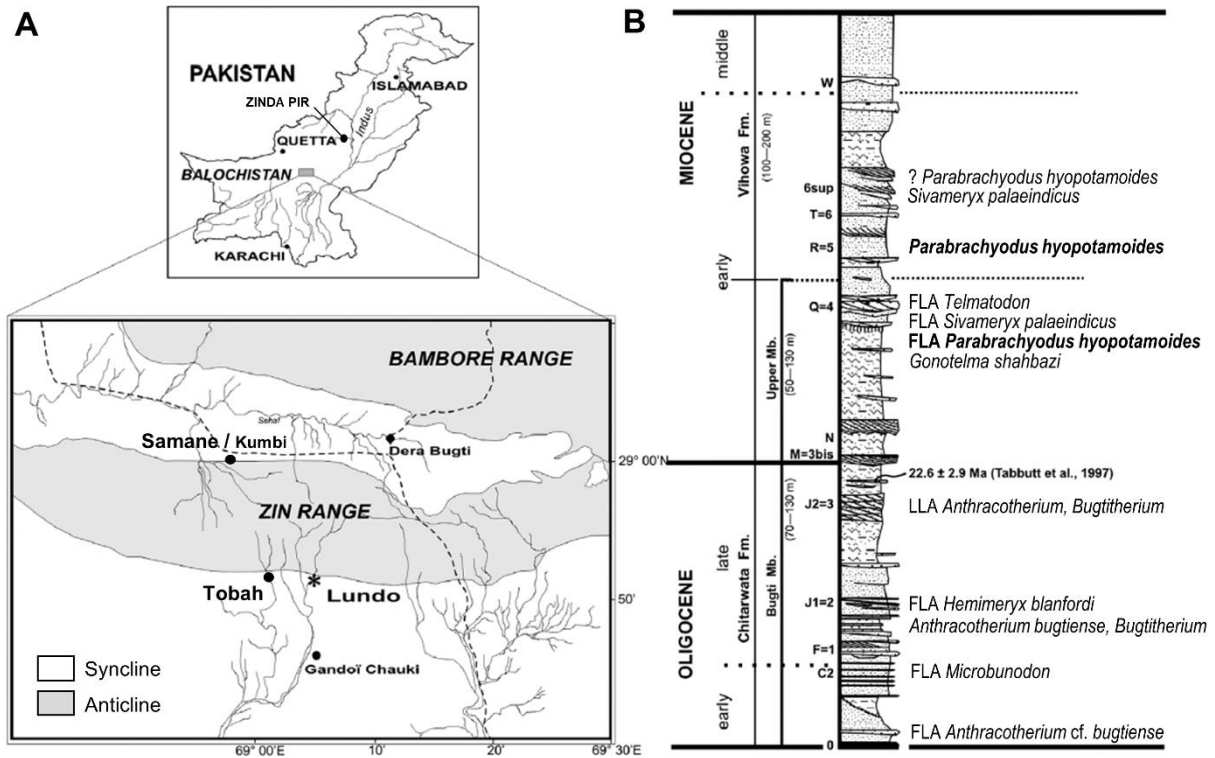


Figure 2. A, geographical position of the Samane Nala sector in the Bugti Hills area (Pakistan). B, stratigraphical position of the level Q = 4 in the synthetic section of the Bugti Hills area, together with anthracothere species distribution in the section (Welcomme et al., 2001; Métais et al., 2009; Antoine et al., 2013; Lihoreau et al., 2016; this study). FLA and LLA stand for first local appearance and last local appearance, respectively.

planes. Sample preparation followed the protocol of [Alloing-Séguier *et al.* \(2014\)](#). Samples were embedded in artificial epoxy resin, then grounded and polished. We then performed 37% phosphoric acid etching of the samples between 30 s and 60 s and rinsed with distilled water. The samples were air dried and coated with conductive material (platinum) before being observed by scanning electron microscope (SEM). For this analysis, we used SEM that allowed magnifications from $\times 40$ to $\times 4000$ (HITACHI S 4000).

Several parameters were evaluated in the description of enamel microstructure, as in [Alloing-Séguier *et al.* \(2014, 2016\)](#) and [Lihoreau *et al.* \(2016\)](#), focusing on Schmelzmuster [distribution of enamel types through enamel thickness, notably the Hunter-Schreger bands (HSB)], enamel thickness [measured perpendicularly from the enamel-dentine junction (EDJ) to the outer enamel surface (OES) at the flanks of the cusp], the interprismatic matrix (IPM) and the prism morphology and direction.

ANATOMY AND PHYLOGENETIC ANALYSIS

The terminology used for the descriptions of tooth morphology (Fig. 3) mainly follows [Boisserie *et al.* \(2010\)](#), as well as [Gomes Rodrigues *et al.* \(2020\)](#) for the deciduous tooth pattern of bothriodontines. The nomenclature used for numerous dental convergent structures between *Parabrachyodus* and Anthracotheriinae is discussed using the work of [Scherler *et al.* \(2018\)](#). Polymorphic dental characters were described with their respective frequency.

All measurements of the unpublished material are given with an accuracy of 0.1 millimetres (mm) and were made with the same digital calliper, by the same operator (Supporting Information, Table S1). The maximum values were retained for the mesiodistal length (Lmd), and the labiolingual lengths (Ll11-3), the measurement protocols of which are specified in Figure 3. Mandibular heights mentioned in the text were taken from the lingual side of the mandible, from its ventral edge to the adjacent tooth socket. Unbiased coefficients

Table 1. Mammals from Samane Nala, level 4 (SAM 4) of the Upper Chitarwata Formation (Dera Bugti area, Bugti Hills, Pakistan).

Creodonta
<i>Hyainailouros bugtiensis</i>
Carnivora
<i>Amphicyon cf. giganteus</i>
Proboscidea
Deinotheriidae
<i>Prodeinotherium pentapotamiae</i>
Elephantoidea
cf. <i>Gomphotherium</i> sp.
Artiodactyla
Sanitheriidae
<i>Sanitherium jeyffreysi</i>
Palaeochoeridae
<i>Pecarichoerus</i> sp.
Suidae
<i>Listriodon affinis</i>
Hippopotamoidea
<i>Parabrachyodus hyopotamoides</i>
<i>Gonotelma shahbazi</i>
<i>Sivameryx palaeindicus</i>
Tragulidae
<i>Siamotragulus bugtiensis</i>
? <i>Siamotragulus indicus</i>
Ruminantia incertae sedis
<i>Bugtimeryx pilgrimi</i>
Perissodactyla
Rhinocerotidae
<i>Brachydiceratherium fatehjangense</i>
<i>Mesaceratherium welcommi</i>
<i>Pleuroceros blanfordi</i>

of variation (CV) were calculated to compare variability between dental measurements. Statistical treatment of the measurements was carried out using R (R Core Team, 2020; v4.0.2). Interpretative drawings, measurements of angles between the lingual slope of the metaconule and the socket of the M3/ (Supporting Information, Table S2), and between the anteroposterior axis of the mandibular symphysis and the dental row, were made from available photographs.

The study of polymorphisms in the jugal dentition of *Par. hypotamoides* and the systematic revision of this species involved the unpublished material from SAM 4 and 5, Safed Nala (Zinda Pir) and fossils from the Natural History Museum (NHM) in London, mostly studied by Lydekker (1883), Pilgrim (1908, 1912) and Forster-Cooper (1913, 1915, 1924). The new material complementing the never-formally-established hypodigm of *Par. hypotamoides* furthers our knowledge of this species, allowing us to recognize all of its synonym species (Supporting Information, Appendix S1) and supporting its inclusion in a character matrix.

We used the latest up-to-date character matrix dealing with Merycopotamini and considering recently introduced informative characters provided by the enamel microstructure and deciduous premolar morphology (Gomes Rodrigues *et al.*, 2020). Six additional taxa were coded: *Bakalovia* spp., *Elomeryx armatus* Marsh, 1894, *Gonotelma shahbazi*, *Parabrachyodus hypotamoides*, *Telmatodon bugtiensis* Pilgrim, 1907 and *T. orientalis* Forster-Cooper, 1924 (Supporting Information, Appendix S2), thereby reaching a total of 76 taxa. These taxa are here first included in a phylogenetic analysis, with the exception of *Elomeryx armatus* (Lihoreau & Ducrocq, 2007). In addition, three original unordered and unweighted characters were added to the 221 already existing to account for the dental peculiarities of the anthracotheres from the Bugti Hills: the alignment of the hypoconulid with the buccal cusps (character 83), the connection of the postectoprotocrista with the lingual

margin of the upper molars (character 117) and the value of the angle between the metaconule and the socket of the M3/ (character 152). The descriptions of these new characters are available in Supporting Information (Appendix S3). The outgroup consists of the basal Eocene artiodactyls *Diacodexis pakistanensis* [Thewissen et al., 1983](#), *Bunophorus* spp. and *Homacodon* [Marsh, 1872](#). The parsimony analysis was performed with PAUP 4.0a169 ([Swofford, 2002](#)) on the new character-taxon matrix (Supporting Information, Appendix S4), through heuristic searches with random step-wise addition taking polymorphism into account, for 1000 replications (with randomized input order of taxa). The robustness of each node was measured via the calculation of Bremer indices (BR) going up to five additional steps. In addition to the new characters and taxa, changes in the coding of the matrix with respect to the previous work of [Gomes Rodrigues et al. \(2020\)](#) are also available in Supporting Information (Appendix S4). The numbers in superscript used after a character number in the main text and figures denote the character state.

SYSTEMATIC PALAEOLOGY

CETARTIODACTYLA [MONTGELARD ET AL., 1997](#)

CETANCODONTA [ARNASON ET AL., 2000](#)

HIPPOPOTAMOIDEA [GRAY 1821 \(SENSU GENTRY AND HOOKER, 1988\)](#)

‘ANTHRACOTHERIIDAE’ [LEIDY, 1869](#)

‘BOTHRIODONTINAE’ [SCOTT, 1940](#)

MERYCOPOTAMINI [LYDEKKER, 1883 \(SENSU LIHOREAU ET AL., 2016\)](#)

PARABRACHYODUS [FORSTER-COOPER, 1915](#)

Type and only species: Parabrachyodus hyopotamoides ([Lydekker, 1883](#)).

Diagnosis: As for the type and only known species.

PARABRACHYODUS HYOPOTAMOIDES (LYDEKKER, 1883)

(FIGS 4-8)

Selected Synonymy (exhaustive synonymy list of 100 synonyms in Supporting Information, Appendix S1):

‘Upper and lower molars of a gigantic species of *Hyopotamus*’; Lydekker, 1882: 107.

Anthracotherium hyopotamoides Lydekker; Lydekker, 1883: 152-154, pl. 24, fig. 2, pl. 25, figs. 1, 3.

Hyopotamus giganteus Lydekker; Lydekker, 1883: 160-164, fig. 1, pl. 24, fig. 3, pl. 25, fig. 2.

Brachyodus giganteus (Lydekker); Depéret, 1895: 407-408.

Brachyodus hyopotamoides (Lydekker); Andrews, 1899: 484.

Brachyodus africanus Andrews; Pilgrim, 1912: 59-62, pl. 22, figs. 2-4 (no figs. 1, 5) (in part).

Telmatodon bugtiensis Pilgrim; Pilgrim, 1912: pl. 24, figs. 2, 3b (no pl. 24, fig. 4), pl. 25, fig. 6 (in part).

Brachyodus pilgrimi Forster-Cooper; Forster-Cooper, 1913: 516-517, fig. 3 (viewed).

Parabrachyodus obtusus (Forster-Cooper); Forster-Cooper, 1915: 404-406, figs. 1-2 (viewed).

Brachyodus gandoiensis Forster-Cooper; Forster-Cooper, 1924: 27-28, pl. 1, figs. 3-6 (viewed).

Brachyodus platydens Forster-Cooper; [Forster-Cooper, 1924](#): 29-31, pl. 2, figs. 2-3 (viewed).

Brachyodus orientalis Forster-Cooper; [Forster-Cooper, 1924](#): 32, pl. 3, figs. 3-4 (viewed).

Brachyodus indicus Forster-Cooper; [Forster-Cooper, 1924](#): 32, pl. 4, fig. 1 (viewed).

Gonotelma major Forster-Cooper; [Forster-Cooper, 1924](#): 49-50, pl. 5, fig. 1 (viewed).

Parabrachyodus Forster-Cooper; [Viret, 1961](#): 948-949.

Brachyodus manchharensis Prasad; [Prasad, 1964](#): 9-12.

Anthracotherium bugtiense Pilgrim; [Pickford, 1987](#): 309-311 (in part).

Parabrachyodus hyopotamoides (Lydekker); [Pickford, 1987](#): 316-319 (in part).

Telmatodon Pilgrim; [Pickford, 1987](#): 320-323 (in part).

Parabrachyodus hyopotamoides (Lydekker); [Welcomme et al., 1997](#): 533, 535.

Parabrachyodus hyopotamoides (Lydekker); [Lindsay et al., 2005](#): 16, table 1 (in part).

Parabrachyodus hyopotamoides (Lydekker); [Bhandari et al., 2010](#): 76, fig. 7A.

Parabrachyodus hyopotamoides (Lydekker); [Antoine et al., 2013](#): tabs. 1-2, fig. 4 [in part].

Holotype: Right maxilla with mesiolabially damaged M3/ and roots of M2/, *GSI B426*, figured by [Lydekker \(1883](#): pl. 24, fig. 2) and housed in the collections of the Indian Museum, Calcutta, India.

Type locality: Exact locality unknown, ‘lower Manchhars of the Bhugti hills, north of Sind’ ([Lydekker, 1882](#): 107), Indus Basin, Pakistan.

Localities: Pakistan: Sulaiman Province: Dera Bugti, Lundo Chur, Kumbi, Samane Nala (levels 4 and 5), Tobah (level Q= 4), all in the Bugti Hills, Zinda Pir area (Z114, Z154, [Lindsay et al., 2005](#); Safed Nala). India: Fategad, central Kutch.

Horizon: Chitarwata Formation (level 4, upper member, [Métais et al.; 2009](#)), Vihowa Formation (level 5, lower member; [Antoine et al., 2013](#)), Khari Nadi Formation ([Patnaik &](#)

Prasad, 2016), seemingly Manchar Formation (lower member; Lydekker, 1882; Raza *et al.*, 1984).

Age: Early Miocene, from *c.* 22 to 19-18 Mya (Lindsay *et al.*, 2005; Métais *et al.*, 2009; Roddaz *et al.*, 2011: fig. 4; Antoine *et al.*, 2013).

New material: the whole new fossil material (22 specimens) used here is housed in the palaeontological collections of the Université de Montpellier (UM). Material from Samane Nala, level 4 (SAM 4) of the upper Chitarwata Formation, Dera Bugti (DB) area, northern flank (19 specimens): right I2/ or I3/ (UM-SAM4-024); right P1/ (UM-SAM4-025); skull with left P3/-M3/ tooth row and P1/-P2/ alveoli (UM-SAM4-001); skull fragment with left P4/-M1/ (UM-SAM4-002); right maxilla with M2/-M3/ (UM-SAM4-003); crown of right M3/ (UM-SAM4-004); worn right M3/ (UM-SAM4-006); right M3/ (UM-SAM4-007); worn left M3/ (UM-SAM4-008); lingual fragment of left M3/ (UM-SAM4-009); distal fragment of left M3/ (UM-SAM4-011); crown of left I/1 (UM-SAM4-026); left P/1 (UM-SAM4-027); fragment of left mandibular symphysis with P/2-P/3 alveoli (UM DB SAM4-014); right M/2 (UM-SAM4-015); worn left M/2 (UM-SAM4-016); fragment of right mandible with M/3 and talonid of M/2 (UM-SAM4-013); fragment of left M/3 without hypoconulid (UM-SAM4-017); talonid and hypoconulid of left M/3 (UM-SAM4-020).

Material from Samane Nala, level 5 (SAM 5) of the Vihowa Formation, Dera Bugti area, northern flank of the Zin anticline: left M3/ (UM-SAM5-001).

Material from Tobah, level Q of the Chitarwata Formation, Dera Bugti area, southern flank of the Zin anticline: right mandible with P/4-M/3 (UM-TOB-001).

Material from the Zinda Pir Dome (Pakistan), Safed Nala: right M/3 (UM-SFN-001).

Other material: Material from the historical field expeditions in the Bugti Hills (Pakistan): ‘Dera Bugti’, ‘Chur Lando’, ‘Kumbi’ and ‘Bugti’ (i.e. for ‘Bugti’, on the flanks of the Zin anticline; see [Pickford, 1987](#): fig. 2), level unknown, Dera Bugti area (82 specimens):

- Material collected by the Geological Survey of India (GSI), housed in the Indian Museum of Calcutta (21 specimens). The revision of the following specimens was in part based on casts housed in the NHM, and on published illustrations. The attributions of some GSI specimens to *Par. hypotamoides* not mentioned here but proposed by [Pickford \(1987\)](#) could not be verified in absence of illustrations or available casts. *Lower dentition* : right P/1-M/2 (GSI B479 / M11076); left P/3-P/4 (GSI B485); left P/3-M/3 (GSI B478); right P/3-M/3 (GSI B420); P/3-M/3 (GSI B458); left M/1-M/3 (GSI B521 / M11062); right M/2 (GSI B429); left M/2-M/3 (GSI B459); right M/3 (GSI B428 / M1541); half right M/3 (GSI B430); broken right M/3 (GSI B431); M/3 (GSI B460). *Upper dentition* : left P2/ (GSI B518 / M11065); left P3/-P4/ (GSI B456 / M10598); left P4/ (GSI B457); palate with right M1/-M3/ and left M3/ (GSI B462; [Pilgrim, 1912](#), pl. 22, fig. 2); skull with left M1/-M2/ and right M1/-M3/ (GSI B461 / M11060; [Pilgrim, 1912](#): pls. 19-20); skull with left M1/-M2/ and right M3/ (GSI B454 / M11064); right M3/ (GSI B426); left M3/ (GSI B427, GSI B433).

- Material collected from several expeditions in the Bugti Hills, studied by [Forster-Cooper \(1924\)](#) and housed in the Bugti collection of the NHM (61 specimens). *Lower dentition* : mandible with left I/2, left P/4-M/3 and right P/4-M/3 (M12724); right P/1-M/1 (M12736); left P/2-M/1 (M12721); right P/3-M/3 (M12723); left P/3-M/3 (M12731); left P/4-M/3 (M12720); right M/1-M/2 (M12732); left M/1-M/3 (M12733, M12734); right M/2-M/3 (M12727); left M/2-M/3 (M12729, M12735); right M/3 (M12726); left M/3 (M12030, M12725, M12730); broken left M/3 (M12722); worn right M/3 (M12719). *Upper dentition* : left P1/-M3/ (M12034); left dP3/-M1/ (M12820); right P3/-M2/ (M96529); skull with left P3/-M2/ and right M3/ (M12821); palate with left dP4/-M1/ and right dP4/ (M43964); left P4/-

M1/ (M43962); right P4/-M2/ (M12713); left P4/-M2/ (M12827); right P4/-M3/ (M11061, M12712, M12717, M12822, M43953); left P4/-M3/ (M12031, M12714, M12715, M12826); right M3/ with worn right P4/-M1/ (M43963); right M1/-M2/ (M43960, M43960); right M1/-M3/ (M12818); left M1/-M3/ (M12032, M12035, M12036, M12718); right M2-3/ (M12039); right M2/-M3/ (M12716, M12817, M12823, M12824), left M2/-M3/ (M12711, M12819, M12825, M43950, M43951); right M3/ (M12033, M43952, M43955, M43958); left M3/ (M43956, M43957, M43959); skull roof (M43949).

Material from the Zinda Pir Dome (Pakistan), collected by the GSI, studied by [Lindsay *et al.* \(2005\)](#) and housed in the Peabody Museum of Harvard University (2 specimens); locality Z154, right M3/ (z2077); locality Z114, left P4/ (z258).

Material from Fategad, central Kutch (India), Khari Nadi Formation (latest Early Miocene), collected by the GSI, studied by [Prasad \(1964, 1967\)](#) and [Bhandari *et al.* \(2010\)](#) and housed in the Indian Museum of Calcutta: palate with left M2/-M3/ and fragment of right M2/ (GSI 18097).

Emended diagnosis (modified from [Pickford, 1987](#)): Medium-sized to large bothriodontine with a unique combination of characters among anthracotheres: main palatal foramen open in front of M1/, I/2 smaller than I/3, large alveoli for lower and upper canines, which are separated from premolars by short diastema, no diastema between lower and upper jugal teeth, P/1 biradicate, preprotocristid of lower premolars with an accessory cusp, P/4 postprotocristid centered with respect to the mesiodistal axis and not fused with the endoprotocristid, P1/-P3/ with two mesial ridges (a preparacrista and an ectoparacrista) and a postparacrista with two accessory cusps, P3/ with distolingual cingular style, P4/ with an endoprotocrista and a large distostyle, pentacusp upper molars with a continuous transverse valley and a low crown, pronounced flare of the lingual flank of the lingual cusps on upper molars, developed loop-like labial styles on upper molars, parastyle formed by preparacrista,

quadricrescentic protocone with an ectoprotocrista connected to a protostyle on the mesial cingulum, postectoprotocrista directed towards the lingual margin of upper molars along the transverse valley, deep ectoprotofoffa and postectoprotofoffa, lack of premeta-preprotocristid connection on lower molars, postentocristid often present, prehypocristid of M/3 with two mesial arms, pinched hypoconulid aligned with lingual cuspids, wrinkled and thick molar enamel with a large zone of radial outer enamel on the bizonal Schmelzmuster, dP3/ with bicuspid anterior lobe and entostyle.

Differential diagnosis: Differs from other bothriodontines by its additional styles and crests on lower and upper jugal teeth. *Parabrachyodus* differs from *Elomeryx* in the lack of junction between the upper molar protocristae and premetacristule. Among bothriodontines from the Bugti Hills: differs from *Telmatodon* and *Gonotelma* mainly in the presence of a paraconule on upper molars. It differs also from *T. bugtiensis* in a less prominent ectostylid (when present) on its M/3. Contrary to *T. orientalis*, the postectoprotocrista joins the lingual margin on its upper molars, and there is an endoprotocrista on P4/. *Parabrachyodus* differs from *Gonotelma shahbazi* in the presence of a postmetafossule, the less steep-sided lingual flank slope of the lingual cusps on upper molars, the alignment of the M/3 hypoconulid with lingual cuspids, and its much larger teeth. The paraconule is well distinct from the protocone compared to *Sivameryx palaeindicus*, and the postparacristule reaches the transverse valley instead of the base of the paracone. Differs from advanced Merycopotamini such as *Sivameryx* and *Hemimeryx blanfordi* in the configuration of the prehypocristid, which does not reach the lingual margin of lower molars, and the more robust mandible with a more obtuse angle between the symphysis and the jugal tooth row.

Comparative descriptions

Cranium: In lateral view (Fig. 4A), the skull is shallow and elongated as in *Brachyodus onoideus* (Dineur, 1981; Orliac *et al.*, 2013). The jugal appears relatively deep compared to that of other bothriodontines such as *Elomeryx* (Lihoreau *et al.*, 2009). The facial ridge runs ventrally along the jugal until the level of the infraorbital foramen. It intrudes on the maxilla where the maxillojugal suture delimits a brief concavity of the jugal, then bifurcates ventrally to reach the facial tuberosity above the M2/. The combination of these cranial characters is found on all available maxillae of *Parabrachyodus* (UM-SAM4-002, M12033, M12717 and M12718), but also on the sole cranium of *Sivameryx*, which preserves this area (Miller *et al.*, 2014). A strong concavity of the face is anterior to the facial tuberosity, so that the snout is narrow at the level of the canine fossa (Fig. 4A, M12821), unlike the condition seen in *Brachyodus aequatorialis* (MacInnes, 1951: pl. 1) and *Br. onoideus* (Dineur, 1981). The infraorbital foramen is located above the P4/ on UM-SAM4-001 and above the M1/ on UM-SAM4-002. There is also a reduced distance between this foramen and the anterior margin of the orbit in the latter with respect to UM-SAM4-001 (64 mm vs. 74.8 mm). The lacrimal contributes to the anterior margin of the orbit and joins a narrow nasal by a short process separating the frontal from the maxillary on UM-SAM4-001. This lacrimonasal contact is absent on other skulls reported to *Par. hyopotamoides* (M11064, M43949) and *Sivameryx* (Rowan *et al.*, 2015). The cranium of SAM 4 is thus an exception. Such a variation of the lacrimonasal configuration is unknown among other anthracotheres (i.e. Hippopotamoidea excluding Hippopotamidae) at the species level. This morphology was highlighted as a derived character in *Hippopotamus*, more generally regarded as a fixed and constant generic character in the whole Hippopotamidae (Boisserie, 2005). The orbits are slightly more dorsally elevated (M43949) than in *Sivameryx*, and are similar to the condition seen in *Brachyodus onoideus* (Orliac *et al.*, 2013), but are not as much elevated as those in

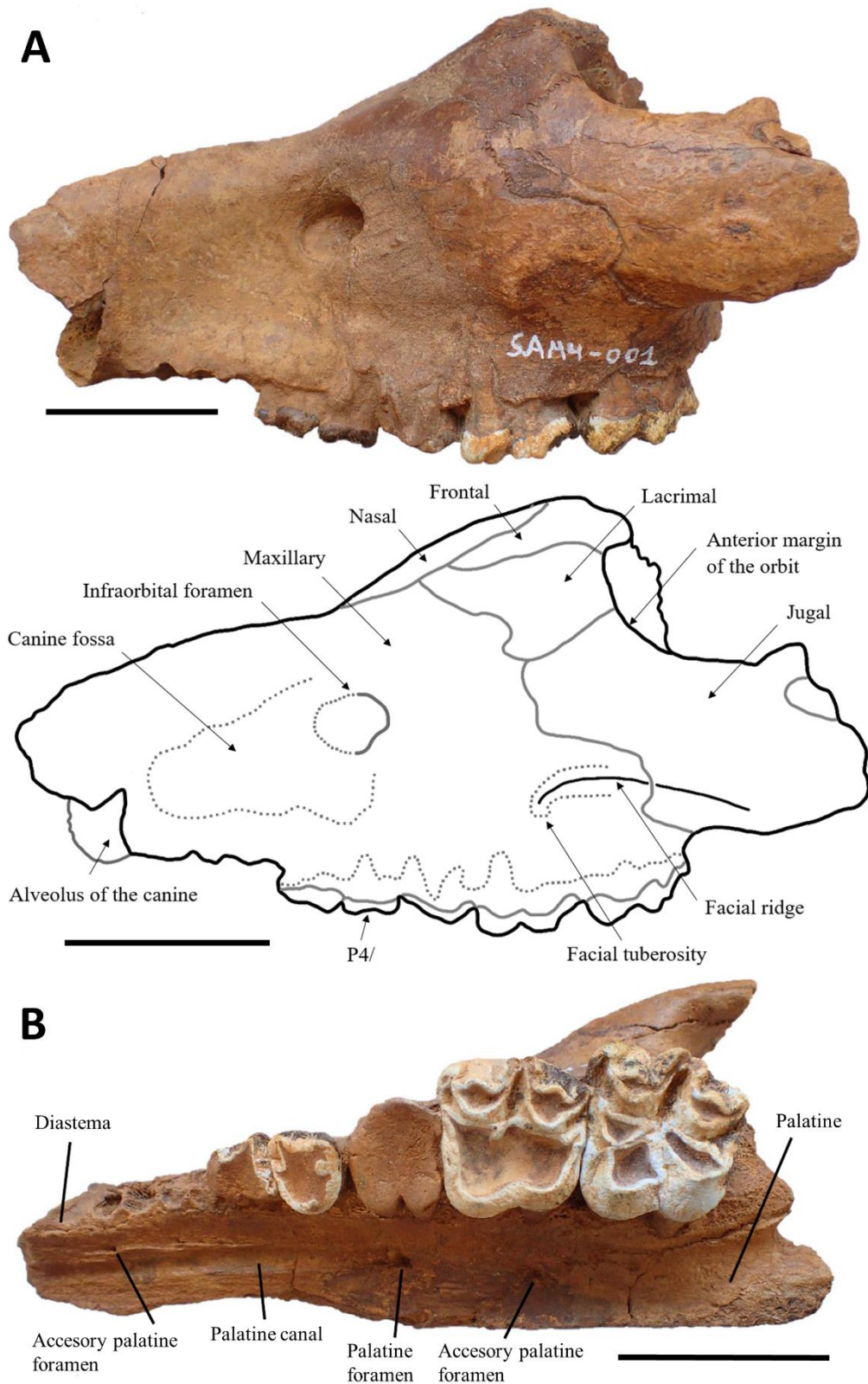


Figure 4. Fragmentary cranium of *Parabrychodus hyopotamoides* from Samane Nala 4 (UM-SAM4-001) in A, lateral view with an interpretative drawing. The grey full lines represent the sutures between bone units or the demarcation of teeth crowns, the grey dotted lines concern depressions on the skull surface. B, ventral view, displaying P1/-P2/ alveoli, and P3/-M3/. Scale bars equal 50 mm.

Merycopotamus dissimilis Falconer & Cautley, 1847 (Lihoreau *et al.*, 2007) or *Libycosaurus bahri* (Lihoreau *et al.*, 2014). There is neither lacrimal foramen nor lacrimal canal, except on M43949. In ventral view (Fig. 4B), the palatine advances between the maxillaries to the posterior part of the M1/, like in all anthracotheres.

The main palatine foramen is situated at the level of the M1/ on the cranium from SAM 4, whereas in *Elomeryx* it is located between the level of the P2/ to P4/ (Lihoreau *et al.*, 2009), the P2/ in *Brachyodus onoideus* (Dineur, 1981: 25) and *Merycopotamus* (Lihoreau *et al.*, 2007), and is between the mesialmost upper premolar (PX/) and the canine in *Libycosaurus* (Lihoreau *et al.*, 2014). Anteriorly, a wide palatal canal forms a groove over the rest of the dental row and has an accessory palatal foramen at the level of the P1/. A second accessory palatal foramen is located on the maxillopalatine suture in front of the M2/ (Fig. 4B). This configuration of the palatal foramina is also exhibited by the M12714 (Forster-Cooper, 1924: pl. 2, fig. 1) and M12826 specimens. Pilgrim (1912: 53, 58) noted a palatal foramen near the P3/ on some GSI specimens, but it is not appreciable on the available casts and illustrations of the referred skulls. Only the M12821 skull with *Parabrachyodus*-like molars clearly displays this character state. The choanae open behind M3/ at the level of the palatine process and the maxillary tuberosity (UM-SAM4-001, -003) as in all bothriodontines.

In dorsal view [only on material published by Pilgrim (1912)], the angle between the sagittal crest and the frontal lines is more obtuse on the skulls M11060 and M43949 ($> 80^\circ$) than on M11064 (60°). Furthermore, the sagittal crests of M43949 and M11064 are longer than on M11060. In the absence of more material likely to quantitatively address this variation, it is not possible to conclude whether or not there is a marked sexual dimorphism like that observed in *Merycopotamus* and *Libycosaurus* (Lihoreau *et al.*, 2007, 2014). The median occipital ridge (M11064) is surrounded by two nuchal fossae also found in *Merycopotamus* (Lihoreau *et al.*, 2007).

Rostral dentition: Of the premaxillary region and rostral teeth of *Par. hyopotamoides*, only an isolated right I2/ or I3/ is known, measuring 38 mm from root to crown (UM-SAM4-024; Fig. 5A). Its root is relatively short and smaller in diameter than the crown. The crown has a spatulate shape, a mesial and a distal pinched crest, and wrinkled enamel that is a characteristic feature of *Par. hyopotamoides*. The distal crest is higher than the mesial crest. A strong lingual cingulum is adjacent to the mesial border. On the skull UM-SAM4-001 (Fig. 4A) the alveolus for the canine has a large diameter (18.3 mm) and it is transversely compressed. The canine is separated from the P1/ by a relatively short diastema only visible on the skull of SAM 4 (19.3 mm; Fig. 4B), while that of *Brachyodus* is long (e.g. [Pickford, 1991](#)).

Upper premolars: The upper jugal teeth are in a contiguous row (UM-SAM4-001 and M12034; Fig. 4B and Fig. 5B), which contrasts with Eocene and Oligocene bothriodontines displaying diastema between their premolars, such as *Bothriodon* and *Bothriogenys* ([Dineur, 1981](#): 159) or *Elomeryx* [Geais \(1934\)](#). P1/ to P3/ are biradicated and exhibit two mesial ridges: a preparacrista and an ectoparacrista. The occlusal pattern of P1/ is known from an isolated specimen from SAM 4 (UM-SAM4-025; Fig. 5C) which displays weak accessory cusps on the postparacrista and looking more like P1/ than P2/ of M12034 in shape and size. The P3/ is larger than the P2/, with a more developed distolingual basin and a squarer shape (M12034; Fig. 5B). In addition, the paracone of the P3/ is flanked by a small distolingual cingulate style (protostyle, Fig. 5C), as in *Anthracotherium* ([Scherler et al., 2018](#), fig. 3). The P3/ has two accessory cusps on the postparacrista (GSI B456; Fig. 5D) and the two mesial ridges reminiscent of Merycopotamini such as *Sivameryx palaeindicus* ([Holroyd et al., 2010](#): fig. 43.4C), are present.

The P4/ is always bicuspidate, except for that of the maxilla which [Forster-Cooper \(1915\)](#) erroneously interpreted as the 'holotype' of the genus *Parabrachyodus* (M12031; Fig.

1A), and for M12826 and M12827, which both lack the protocone (20 %, 3/15 P4/ with a well-preserved occlusal surface). In the classic pattern of P4/ (UM-SAM4-002; Fig. 5E), three ridges arise from the protocone with a rounded contour and less selenodont than forms like *S. palaeindicus*. The pre- and post-paracristae are divergent in the same way as the latter, in contrast to *Merycopotamus* where they tend to parallelise (Lihoreau *et al.*, 2007). A strong cingulum surrounds the entire tooth and opens distally into a large distostyle (M12712). The latter is in contact with the postprotocrista like in *Telmatodon* (Forster-Cooper, 1924), whereas it appears free most of the time in bothriodontines such as *Bothriogenys orientalis* Ducrocq, 1997 (Ducrocq, 1997). In *Par. hyopotamoides*, an additional crest is similar in position to the postprotocrista known in *Myaingtherium* Tsubamoto *et al.*, 2011 (Tsubamoto *et al.*, 2011) and in some anthracotheriines (Scherler *et al.*, 2018). We interpret it as an additional ‘endoprotocrista’, regarding the more lingual position of the postprotocrista in Bothriodontinae (see Discussion). One-third of the P4/ specimens have an endoprotocrista with a vacant distal end as on the P4/ of SAM 4 with a preserved occlusal pattern (Fig. 5E). The other two-thirds show an endoprotocrista that joins the base of the paracone (GSI B456, M11061 or M12822). It is worth noting that two P4/s attributed to *S. palaeindicus* from SAM 4 similarly show a variation in the orientation of the postprotocrista, directed towards the distostyle or the base of the paracone. This was also observed on some P4/ of *S. palaeindicus* studied by Forster-Cooper (1924: 33).

Upper deciduous dentition: The only known and unpublished dP3/ (M12820; Fig. 5F) bears four main cusps and three accessory cusps as *Merycopotamus* (Gomes Rodrigues *et al.*, 2020), but it is larger. On the same specimen, the dP4/ is a smaller copy of the adjacent M1/, whose protocone possesses the characteristic features of *Parabrachyodus* (see also M43964). In addition to the four main cusps, the dP3/ is characterized by an entostyle and accessory cusps (lingual parastyle and postparaconule), whose appearance is delayed during the

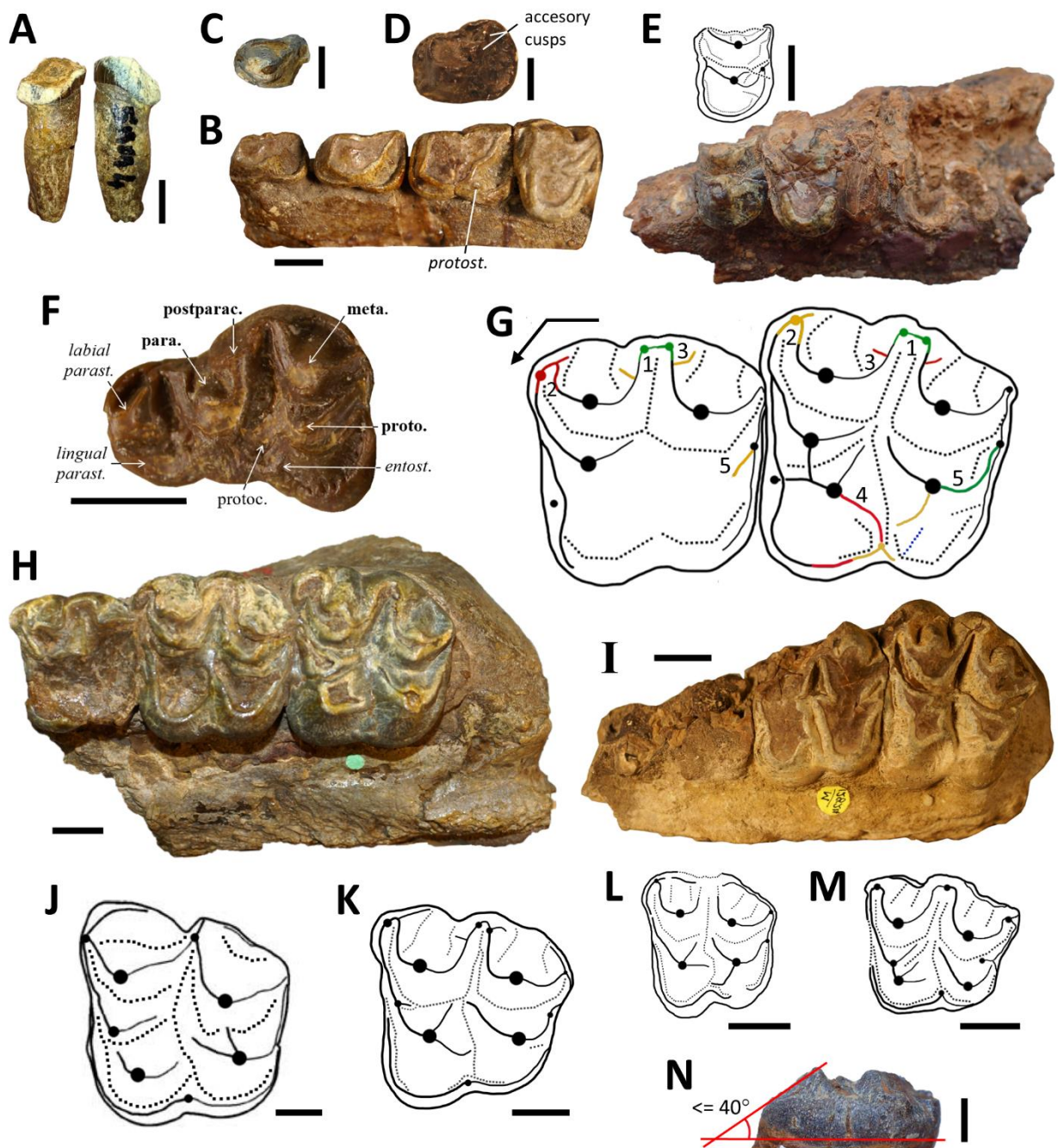


Figure 5. Upper teeth of *Parabrachyodus hyopotamoides*. A, left upper incisor (I2/ or I3/) in lingual (left) and labial (right) view (UM-SAM4-024). B, P1/-P4/ from a left maxilla (M12034) in occlusal view. C, right P1/ (UM-SAM4-025) in occlusal view (mirror). D, left P3/ (M10598) in occlusal view. E, left maxilla with P4/-M1/ in occlusal view, with a drawing of P4/. F, left dP3/ (M12820) in occlusal view. Abbreviations derived from the nomenclature introduced in Figure 2: protoc., protocrista. G, dental variation of *Parabrachyodus hyopotamoides* figured on composite upper molars ($N = 26$ for M3/; $N = 11$ for M2/). Variable characters are coloured. Character frequency: black: 100%; red: (75–99%); yellow: (50–74%); green: (25–49%); blue: (0–24%). The presence/absence of the coloured character is evaluated. 1, mesostyle divided into two slender apices; 2, parastyle of the same size or smaller than

mesostyle; 3, wing-like labial cingulum; 4, postectoprotocrista reaching the lingual edge of the tooth; 5, double curvature of the postmetacristule. The arrow indicates the mesiolingual direction. Teeth are not to scale. H, left maxilla with M1/-M3/ (M12718) in occlusal view. I, right maxilla with P4/-M3/ (M12824) in occlusal view (mirror). Comparisons with drawings of (J) left M3/ of *Brachyodus onoideus* in occlusal view, modified from [Ducrocq & Lihoreau \(2006\)](#); K, left M3/ of *Telmatodon orientalis* (M12040, holotype) in occlusal view; L, right M3/ of *Gonotelma shahbazi* (UM-SAM4-010) in occlusal view (mirror); M, left M3/ of *Sivameryx palaeindicus* (UM-SAM4-005) in occlusal view. N, M3/ of *Par. hyopotamoides* (UM-SAM5-001) in distal view, showing the low value of the angle between the lingual slope of the metaconule and the socket. Scale bars all equal 10 mm.

development of cusps (Gomes Rodrigues *et al.*, 2020: table 2). By contrast, only the postparaconule is present in upper deciduous premolars of *Elomeryx armatus* (Scott, 1940: fig. 122).

Upper molars: The teeth from SAM 4 have a morphological disparity (illustrated in Fig. 5G) also encountered in other sites of the Bugti Hills, as described hereafter. The interindividual variation does not allow us to subdivide the material into coherent taxonomic units in a small series from a single locality (here SAM 4). Pilgrim (1912: 49) already underlined the difficulty of distinguishing, based on stable characters, the two species *Brachyodus giganteus* (Lydekker, 1883) and *Br. hyopotamoides* then discriminated by himself and Lydekker (1883). Thus, the wide, looped mesostyle surrounding a deep, transverse valley without ectocrista is divided into two slender apices connected to each other (issued from the postparacrista and premetacrista) in less than half of the specimens (43 %, 13/30; Fig. 5G). The presence of a mesostyle with two apices is also common in *Elomeryx armatus* (Scott, 1940: fig. 122) and *E. borbonicus* Geais, 1934. Each of these character states (mesostyle composed of one or two apices) here certainly depend on the degree of tooth wear.

For the whole upper teeth sample, the normality assumption is rejected only for the labiolingual length of the mesial lobe of M3/ (Shapiro-Wilk test with $p < 0.05$, Table 2). On some M3/s (UM-SAM5-001 and M43951), this part of the tooth is excessively extended lingually, and as such it is reminiscent of the more triangular shape of *Telmatodon* (Fig. 5K) and *Gonotelma* (Fig. 5L). In addition, the parastyle resulting from the preparacrista and not from the labial cingulum, unlike *Brachyodus* (Fig. 5J; Lihoreau & Ducrocq, 2007), is larger than the mesostyle on one-third of the M3/s (5/15, e.g. M12034 and M12035). They are otherwise equal (Fig. 5G), which gives a square shape to the teeth. Since the origins of the variability in labiolingual width are diverse, it is not possible to discriminate between individuals solely on such a difference in shape (see Fig.5H vs. Fig.5I). The metastyle is

reduced compared to the other two labial styles. The development of the cingula is not the most variable characters of *Par. hyopotamoides* (Fig. 5G; *contra* [Viret, 1961](#)). In fact, the cingulum surrounding the protocone is only reduced in one specimen of SAM 4 (UM-SAM4-001; Fig. 4B) and we found a similar polymorphism in the entire sample for M3/ (77 %, 17/22). When a labial wing-like cingulum is present (75%, 24/32 of M2/ and M3/; UM-SAM4-001 and -007; Fig. 4B, 5G), it joins the postparacrista and the premetacrista, and thus draws the loop of the mesostyle.

The paraconule is separated from the protocone by a small, transverse fossa, which contrasts with the advanced fusion of these cusps seen in *Sivameryx* (Fig. 5M; [Grossman et al., 2019](#)). In addition, the postparacristule joins the transverse valley in the same way as in *Elomeryx*, whereas it connects to the base of the paracone in *S. palaeindicus* ([Ducrocq & Lihoreau, 2006](#)). A protostyle adorns the mesial cingulum as observed in Anthracotheriinae ([Scherler et al., 2018](#)), *Geniokeryx* [Ducrocq, 2020](#) and *Epirigenys* [Lihoreau et al., 2015](#). As in the latter, an accessory ridge could be occasionally noted in the distal transverse fossa (M12715 and M43959). The retention of both the protostyle and this crest underscores the primitiveness of *Par. hyopotamoides* compared to other Miocene bothriodontines. The species is unique in that a crest we identified as an ectoprotocrista constantly connects the protocone to the protostyle (Fig. 5G). The ectoprotocrista is clearly separated from the preprotocrista at the apex of the protocone on the less worn specimens (M11061 and M43961). In addition, almost all M3/ have a postectoprotocrista running along the transverse valley to the lingual edge (88 %, 22/25), where it meets or not an entostyle (68 %, 17/25 M3/; Fig. 5G). Such orientation of the postectoprotocrista is half as common on M2/ (40%, 4/10). This character is otherwise found on the single known M3/ of *Telmatodon bugtiensis* ([Pickford, 1987](#)). The prominence of this crest always tends to deviate the transverse valley distally, which is observed to a lesser extent in *Gonotelma* (Fig. 5L), *Sivameryx* (Fig. 5L) and even *Brachyodus*

(Fig. 5J), whilst it is almost absent in *Hemimeryx* and most Merycopotamini lacking this distal crest (Lihoreau *et al.*, 2016, fig. 2D-E). The ectoprotofossa and postectoprotofossa lingual to the ectoprotocrista and postectoprotocrista, respectively, protrude those additional cristae (Fig. 5G-I), thereby implying a multiplication of the number of wear surfaces. The arrangement of the cristae and fossae on the conical protocone is hence different from the selenodont pattern exhibited by other bothriodontines. The distinction of this original pattern of the protocone is enough to recognize *Par. hyopotamoides*, even for worn or fragmented M3/ from SAM 4 (UM-SAM4-006 and -009). It should be noted that specimens attributed to *Sivameryx palaeindicus* may occasionally exhibit some of the peculiarities observed on the protocone of *Par. hyopotamoides* (Forster-Cooper, 1924: pl. 4, fig. 7; Lydekker, 1883: pl. 23, fig. 6).

We distinguished two morphs for the postmetacristule labial to the postmetafossule: one with a double curvature before a large distostyle (52 %, 17/33 upper molars; UM-SAM4-001 and M12036; Fig. 4B) and another with a single curvature but less common here (UM-SAM4-011; Fig. 5G on the M2/). Also, two molars along the same tooth row may vary in types of curvature for their postmetacristule (M12718; Fig. 5H), and this may be related to the differential wear of M2/ and M3/. The ectometacristule is either weak (UM-SAM4-009) or protruding (UM-SAM4-011) on M2/ and M3/, almost twice as present on M3/ (73 %, 19/26) than on M2/ (40 %, 4/10), and this character tends to disappear in other Miocene bothriodontines as well. Moreover, M1/ do not develop an ectometacristule, unlike *Bakalovia* and *Elomeryx* from the Eocene-Oligocene (Hellmund, 1991; Böhme *et al.*, 2013). The specimens UM-SAM4-007 and UM-SAM4-011 show that a secondary ectometafossule, lingual to the ectometacristule, is sometimes present on M3/ (19 %, 5/26; Fig. 5G). The M3/ UM-SAM4-004 - and most of the specimens to a lesser extent - is covered with thick wrinkled enamel on the lingual tubercles. This upper molar also shows the shallow aspect of

the crown, which is characteristic of *Par. hyopotamoides* (Fig. 5N; Bhandari *et al.*, 2010). The two lingual roots of the M3/ from SAM 5 (UM-SAM5-001) are well-preserved and distinct, whereas the labial roots are fused. The angle between the lingual flank of the metaconule and the collet of the M3/ (Fig. 5N) is on average closer to that observed on teeth of *Telmatodon* and *Elomeryx* (between 40-45°), whereas it is more obtuse (between 50 and 60°) in *Gonotelma*, *Brachyodus*, and all Merycopotamini (Supporting Information, Table S2).

The M1/ are significantly smaller than M2/, and the M2/ are significantly smaller than M3/, even if the overlap between M1/-M2/ is lesser than the overlap between M2/-M3/ (Table 2). The dimensions of the jugal teeth from SAM 4 (Supporting Information, Table S1) are included in the range of variation of all the specimens we attributed to *Par. hyopotamoides* from the collections of the Bugti Hills. In addition, no biometric discrimination has been retrieved, either considering the deposit of origin (i.e. Dera Bugti, Lando Chur, Samane Nala, and Bugti Hills) or the ancient attribution (the museum species name of the specimens) with mesiodistal or labiolingual length 1 (Table 3).

Mandible: The external flank of the mandible has two foramina: one below the P/1-P/2 contact as observed on the symphysis UM-SAM4-014, and another below the P/3-P/4 contact (M12736, Fig. 6A). The mandibular height under the P/2-P/3 is greater on UM-SAM-014 (57.7 mm) than on UM-TOB-001 (47.3 mm), hence it is variable. So is the mandibular height below M/3, which is nonetheless normally distributed here (Shapiro-Wilk test with $p < 0.05$, Table 4). The mandible corpus is wider at the M/3 than mesially (e.g. UM-TOB-001; Fig. 7A), and it is also much higher under the M/3 (e.g. 88.9 mm on UM-SFN-001; Fig. 7C). The mandibular symphysis ends up between P/1-P/2 in all the specimens referable to *Par. hyopotamoides* (e.g. Fig. 6B). In sagittal section, its dorsal margin is convex, at least distally, on UM-SAM4-014 and M12724 (Fig. 6B), and its ventral margin (M11076, M12724, and M12731) is always straight (convex in *Brachyodus*). The greatest distal height of the

Table 2. Measurements of upper jugal teeth of *Parabrachyodus hyopotamoides* (in mm) from the historical quarry sites ‘Dera Bugti’, ‘Chur Lando’ (= Lundo Chur), ‘Bugti’, ‘Kumbi’ (only those conserved in the NHM) and from Samane Nala. Abbreviations: *N*, number of specimens measured; Lmd, mesiodistal length; Lmd, mesiodistal lengths; Lll1-3, labiolingual lengths; SD, standard deviation; CV, unbiased coefficient of variation (%); W, Shapiro–Wilk test (ns, normal distribution cannot be rejected; s, normal distribution is rejected; $P < 0.05$); t-test, student test between mesiodistal length (Lmd) of M1/ and M2, and between mesiodistal length of M2/ and M3/, the lines concerned are in bold; s, mean values significantly different.

Tooth		<i>N</i>	Mean	Min	Max	Sd	CV	W	<i>t</i> -test
P1/	Lmd	2	18,7	18,4	19,0				
	Lll	2	12,3	12,0	12,6				
P2/	Lmd	2	21,0	20,6	21,4				
	Lll	2	15,4	14,7	16,0				
dP3/	Lmd	1	22,8						
	Lll1	1	10,2						
	Lll2	1	16,6						
P3/	Lmd	3	22,6	19,0	25,0				
	Lll	3	18,1	15,6	19,8				
dP4/	Lmd	2	21,2	20,8	21,6				
	Lll1	2	20,8	20,3	21,2				
	Lll2	2	21,4	20,6	22,2				
P4/	Lmd	13	18,2	13,7	22,2	2,3	12,6	ns	
	Lll	14	21,7	19,5	24,3	1,2	5,5	ns	
M1/	Lmd	15	26,5	21,3	32,1	2,6	9,8	ns	} s
	Lll1	13	29,5	26,7	34,7	2,3	7,8	ns	
	Lll2	17	29,1	23,0	35,8	2,8	9,6	ns	
M2/	Lmd	31	35,0	30,3	39,2	2,3	6,6	ns	} s
	Lll1	30	38,3	31,1	45,0	2,9	7,6	ns	
	Lll2	26	36,9	28,5	42,9	2,8	7,6	ns	
M3/	Lmd	42	38,1	31,9	43,3	2,7	7,1	ns	} s
	Lll1	38	42,9	32,5	48,9	3,7	8,6	s	
	Lll2	41	40,6	29,8	46,8	3,4	8,4	ns	

Table 3. Results of the non-parametric analysis of variance (KW, Kruskal–Wallis chi-squared value; d.f., degree of freedom; ns, normal distribution cannot be rejected; s, normal distribution is rejected; $P < 0.05$) of measurements of jugal teeth of *Parabrachyodus hyopotamoides* (P4/ to M3/ included) between subgroups according to the deposit of origin or the ancient attribution of the material. N is the number of teeth considered in the whole sample. No biometric discrimination is retrieved.

Non-parametric tests; grouping according to:		
P4/: M3/ (N = 91)	Deposit of origin (d.f. = 3)	Ancient attribution (d.f. = 9)
Lmd	ns (KW=3.42, $P = 0.33$)	ns (KW = 7.38, $P = 0.60$)
Lll1	ns (KW=6.26, $P = 0.10$)	ns (KW = 9.25, $P = 0.42$)

symphysis (31.6 mm) makes it more robust than that of *Hemimeryx* (Lihoreau, 2003: fig. I.25), a bothriodontine with similar dental proportions (Lihoreau *et al.*, 2016, table 1). The angle between the anteroposterior axis of the symphysis and the jugal tooth row is 35.0° (M12724, Fig. 6B), so it is much more obtuse than in *Elomeryx*, *Hemimeryx* or *Sivameryx* (Lihoreau, 2003: fig. I.16). All these characters bring the symphysis of *Par. hyopotamoides* closer to that of the small Libyan anthracothere *Afromeryx zelteni* Pickford, 1991 (Pickford, 1991: pl. 6), except for its robustness and the absence of a genial spine. There is a marked mandibular constriction between c and P/1 without the intermediate protrusion characteristic of *Hemimeryx* and *Sivameryx* (Fig. 6D). Neither the coronoid process nor the angular process was preserved. The gonial region is slightly projected ventrally below the horizontal branch of the mandibles M12723, M12726 and M12732 (Forster-Cooper, 1924: figs. 28, 40), and thus resembled that of *Brachyodus* (Dineur, 1981: pl. 9) more than that of *Libycosaurus* (Lihoreau *et al.*, 2014).

Lower incisors and canines: The arrangement of the lower incisors is known from the M12724 mandible (Forster-Cooper, 1924: fig. 29), where a socket and a broken incisor are preserved (Fig. 6C). The incisor is interpreted as I/2, and the alveolus as the adjacent I/3. Indeed, in frontal view, a small ventral chin foramen, mesial to the preserved incisor, could be in the same position as the intermediate foramen between the I/1 and I/2 of *Merycopotamus medioximus* Lihoreau *et al.*, 2004b (Lihoreau *et al.*, 2004b), and reveals the existence of the I/1. The diameter of the I/2 alveolus (8.7 mm) is smaller than that of the I/3 alveolus (12.4 mm) (Fig. 6D), unlike in *Elomeryx*. Only the crown of a left I/1 from SAM 4 (UM-SAM4-026, Lmd = 12 mm) documents this dental locus. There is no diastema between c and I/3. On the M12736 mandible (Forster-Cooper, 1924: fig. 41) and UM-SAM4-014 in frontal view, the outline of the canine socket is large and clearly elliptical, hence not premolariform, in contrast to *Brachyodus* (MacInnes, 1951; Dineur, 1981).

Lower premolars: The occlusal structure of P/1-P/2 is best preserved on the M12736 mandible, where all premolars have an accessory cuspid on their preprotocristid (Fig. 6A) like in *Hemimeryx* (Lihoreau *et al.*, 2016). The P/1 has two separate alveoli (Fig. 6D), whereas those of *Brachyodus* and *Afromeryx* are single-rooted. An isolated crown of a P/1 from SAM 4 (UM-SAM4-027) also possesses a fused upper part of the roots. The postprotocristid is distolingually oriented on the P/3 of M12736 (Fig. 6A), and is clearly straight and distal in other specimens (M12721, M12723 and M12731), unlike the condition observed in *Elomeryx* and Merycopotamini. This tooth displays a well-preserved endoprotocristid on GSI B479 (Pilgrim, 1912: pl. 25, fig. 6). The P/4 has a rectilinear postprotocristid centered with respect to the median axis (Fig. 6E). It is split from the protoconid without partially fusing with the distolingually directed endoprotocristid (M12720 and UM-TOB-001; Figs 6E, 7A), which is a known primitive character also present in *Bakalovia* and *Elomeryx* (Hellmund, 1991). Despite the lack of distolabial cristid, a deep postprotocristid is retained. An accessory mesiolingual ridge joining the preprotocristid is only visible on the M12720 P/4 (Fig. 6E), but not on the specimens M12721, M12731 and M12736 (Fig. 6A). The advanced occlusal wear of three other known P/4s, including that of the mandible from Tobah (Fig. 7A), discard observing this feature. The lingual cingulid of the P/4 does not form a clear wall, unlike in Merycopotamini (Lihoreau *et al.*, 2019), but it begins near the distal edge of the tooth.

Lower deciduous dentition: The only mandible with a dP/4 we attribute to *Parhyopotamoides* (GSI B478), for which only an original drawing is available, was initially considered as *Telmatodon bugtiensis* by Pilgrim (1912: pl. 24, fig. 2). This deciduous tooth has a paraconid mesial to the primoconid but no postectoparacristid. This combination of characters is only found on dP/4 of *Afromeryx zelteni*.

Lower molars: Labial cuspids of lower molars are broad and less crescentic than in *Gonotelma*, *Hemimeryx* and *Sivameryx* known from the Bugti Hills. This aspect is reinforced

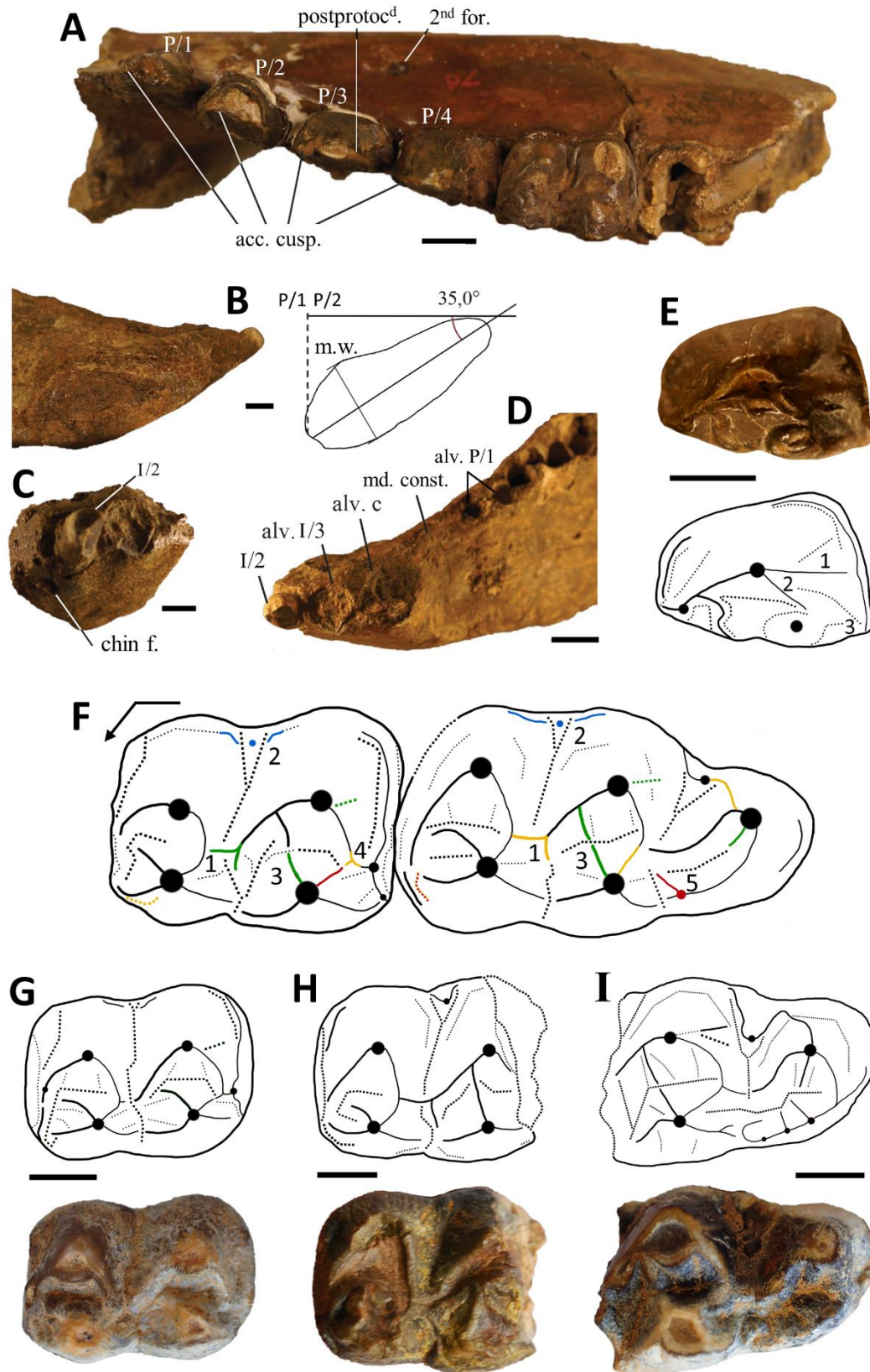


Figure 6. Mandibles and lower teeth of *Parabrachyodus hyopotamoides*. A, right mandible with P/1-M/1 and symphysis (M12736) in occlusal view; 2nd for., second mandibular foramen; acc.cusp., accessory cuspids. B, left mandible with I/2-M/3/ and symphysis (M12724) in sagittal view of the

symphysis with interpretative drawing; m.w., maximal width; C, frontal view of the mandible M12724; chin f., chin foramen; D, frontolateral view of the mandible M12724; alv. c., alveolus of the canine; alv. I/3, alveolus of the I/3; alv. P/1, alveolus of the P/1; md. const., mandibular constriction; E, left P/4 (M12720) in occlusal view (mirror view). 1, centred postprotocristid; 2, no fusion between postprotocristid and endoprotocristid; 3, lack of lingual cingulid wall; F, dental variation of *Parabrachyodus hyopotamoides* figured on composite lower molars ($N = 18$ for M/3; $N = 12$ for M/2). Variable characters are coloured. Character frequency: black: 100%; red: (75–99%); yellow: (50–74%); green: (25–49%); blue: (0–24%). The presence/absence of the coloured character is evaluated. 1, prehypocristid with two arms (one median); 2, labial cingulid developed in ectostylid; 3, preentocristid joins the prehypocristid towards the apex of hypoconid; 4, triple connection; 5, at least one postentostylid paired with an accessory cristid. The arrow indicates the mesiolingual direction. Teeth are not to scale. G, right M/2 (UM-SAM4-015) in occlusal view (mirror view) with interpretative drawing; H, left M/3 without hypoconulid (UM-SAM4-017) in occlusal view; I, left M/3 without trigonid (UM-SAM4-020) in occlusal view. Scale bars all equal 10 mm.

by the broad labial ribs of *Parabrachyodus*. The lingual cuspids are also broad whereas they are reduced to an apex in Merycopotamini. The metaconid is always quadricrescentic (Fig. 6F) like in *Sivameryx* and *Afromeryx*, and it is thus clearly distinct from that of *Brachyodus* (Holroyd *et al.*, 2010). Sixty-five per cent (17/26) of the lower molars we observed possess an ectometafossid, whereas the premetacristid is consistently present. The preprotocristid does not reach the premetacristid, which is often considered as a character of Merycopotamini (Lihoreau *et al.*, 2016). Labial to the trigonid, there is a small ectostylid on the M/1 (M12731), which is rarely present on M/2 and M/3 (11%, 3/28 specimens; Fig. 6G vs. Fig. 6H, summarized in Fig. 6F) where the cingulid is often discrete. In contrast, it is protuberant on the M/3 ascribed to *Telmatodon bugtiensis* (Forster-Cooper, 1924: fig. 35).

The shape of the prehypocristid is variable. It is frequently divided into two mesial arms on the M/3 on which this character is observable (57 %, 8/14), whereas it more often consists in a single cristid on the M/2 (33 %, 4/12 specimens with a prehypocristid divided into two arms). The main arm of the prehypocristid is either oriented lingually toward the postmetafossid (UM-SAM4-015, -016 and M12734; Fig. 6G) or reaches the distal wall of the trigonid ('median' configuration, UM-SAM4-017; Fig. 6H). The main arm of the prehypocristid is more often median on the M/3 (71 %, 10/14) than on the M/2 (33 %, 4/12). A similar polymorphism of the prehypocristid is known in other bothriodontines, such as *Elomeryx armatus* (Macdonald, 1956: figs. 5, 7), and for the two M/3 referred to as *Hemimeryx blanfordi* by Lihoreau *et al.* (2016) (Forster-Cooper, 1924, fig. 44 vs. pl. 6). In addition, the lingual arm of the prehypocristid, although sometimes long (M12731 and M12734), never reaches the lingual margin of the lower molars inasmuch as it is restricted by the postectometacristid and the protruding ectoentocristid (UM-SAM4-016), which tend to close the transverse valley. In this sense, the crest pattern observed in *Parabrachyodus* is reminiscent to that of *Brachyodus* (*contra* Dineur, 1981; Pickford, 1987) in which the lingual

arm of the prehypocristid is also limited by the postectometacristid. This is in contrast to the condition seen in *Libycosaurus*, *Merycopotamus* and *Sivameryx* where the lingual arm of the prehypocristid meets the lingual margin of the tooth (Lihoreau & Ducrocq, 2007).

On almost half of the lower molars on which the preentocristid can be seen (48 %, 13/27 M/2 and M/3; Fig. 6F), this cristid is directed towards the apex of the hypoconid. It is otherwise oriented mesially towards the trigonid wall. A possible contact between the preentocristid and the prehypocristid is materialized on three specimens by the presence of an accessory ridge distinct from the ‘endohypocristid’ known in some species of *Bothriogenys* (Ducrocq, 1997), in that its basal part is linked to the prehypocristid instead of the apex of the hypoconid (UM-SAM4-020, GSI B521 and M12725; Fig. 6I). The posthypocristid can either directly join the prehypocristid on the M/3 and the lingual distostylid on the M/2 (UM-SAM4-015, and M12729; Fig. 6G), or form a talonid wall with the postentocristid when present (69 %, 18/26 lower M/2 and M/3; UM-SAM4-013 and -020). In *Bothriogenys gorringei* (Andrews & Beadnell, 1902), the M/3 shows the same polymorphism regarding the accessory ridge of the hypoconid, but also on the direction of the posthypocristid as evidenced by Ducrocq (1997: 15). The uncommon posthypofossid (33 %, 9/27 of M/2 and M/3) found on UM-SAM4-020 is accompanied by a distal accessory ridge on this tooth (Fig. 6I).

The hypoconulid is loop-like and transversely compressed, as in all Bothriodontinae. It is also pinched mesially and aligned with the lingual cuspids, unlike *Telmatodon bugtiensis* (Pilgrim, 1907: pl. 12, fig. 4) and *Brachyodus onoideus* (Ducrocq & Lihoreau, 2006: fig. 1G). The morphology of this cuspid is similar to that of Anthracotheriinae on some specimens (UM-SAM4-020, M12722 and M12725; Fig. 6I), in part due to the short mesiolingual ectohypocristid occasionally leaving its apex (44 %, 7/16 of M/3; Fig. 6F). Regarding the postectostylid, the labial cingulid connects to the hypoconulid on over two-thirds of the M/3. In lingual view, we frequently observed a postentostylid on the posthypocristid (89 %,

16/18 of M/3), accompanied by a ridge closing the transverse fossa (76 %, 13/17 of M/3). The M/3 UM-SAM4-020 (Fig. 6I) displays three of those stylids arising from the marked distal cingulid, which is also well developed on the M/2 and absent on the M/3 of *Hemimeryx* (Lihoreau *et al.*, 2016). Here, the largest of the postentostylids is, therefore, not homologous to the entoconulid of anthracotheriines. It is worth noting that a similar multiplication of postentostylids is also observed on a M/3 of *S. palaeindicus* from Tobah. The combination of a low crown, a postentocristid, an ectohypocristulid and a pinched hypoconulid closed by accessory cristids allowed us to recognize the only known lower jugal tooth of *Par. hyopotamoides* from Zinda Pir (UM-SFN-001; Fig. 7B, C).

The lengths and widths of the lower molars of *Par. hyopotamoides* have higher unbiased coefficients of variation than the upper molars (Table 4), and the range of measurements for M/3 reaches 20 mm for the length. Variations of this order are expected for an anthracothere of the size of *Parabrachyodus*, because the same observations can be made for the molars of *Libycosaurus bahri*, equivalent in size to *Par. hyopotamoides* based on the proportions of molars (Lihoreau *et al.*, 2014: table 7). There is no significant difference between the mesial (Ll1) and distal width (Ll2) of the lower molars (t-test with $p < 0.05$; $N = 38$, $t = -0.50$, d.f. = 74, $P = 0.61$) even though those of the small series from SAM 4 (Supporting Information, Table S1) display a smaller width mesially than distally. In the new specimens here described, some molars have a broader talonid (Fig. 7A), while others display a broader trigonid (Fig. 7B). The size of the M/1 (approximated as the labiolingual length of the talonid instead of the mesiolingual length, due to the presence of the hypoconulid lobe on M/3, more elongated) is reduced compared to the M/2-M/3, in the same proportion as that which we observed on the upper molars (Fig. 7A; Table 4). Furthermore, the labiolingual length of the talonids of *Telmatodon* and *Hemimeryx* falls within the lower limit of that of *Par. hyopotamoides* with which they could be confused. Due to the paucity of specimens

Table 4. Measurements of lower jugal teeth of *Parabrachyodus hyopotamoides* (in mm) from the historical quarry sites ‘Dera Bugti’, ‘Chur Lando’ (= Lundo Chur), ‘Bugti’, ‘Kumbi’ (only those conserved in the NHM), and from Samane Nala, Tobah and Safed Nala. Abbreviations: *N*, number of specimens measured; Lmd, mesiodistal length; Lmd, mesiodistal lengths; Lll1-3, labiolingual lengths; SD, standard deviation; CV, unbiased coefficient of variation (%); W, Shapiro–Wilk test (ns, normal distribution cannot be rejected; s, normal distribution is rejected; $P < 0.05$); t-test, student test between labiolingual length 2 (Lll2) of M/1 and M/2, and between labiolingual length 2 of M/2 and M/3, the lines concerned are in bold; s, mean values significantly different; hM/3, mandibular height below M/3.

Tooth		<i>N</i>	Mean	Min	Max	Sd	CV	W	<i>t</i> -test
P/1	Lmd	2	16,1	16,0	16,1				
	Lll	2	8,3	8,2	8,4				
P/2	Lmd	2	20,2	18,3	22,0				
	Lll	2	12,6	12,5	12,7				
P/3	Lmd	4	21,9	19,8	23,2	1,5	6,8	ns	
	Lll	2	13,2	12,0	14,4				
P/4	Lmd	7	22,5	19,1	25,2	2,1	9,3	ns	
	Lll	6	16,6	13,8	19,5	2,0	12,0	ns	
M/1	Lmd	7	24,8	22,2	28,4	2,6	10,5	ns	
	Lll1	4	17,3	15,6	20,4	2,1	12,1	ns	
	Lll2	7	19,3	16,8	21,7	1,8	9,3	ns	
M/2	Lmd	14	32,5	27,6	36,9	2,9	8,9	ns	s
	Lll1	14	24,5	20,9	27,9	2,1	8,6	ns	
	Lll2	17	26,4	21,1	30,5	2,6	9,8	ns	
M/3	Lmd	18	53,0	43,7	63,8	5,3	10,0	ns	s
	Lll1	20	29,5	24,0	35,9	3,3	11,2	ns	
	Lll2	22	29,3	22,2	35,9	3,2	10,9	ns	
hM/3	Lll3	18	19,4	14,9	23,9	2,5	12,9	ns	
		12	72,7	58,5	88,9	10,4	14,3	ns	

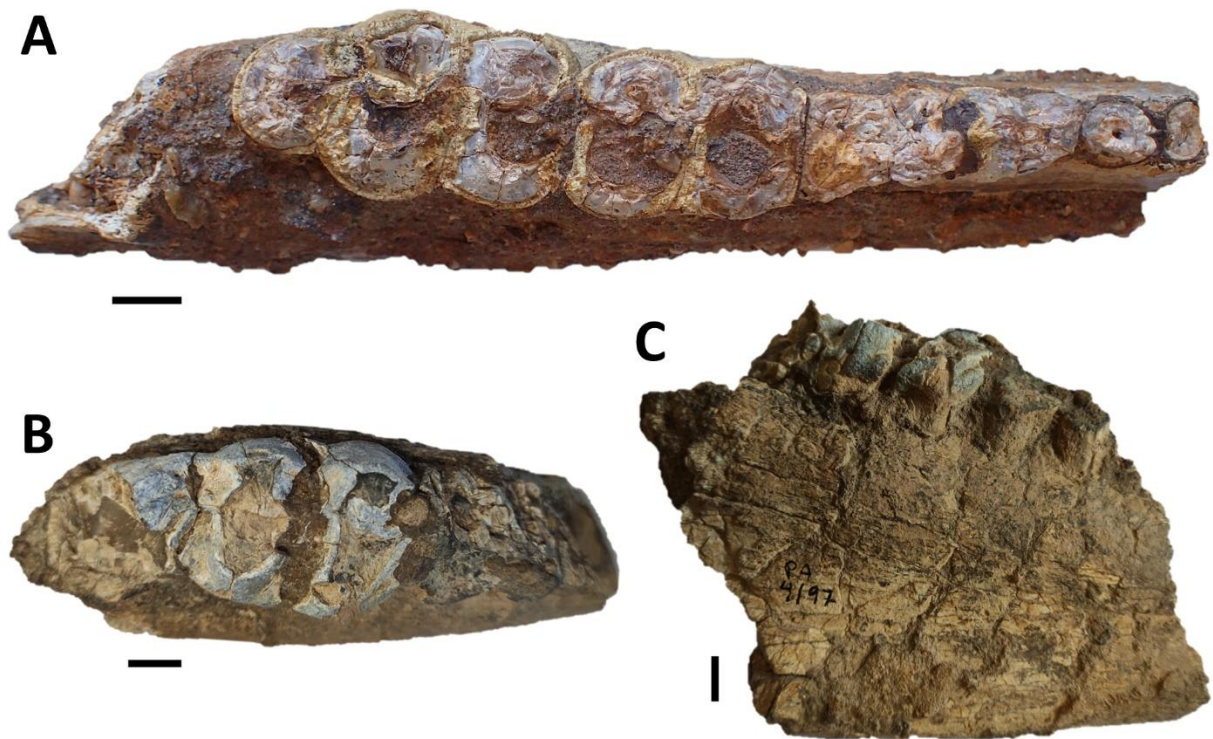


Figure 7. Hemi-mandible fragments of *Parabrachyodus hyopotamoides* from A, Tobah (Bugti Hills), right alveoli of P/3, and P/4-M/3 (UM-TOB-001) in occlusal view, and B, C, Safed Nala (Zinda Pir Dome), right M/3 (UM-SFN-001) in occlusal (B) and labial (C) views. Scale bars equal 10 mm.

attributed to the formers, we consider that this difference cannot be assessed with confidence here.

Enamel microstructure

On the vertical section, enamel thickness averages 2210 μm with maximal measured value of 2381 μm . This is higher than what has been observed so far in bothriodontines, notably with the thick enamel of *Brachyodus onoideus*, which is close to 1500 μm (Alloing-Séguier *et al.*, 2014). This enamel thickness is close to values measured for *Paenanthracotherium bergeri* Scherler *et al.*, 2018 and the early hippopotamines *Saotherium* Boissérie, 2005 and *Hexaprotodon* Falconer & Cautley, 1836 (Alloing-Séguier *et al.*, 2014, see also: Scherler *et al.*, 2018, for *Paenanthracotherium* attribution). The Schmelzmuster (Fig. 8A) shows an inner zone with little development of inner radial enamel (4%), a large decussation zone with Hunter-Schreger Bands developed for 75% of the whole thickness, and a large outer zone of radial enamel (21%). Due to the weak development of inner radial enamel, the Schmelzmuster can be regarded as bizonal, following Alloing-Séguier *et al.* (2014). In the decussation zone, bands are from 45 to 117 μm (with a mean of $84.8 \pm 25 \mu\text{m}$) with about 12 to 17 prisms per band. There is a high decussation angle with several transitional prisms (almost five; Fig. 8B). Bands vary slightly in width from the EDJ to the OES (Fig. 8A) displaying a regular aspect. They are strongly bent in the inner third of the enamel thickness, rising at an angle of $57 \pm 8^\circ$ with the EDJ and reaching the outer radial enamel perpendicularly to the OES. We did not observe anastomosis or bifurcation of the bands.

On horizontal sections, the Schmelzmuster displays radial enamel with some blurry decussations near the EDJ that quickly disappear to become strict radial enamel with some

synchronous prism undulations (three) in the inner two-thirds of enamel thickness. Radial enamel then becomes straight to the OES.

Mean prism diameters is $4.5 \pm 0.4 \mu\text{m}$ (between 4 and 5.2 μm). Prism angles with EDJ equal $\sim 54.6 \pm 6^\circ$ and reach OES perpendicularly. IPM forms inter-row sheets in the HSB zone and in the short inner radial zone. IPM crystallites are nearly perpendicular to prisms (Fig. 8C). In the outer radial portion, IPM forms closed coats.

Comparisons indicate more similarities with *Merycopotamini* than with *Brachyodus*, notably due to the marked development of the outer radial enamel, the large and blurry HSB, the low number of prism undulations in horizontal section and the development of inter-row sheets from the EDJ (Fig. 8D).

PHYLOGENETIC ANALYSIS

The heuristic searches yielded 208 equally most-parsimonious trees of 1558 steps each. A prominence of homoplastic characters has been obtained (consistency index = 0.195) as expected for an intra-ordinal analysis, but the phylogenetic results are quite structured (retention index = 0.625), as summarized by the well-resolved strict consensus tree (Fig. 9). The major polytomies concern relationships within the Hippopotamidae + Bothriodontinae clade erected in [Lihoreau et al. \(2015\)](#). This clade is well supported [Bremer index (BI) = 5] by 24 non-ambiguous synapomorphies of which five are also non-homoplastic among artiodactyls, including the Schmelzmuster composed of three layers (168¹, with intraclade reversions) and the presence of bent instead of straight HSB (176¹). The trees differ from each other mainly in the resolution of the relationships between the four subclades (*Bothriodon* + *Aepinacodon*), ((*Brachyodus* spp. + *Bothriogenys andrewsi*) + *Bo. gorringei* + *Bo. fraasi*), (*Bo. orientalis* + *Epirigenys* + Hippopotamidae), and the clade A including *Parabrachyodus*

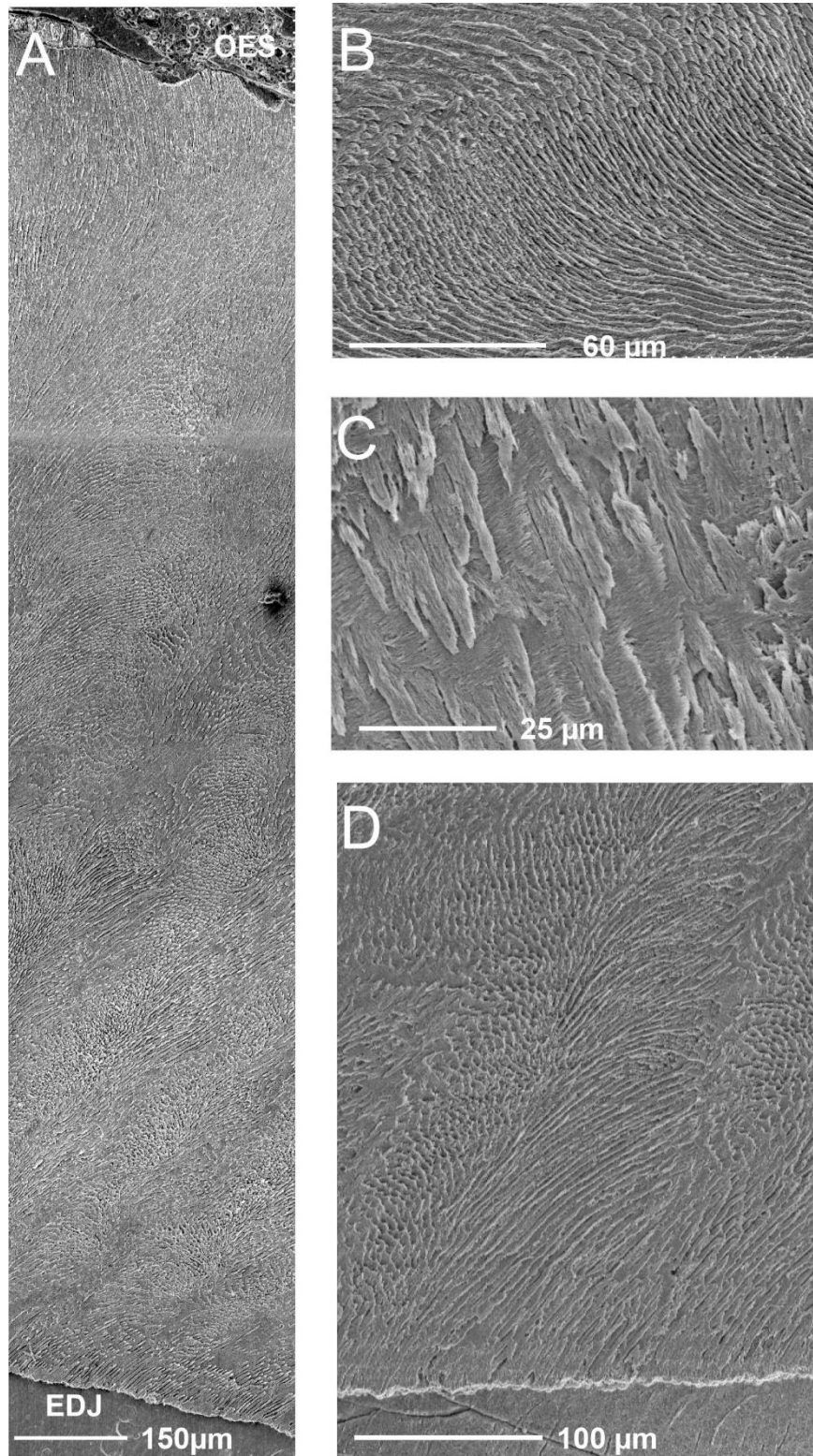


Figure 8. Enamel microstructure of *Parabrachyodus hyopotamoides*. A, vertical section of enamel from EDJ (bottom) to OES (top). B, detail of the decussation of several transition prisms in vertical section. C, detail of the angulation between IPM crystallites and prisms in vertical section. D, detail of the inter-row sheets in vertical section. EDJ, enamel dentine junction; OES, outer enamel surface; IPM, interprismatic matrix.

hyopotamoides. This uncertainty is consistent with the need for a revision of the evolutionary history of *Brachyodus* and *Bothriogenys* (Lihoreau *et al.*, 2019) whose monophyly is not supported here.

Parabrachyodus hyopotamoides is hence positioned among Bothriodontinae in a separate clade from the one including *Brachyodus* (clade A), supported by nine non-ambiguous traits (BI= 3). Its topology consists of a branching sequence with the Merycopotamini *sensu* Lihoreau *et al.* (2016) as crown group, with the enigmatic *Bakalovia* as the earliest offshoot (node A), including the monophyletic genus *Elomeryx* (node B), *Par. hyopotamoides* and the other endemic taxa from the Bugti Hills (node D). It is worth noting that the Merycopotamini (*Afromeryx*, *Hemimeryx*, *Libycosaurus*, *Merycopotamus* and *Sivameryx*) are resolved here as a paraphyletic group because of the newly added genus *Gonotelma*, which is the sister-taxon of *Afromeryx* (node H). These two genera are only united by synapomorphies of their lower molars (67⁰, 80¹, 83¹). Furthermore, the non-ambiguous synapomorphies defining the tribe Merycopotamini (Lihoreau *et al.*, 2016) appear sequentially in our topology: the pinched hypoconulid (79¹), the labially connecting preparacrista of the parastyle (130²), and the absence of ectocristyle (133¹) for clade A; the presence of accessory cuspids on the preprotocristid of lower premolars (19¹), which is also non-homoplastic at node B; and the loss of the connection between the premetacristid and the preprotocristid of lower molars (50¹), the loss of the paraconule of upper molars (127¹) and the marked development of outer radial enamel (171¹) for clade D.

The clade D, including (*Parabrachyodus* + *Telmatodon*), *Gonotelma* and the Merycopotamini *sensu* Lihoreau *et al.* (2016), is among the strongest ones (BI= 4). It is defined by 13 non-ambiguous synapomorphies (two of which are above-mentioned) including the more extensive development of the I/1 (4²), the preparacrista composed of two mesial ridges on P1/-P3/ and the multiplication of accessory cusps on their postparacrista (93¹, 94¹),

the loss of the junction between the protocone and the metaconule, characteristic of the upper molars of *Elomeryx* (119⁰), or the presence of two external foramina on the mandible instead of one (159²). It is relevant to mention that the enamel microstructure and the occlusal morphology of the dP3/ strongly supports this clade with almost half of the non-ambiguous synapomorphies (6 on a total of 13 synapomorphies). Hence, three of them are related to the enamel microstructure (168⁰, 170¹ and 171¹), namely that the Schmelzmuster is composed of two layers (168⁰), HSB occupy less than a quarter of its surface (170¹) and the marked development of outer radial enamel (171¹). Three non-ambiguous traits are related to character states of the dP3/ (213¹, 219¹, 223⁰), known by only one specimen for *Parabrachyodus*. Thus, there is an entostyle (219¹) and no connection between the protocone and the metacone (223⁰). The bicuspidate anterior lobe of the dP3/ (213¹) is also a non-homoplastic trait.

The resolution in clade D is good despite the low scoring for *Gonotelma shahbazi* (79/224 characters), *Telmatodon bugtiensis* (75/224 characters) and *T. orientalis* (90/224 characters). Altogether, *Parabrachyodus* and its 'relatives' from the Bugti Hills appear paraphyletic in this first attempt to include them in a cladistic analysis. *Telmatodon* forms a clade with *Par. hyopotamoides* (node E), supported by four non-ambiguous synapomorphies (63¹, 108¹, 143¹ and 152⁰) such as the gentle slope of the metaconule (152⁰) compared to all other anthracothere groups (non-homoplastic in this context). *Parabrachyodus hyopotamoides* is related to *Telmatodon bugtiensis* (node F) rather than to *T. orientalis* (both *Telmatodon* species are here considered valid due to the nature of the material attributed to each of them, see Supporting Information, Appendix S2) by only two non-ambiguous synapomorphies, one of which is also non-homoplastic and concerns the lingual development of the postectoprotocrista on the M3/ (117¹).

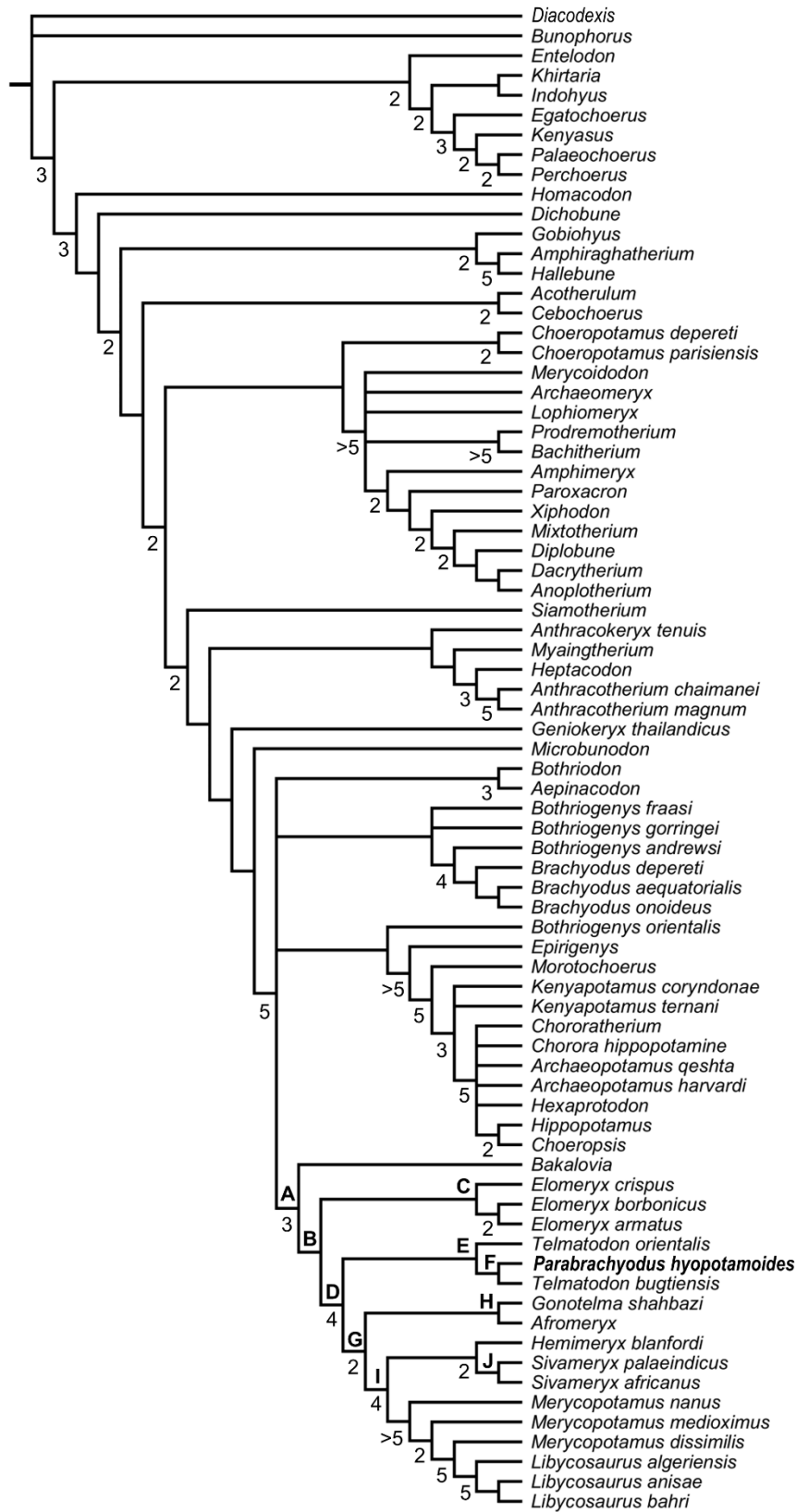


Figure 9. Phylogenetic results. Strict consensus tree of the 208 most parsimonious trees of 1558 steps each (CI = 0.195, RI = 0.625). Letters above the branches at nodes refer to the clades discussed in the phylogenetic analysis section of the main text. Values under the branches at nodes are Bremer indices (BI) when > 1.

The next node (G, BI= 2) grouping *Gonotelma shahbazi*, *Afromeryx zelteni* and the rest of Merycopotamini, is supported by four non-ambiguous synapomorphies, including the non-ambiguous anterior position of the main palatal foramen (166¹), the abrupt change in direction of the preprotocristid of P/4 (44²) and, especially, the lingual position of the postprotocristid of the P/4 (41¹), which is non-homoplastic at the artiodactyls scale. There are also two non-ambiguous synapomorphies supporting the clade I (BI= 4) that are related to the P/4 morphology: a fusion of the postprotocristid and endoprotocristid (32²) converging with the subclade (*Brachyodus* spp. + *Bothriogenys* in part) and the presence of a hypoconid (39¹). It is worth noting that *Sivameryx palaeindicus* and *S. africanus* are brought together (clade J) only by the presence of a paraconule (127⁰), which is considered in this topology as a reversion within clade D, occurring also for *Parabrachyodus hyopotamoides*. Specifically, it is one of the six non-ambiguous autapomorphies of *Par. hyopotamoides*, notably including the already mentioned convergences with Anthracotheriinae, such as an ectohypocristulid developed on the M/3 (77²) and the presence of a protostyle on upper molars (151¹).

DISCUSSION

SYSTEMATICS OF *PARABRACHYODUS HYOPOTAMOIDES*

Based on unstable dental characters, early authors like Lydekker, Pilgrim and Forster-Cooper created up to ten species of *Brachyodus* (*Br. africanus*, *Br. gandoiensis*, *Br. giganteus*, *Br. hyopotamoides*, *Br. indicus*, *Br. manchharensis*, *Br. obtusus*, *Br. orientalis*, *Br. pilgrimi* and *Br. platydens*). Our analyses of character variance (namely the multiplication of original crests and styles around the protocone of upper jugal teeth) led us to synonymize these species with *Par. hyopotamoides*. For example, *Brachyodus platydens* (Fig. 5I; [Forster-Cooper, 1924](#)), described by the flattest upper molars of the historical collections, cannot be

maintained because its definition is based on a degree of wear. The square shape of the upper molars of *Br. gandoiensis* is the only distinctive feature on which this species was founded (Forster-Cooper, 1924: 27-28), but we have shown that the shape of the upper molars in our sample highly depends on characters submitted to intraspecific variability. Moreover, the mesostyle is not loop-shaped but pinched in the type species of *Brachyodus* (e.g. Fig. 5J). The absence of biometric discriminations between upper teeth invalidates *Brachyodus orientalis* defined essentially from upper molars smaller than other specimens (Fig. 5H; Forster-Cooper, 1924: 32) but with morphology equivalent to all the synonym of *Par. hyopotamoides*. On the basis of the morphology of the paraconule, upper molars from the Bugti Hills attributed to *Brachyodus africanus* belong to *S. palaeindicus* (e.g. GSI B463; Pilgrim, 1912: pl. 22, fig. 1) and to the larger *Par. hyopotamoides* (e.g. GSI B462; Pilgrim, 1912: pl. 22, fig. 2). Pilgrim (1912: 50) considered the M/3 displaying postentostylids as pertaining to *Brachyodus giganteus*, the M/3 lacking the postentostylid belonging to *Br. hyopotamoides*. However, as we have shown, this character is commonly subjected to intraspecific variability in close relatives of *Par. hyopotamoides*. The single-cuspidate P4/ were grouped in *Parabrachyodus obtusus* (= *Br. obtusus*) by Forster-Cooper (1915, 1924: 33) based on this criterion, interpreted as a dental anomaly by Viret (1961) among those that can appear in isolated series of anthracotheres (Ducrocq *et al.*, 1995). Considering the frequency of this character state in the studied series of anthracotheres, it is included in the common variability of *Par. hyopotamoides*, as it is for the P4/ of some hippopotamids (Boisserie, 2005: fig. 5D).

Even after attempts to resolve the systematics of *Par. hyopotamoides* (Viret, 1961; Pickford, 1987), the diagnostic characters of this species remained partially misunderstood, with the strength of the convex labial ribs on paracone and metacone or the loop-like styles on upper molars being considered here as plesiomorphic characters shared with all bothriodontines from the Bugti Hills. Our biometric analysis shows that a smaller mesial than

distal width of the lower molars was erroneously considered by [Dineur \(1981\)](#) and [Pickford \(1987\)](#) as a distinctive character between *Parabrachyodus* and *Brachyodus*. Conversely, the M/3 of *Parabrachyodus* is not defined by a trigonid larger than the talonid as suggested by [Forster-Cooper \(1913\)](#), despite the proportions of the first M/3 allocated to the genus (Fig. 1B). Furthermore, drawings of early authors show that the presence of the ectoprotocrista linked to a protostyle (a diagnostic character of *Par. hyopotamoides*) was not considered as a relevant feature (Fig. 1A). It is noteworthy that [Pilgrim \(1912: 55\)](#) was the first to mention some character states of *Parabrachyodus* (= *Brachyodus 'giganteus'*) such as the 'rudimentary additional cusp' on P3/ underscoring the anthracotheriine affinity of this tooth, without interpreting them as diagnostic.

The sample of *Parabrachyodus* is comprehensive in the Bugti Hills, with at least 107 specimens (mostly molars) when including the remains newly described here. All these remains belong to the single species of the genus, *Par. hyopotamoides*. [Pickford \(1987\)](#) stressed the difficulties of discriminating the lower molars of *Par. hyopotamoides* from those of *Telmatodon* and *Hemimeryx*, presumably because the lower molars display a greater number of polymorphic traits and are less represented in number of specimens than the upper molars. Also, the convergent morphology of the hypoconulids of *Anthracotherium* and *Parabrachyodus* probably brought confusions in distinguishing these genera (e.g. [Welcomme & Ginsburg, 1997: 1002](#)), further inspiring the assignment of *Parabrachyodus* in the Anthracotheriinae instead of the Bothriodontinae ([Pickford, 1987: fig. 4](#)), as such following [Lydekker \(1883\)](#) who considered this anthracothere as a representative of *Anthracotherium*. However, the upper molars are more distinctive. *Gonotelma major* is defined by a worn upper molar with a paraconule ([Forster-Cooper, 1924: pl. 5, fig. 1](#)) and it is here considered as a junior synonym of *Par. hyopotamoides*. We concur with [Pickford \(1987\)](#) in considering

Gonotelma a monospecific genus with small tetracuspitate molars, first interpreted as pentacuspitate (Pilgrim, 1908; Pilgrim, 1912).

AGE AND GEOGRAPHICAL DISTRIBUTION OF *PARABRACHYODUS*

In addition to the series of *Parabrachyodus hyopotamoides* from SAM 4 (c. 21 Mya), the isolated M3/ UM-SAM5-001 is the first reported occurrence of a fossil from SAM 5, which extends the age formally given to *Par. hyopotamoides* to approximately 19 Mya (Roddaz *et al.*, 2011; Antoine *et al.*, 2013). We thus confirm the presence of the species in the Vihowa Formation (e.g. Antoine *et al.*, 2013; Nanda *et al.*, 2017). *Parabrachyodus hyopotamoides* is also recorded with confidence in the Zinda Pir Dome, Sulaiman Province of Pakistan, about 200 km north of the Bugti Hills, through three isolated specimens in localities Z114, Z154 (Lindsay *et al.*, 2005) and Safed Nala. The “Interpretation B” of Lindsay *et al.* (2005: fig. 6B) for the correlation of the Zinda Pir localities to Geomagnetic Polarity Time Scale (GPTS) being the most satisfactory (Antoine *et al.*, 2013: 416), the localities Z114 and Z154 then lie between the magnetochrons C6AA and C6Bn. The corresponding approximate age is 21.95 Mya (Speijer *et al.*, 2020; J. Barry, pers. comm., 2022), which makes it the oldest known occurrence of *Par. hyopotamoides*. The species is also documented in the Khari Nadi Formation (Kutch Basin, Gujarat, India), via a palate with molars that have, among other traits, the characteristic morphology of the protocone and a large distostyle (Bhandari *et al.*, 2010: fig. 7A). It is also accompanied by *Sivameryx palaeindicus* in the Kutch fauna. This assemblage could be younger than Samane Nala 4 and 5 according to Bhandari *et al.* (16.5 +/- 0.5 Mya). However, they precisely considered a Last Local Appearance (LLA) of 16.5 Mya for *Par. hyopotamoides* to propose the most likely age of the Kutch mammal fauna. It is unclear whether or not *Parabrachyodus* also occurs in the Level 6 of the Chitarwata Formation (c. 17,5-18 Mya, Roddaz *et al.*, 2011; Antoine *et al.*, 2013: fig. 16.4) and *Par. hyopotamoides*

is certainly not documented in younger levels in the Bugti Hills. Nevertheless, a gap is observed in terms of fossil-yielding levels in the concerned overlying sequence, i.e. between the poorly-documented Level 6sup ('Assemblage B') and the middle Miocene 'Assemblage C' (Level W; [Antoine *et al.*, 2013](#)). In any event, the biochronological age of the Kutch fauna is potentially questionable (*contra* [Bhandari *et al.*, 2010, 2021](#); [Sehgal & Bhandari, 2014](#); [Patnaik & Prasad, 2016](#)). Conversely, it may restrain the use of anthracotheriid species from the Bugti Hills for biochronological purposes ([Antoine *et al.*, 2013](#): 413).

[Russell & Zhai \(1987\)](#) reported one P4/ and one M/2 from the Benara fauna in Georgia ([Gabounia, 1966](#): fig. 9d, e) referred to as *Parabrachyodus*. The upper premolar lacks the two distal ridges and large distostyle characteristic of this genus, and it is more oblong transversely. The lower molar is too small to belong to this taxon; its selenodont morphology with pinched lingual cuspids and the connection between the preprotocristid and the premetacristid are consistent with *Elomeryx* instead. According to the provided drawing, it could also be a worn, ruminant-like lower tooth. A fragmentary pentacuspitate upper molar from the Dingdangou fauna (China) has been interpreted as *Parabrachyodus* sp. ([Wang & Qiu, 2004](#)), but it has more selenodont ridges than unambiguous representatives of this genus, and the postparacristule joins the base of the paracone rather than the transverse valley. In this context, it is more likely that this tooth belongs to *S. palaeindicus* than to *Par.*

hyopotamoides. Hence, no occurrence of *Parabrachyodus* is documented in Oligocene-Miocene deposits of China, and there is no dispersal event either between the north and south sides of the Tibetan Plateau involving this bothriodontine during the Early Oligocene (*contra* [Li *et al.*, 2016](#); [Wang, 2020](#); [Li *et al.*, 2022](#)). The occurrence of *Parabrachyodus* sp. in the Irrawaddy area of Myanmar (Burma) immediately east of the Indian subcontinent ([Bhandari *et al.*, 2010](#)) remains uncertain due to the lack of illustration for the referred specimen. The

provided measurements of the concerned M3/ (46.5 × 54.9 mm) fall outside the range of variation defined for *Par. hyopotamoides* in this study (Table 2).

In the current stage of our knowledge, *Par. hyopotamoides* seems to be restricted to the western part of the Indian subcontinent and it is not formally known in the Palaeogene, in contrast with what the compilation of Sulaiman Range faunas studied by [Raza & Meyer \(1984\)](#) and [Pickford \(1987\)](#) may have suggested. Despite the ‘gigantic *Hyopotamus*’ known ‘from Sind’ ([Lydekker, 1882: 107](#)), *Parabrachyodus* is not mentioned in the Manchar Formation, with maybe the exception of ‘cf. *Brachyodus* sp.’ listed by [Raza et al. \(1984, table 2\)](#) in its lower member. Given that the Sind deposits lie south of the Bugti Hills and north of the Kutch Province ([Bhandari et al., 2010: fig. 1](#)), fossils of *Par. hyopotamoides* are also likely to occur in the Manchar Formation. Fossil collections without any stratigraphical context in the Bugti Hills where Oligocene sediments have been identified (M12030 and M12033) are suspected to somewhat pre-date the Oligocene-Miocene transition ([Forster-Cooper, 1913; Antoine et al., 2013: fig. 16.4](#)) as those referred to as *Hemimeryx blanfordi* have been in the same work of Forster-Cooper ([Lihoreau et al., 2016](#)). This occurrence of *Hem. blanfordi* in the Late Oligocene of the Bugti Hills together with the basal phylogenetic position of the clade (*Par. hyopotamoides* + *Telmatodon*) support the potential appearance of *Parabrachyodus* as early as in the Late Oligocene.

PHYLOGENETIC RELATIONSHIPS BETWEEN BOTHRIODONTINES FROM THE BUGTI HILLS

The three genera, *Gonotelma*, *Parabrachyodus* and *Telmatodon*, recorded in the Bugti Hills can be seen as early Merycopotamini *sensu* [Lihoreau et al. \(2016\)](#) in the present study. We refute the hypothesis that *Gonotelma shahbazi* is more related to *Sivameryx* than to *Afromeryx*

zelteni due to the shared retention of the paraconule (Lihoreau & Ducrocq, 2007). First, the absence of a postparacristule on the M3/ of *G. shahbazi* shows that there is no paraconule (Fig. 5L). In comparison, the holotype of *Telmatodon orientalis* (Forster-Cooper, 1924) has a reduced paraconule with a vestigial cristule (Fig. 5K). Second, the presence of the paraconule is here considered as a derived character that appeared independently in *Sivameryx* and *Parabrachyodus*. The position of *Gonotelma* as sister-group to *Afromeryx* instead supports the hypothesis of closer phylogenetic relationships with this small Libyan merycopotamine (Pickford, 1987, 1991). Shared characters relating to the morphology of the lower molars of these genera explain they are close relatives, while only the similarity of their upper molars had been pointed out by Pickford (1987, 1991). As *Telmatodon* is closer to *Parabrachyodus* than to *Gonotelma*, the hypothesis of a synonymy between *Telmatodon* and *Gonotelma* (Viret, 1961; Kumar & Kad, 2003) is not verified by the present analysis, despite their general similarity. These findings involving the phylogenetic position of *Telmatodon* and *Gonotelma* suggest that they do not constitute a clade with *Parabrachyodus* contrary to what Pickford (1987: fig. 4) had informally proposed. Instead, *Parabrachyodus* and *Telmatodon* can be seen as a lineage that appears to be restricted to the Indian subcontinent during the Early Miocene. These conclusions remain uncertain insofar as the scarce fossil material for *Telmatodon* and *Gonotelma* (lacking lower premolars, rostral teeth, mandible and skull) has not allowed us to discriminate their diagnostic characters as precisely as for *Par. hyopotamoides*. In all cases, the phylogenetic proximity of these three associated early merycopotamines together with their size differences (*Parabrachyodus* and *Telmatodon* being gigantic compared to *Gonotelma*), contradict the existence of a body size increase through time in this lineage, as argued by Pickford (2009) for the African merycopotamines *Afromeryx* and *Libycosaurus*.

Of the two distal ridges of the protocone of P4/ of *Parabrachyodus*, the one that joins the distostyle can be interpreted at first as the postectoprotocrista and the other one, shorter

and labially situated, as the postprotocrista, considering the convergent condition in *Anthracotherium* (Scherler *et al.*, 2018). In the context of the basal position of *Par. hyopotamoides* in relation to Merycopotamini such as *Sivameryx palaeindicus* (also documented in the Bugti Hills), the hypothesis of homology involved by this terminology implies that a reduction of the postectoprotocrista - accompanied by a lingual displacement of the postprotocrista and its development until it reaches the distostyle - would have led to the occlusal pattern of the P4/ of this tribe (Fig. 10A). In view of the configuration of the distal crest of the P4/ of *Elomeryx* (Kostopoulos *et al.*, 2012: fig. 4) resembling those of Merycopotamini, two hypotheses are equally parsimonious. Since *Par. hyopotamoides* is the first branching species of the clade excluding *Elomeryx* together with species of *Telmatodon*, it may be expected that the *Parabrachyodus*-like postprotocrista has been lost and the postectoprotocrista is retained in all Merycopotamini (Fig. 10B). The postprotocrista of *Par. hyopotamoides* can be seen as an additional ‘endoprotocrista’ (formed from an enamel fold or a fossa) and the postectoprotocrista as the true postprotocrista that connects to the distostyle, inherited from a common ancestor with *Elomeryx* (Fig. 10C). Since the single known P4/ of *Telmatodon orientalis* (Fig. 10; Forster-Cooper, 1924: pl. 5, fig. 5) has a two-crested protocone, with one distal crest, the second proposal is the most likely in the context of the present topology (the P4/ of *Gonotelma* being unknown). This autapomorphic scenario (Fig. 10C) is consistent with the overall trend towards the addition of styles and ridges, which have only been reported on the jugal teeth surrounding the P4/ of *Par. hyopotamoides*, namely the small distolingual style on the P3/ and the protostyle and ectoprotocrista of upper molars.

IMPLICATIONS FOR THE DEFINITION OF MERYCOPOTAMINI

The paraphyly of Merycopotamini *sensu* Lihoreau *et al.* (2016) as well as the weak support of the clade, assuming that *G. shahbazi* (the sister-species to *A. zeltani*) is part of it, highlights

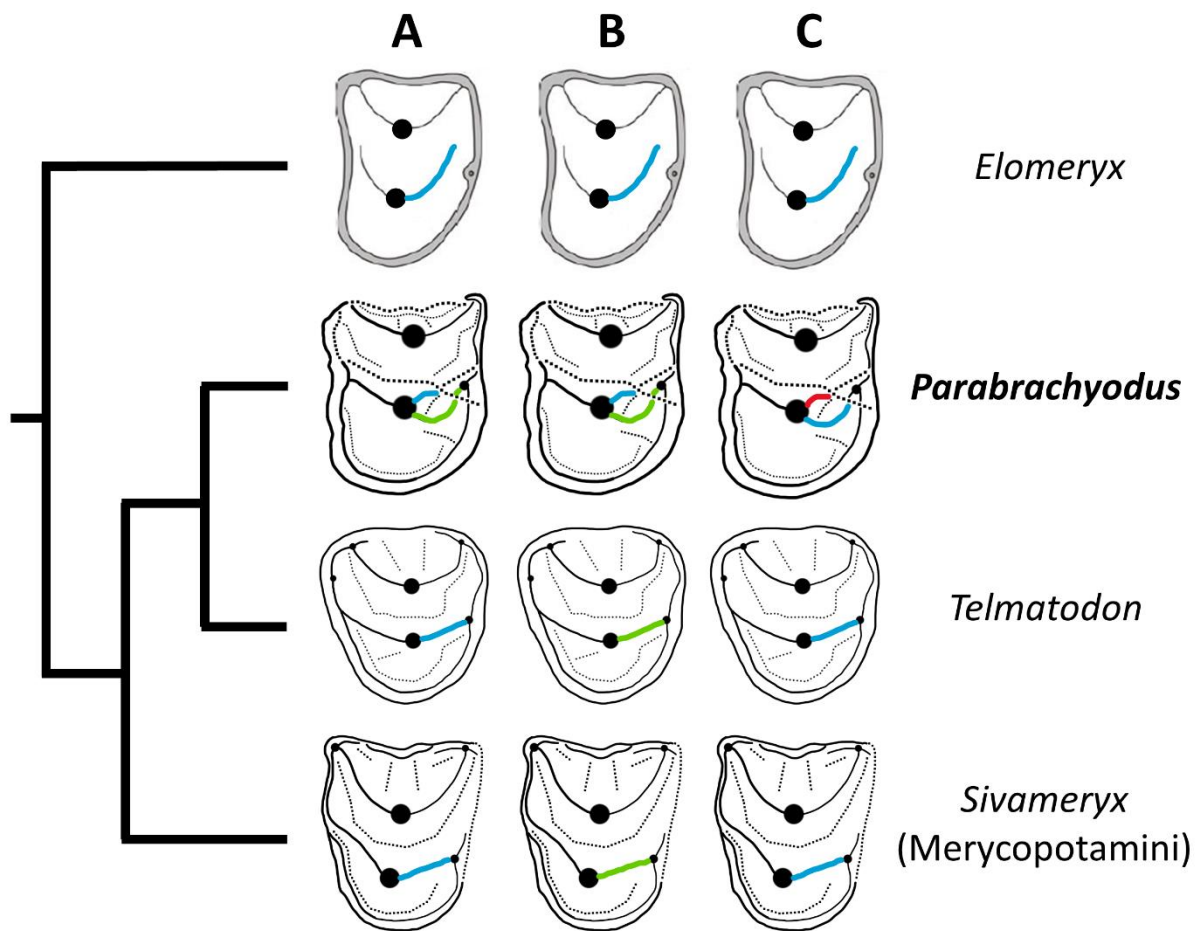


Figure 10. Three hypotheses of homology for the cristae of P4/ within the clade B due to the inclusion of *Parabrachyodus hyopotamoides*, through scenarios sketched on a simplified topology. A, hypothesis 1, convergence with the Anthracotheriinae; B, hypothesis 2, reviewed homology of the distal crest of *Telmatodon* and the Merycopotamini; C, hypothesis 3 (this work), additional endoprotocrista of *Par. hyopotamoides*. Coloured characters: blue, postprotocrista; green, postectoprotocrista; red, endoprotocrista. Drawing of the P4/ of *Elomeryx* modified from [Kostopoulos et al. \(2012\)](#). Drawings are not to scale.

the need for a more inclusive diagnosis of the tribe. Two-thirds of the non-ambiguous synapomorphies that made Merycopotamini a clade at the time of its definition were then interpreted as convergences with *Elomeryx* and *Bothriodon* (Lihoreau *et al.*, 2016). The phylogenetic position of *Parabrachyodus* with respect to *Elomeryx* on the one hand and Merycopotamini on the other hand establishes the suspected link between *Elomeryx* and Merycopotamini (Lihoreau & Ducrocq, 2007; Böhme *et al.*, 2013, Rincon *et al.*, 2013). Hence, 7 out of 9 characters defining Merycopotamini *sensu* Lihoreau *et al.* (2016) are retrieved as unambiguous synapomorphies in the branching sequence leading to the robust node comprising *Par. hyopotamoides* (Fig. 11). For instance, the pinched loop-like hypoconulid on M/3, the parastyle issued from the preparacrista and the absence of ectocristyle on upper molars are actually inherited from a common ancestor with *Elomeryx* and *Bakalovia*. Thus, considering the first diagnosis of Merycopotami (Lihoreau *et al.*, 2016), *Par. hyopotamoides* differs in only three out of 13 traits relative to the morphology of the cristids of the protoconid on P/3 and P/4, namely the orientation of the P/3 postprotocristid, the position of the P/4 postprotocristid and the direction of the P/4 preprotocristid. Nevertheless, the occlusal pattern of lower P/4 has proved to be of great interest for distinguishing Merycopotamini from each other (Lihoreau *et al.*, 2019: fig. 4).

Considering the robust relationship between *Elomeryx* and Merycopotamini through the inclusion of *Par. hyopotamoides*, and the primitive condition of its P/4 compared to Merycopotamini *sensu* Lihoreau *et al.* (2016) (Fig. 11), we suggest a redefinition of Merycopotamini encompassing the basal position of *Parabrachyodus* and its relatives *Telmatodon* and *Gonotelma*. Interestingly, the new traits of the larger tribe concern mainly the eruption of tubercles appearing subsequently during the development of the dP3/, recently considered as bearing strong diagnostic characters (Gomes Rodrigues *et al.*, 2020), the preferential development of the I/1 among the lower incisors, the multiplication of tubercles

and crests on the P3/ and that of the number of mandibular foramen; hence very different characters from the previous definition. Nonetheless, the critical role of the enamel microstructure in distinguishing this clade (Alloing-Séguier *et al.*, 2014; Lihoreau *et al.*, 2016) is here reinforced, the substantial development of radial outer enamel being completed by the Schmelzmuster composed of two layers and weakly developed HSB. This diagnosis also clearly distinguishes merycopotamines from *Elomeryx* through the lack of connection between the protocone and the metaconule, closing the transverse valley on upper molars, except for *E. borbonicus* (e.g. Geais, 1934; Hellmund, 1991; Lihoreau *et al.*, 2009: fig. 3), and between the premetacristid and the preprotocristid on lower molars. We note a tendency for the number of protocone crests to decrease in the extended tribe, from *Parabrachyodus* with a quadricrescentic protocone to *Afromeryx*, *Gonotelma*, *Hemimeryx*, *Sivameryx* and *Telmatodon* with three crests, and *Libycosaurus* and *Merycopotamus* with only two crests. Finally, this lineage is also characterized by a tendency to complexify the occlusal morphology of the *Parabrachyodus*-like P/4, as suggested above. A mesial curvature of the preprotocristid and a lingual orientation of the postprotocristid are acquired in *Afromeryx*, the hypoconid and a partial fusion of the postprotocristid and endoprotocristid in *Hemimeryx* and *Sivameryx*, the distal crest of the entostylid in *Merycopotamus*, and a multiplication of accessory cusps mesially to the preprotocristid are independently developed in *Hemimeryx* and *Libycosaurus* (Fig. 11; Lihoreau *et al.*, 2019).

PALAEOBIOGEOGRAPHICAL IMPLICATIONS

The northern distribution of *Brachyodus* relative to the Himalaya Range during the Early to Middle Miocene (Ducrocq *et al.*, 2003) indicates that these mountains must have constituted a barrier to dispersal for this genus and vice versa for *Parabrachyodus* from India, inasmuch as no specimen from China similar to those from the Indian subcontinent is documented. An

alternative hypothesis for their non-overlap is a mutual exclusion for ecological reasons. *Elomeryx cf. borbonicus* is known from two jugal teeth in the Zinda Pir Dome in Z108 locality (Ducrocq & Lihoreau, 2006), an older locality than those that have yielded the oldest material of *Parabrachyodus* (Z114 and Z154; Lindsay *et al.*, 2005: fig. 6B). The occurrence of this European species in Pakistan shows that the palaeobiogeography of the Late Oligocene and the Early Miocene allowed interchanges with Europe, as massively illustrated by mammalian assemblages of the Early Miocene in general (e.g. Antoine *et al.*, 2010, 2013). In Burdigalian times (late Early Miocene), the two concomitant dispersal events involving *Sivameryx* on the one hand and *Gonotelma* and *Afromeryx* on the other (Proboscidean Datum Events, Fig. 11), via the probable connection of the Indus with the Tiger-Euphrate drainage basin, provide evidence that a passageway to Africa was also open from Pakistan (e.g. Barrier *et al.*, 2018; Grossman *et al.*, 2019; Lihoreau *et al.*, 2019). An origin for Merycopotamini, rooted by *Par. hyopotamoides*, in this north-western province of the Indian subcontinent (i.e. Pakistan), is therefore consistent with this second phase of dispersal in the evolutionary history of this lineage of bothriodontines (Fig. 11).

Unlike the small merycopotamines, *Par. hyopotamoides* appears to be endemic to the Indian sub-continent. The absence of dispersal towards Africa is probably linked to its extinction just before the contact between the two continents (Fig. 11). *Parabrachyodus hyopotamoides* displaying the thickest enamel among bothriodontines, allowing more resistance to wear that could explain the strong wear gradients of molars rows (Alloing-Séguier *et al.*, 2014: 691), the flattest occlusal surface among bothriodontines and molars with a selenodonty less marked than in other merycopotamines, we question if a high degree of ecological specialization may explain its extinction.

The basal position of *Parabrachyodus* in relation to Merycopotamini, its relatively short temporal range and atypical morphology (for a bothriodontine), as well as a fossil record

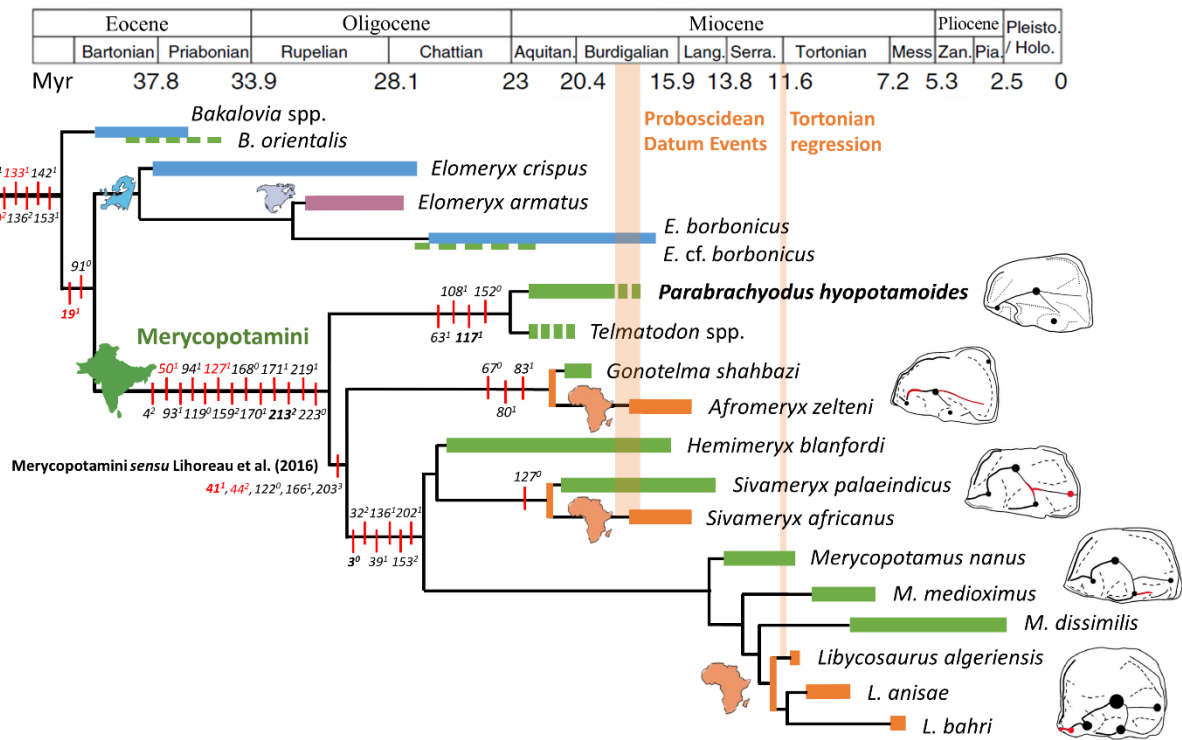


Figure 11. Part of the consensus tree mapped on the geologic time scale (Gradstein *et al.*, 2012) and the geographic distribution of selected bothriodontines. The temporal extensions of taxa are coloured according to their geographical distribution, those in non-full lines are uncertain. Green, Indian subcontinent; blue, Europe; purple, North America; orange, Africa. The non-ambiguous synapomorphies are placed at the nodes discussed in this work, the character states are summarized in the Supporting Information (Appendix S2); the non-ambiguous synapomorphies defining Merycopotamini in the analysis of Lihoreau *et al.* (2016) are in red; the non-ambiguous and non-homoplastic synapomorphies are in bold. Drawings of the P/4 are (from top to bottom) *Parabrachyodus hyopotamoides* (this study), *Afromeryx zelteni*, *Sivameryx africanus*, *Merycopotamus medioximus* and *Libycosaurus anisae* (Lihoreau *et al.*, 2019). The characters highlighted in red on the P/4 are those acquired in the clade involved. Drawings are not to scale. Spatial and temporal distributions are from Lihoreau *et al.* (2007, 2016, 2019), Bhandari *et al.* (2010), Holroyd *et al.* (2010), Kostopoulos *et al.* (2012), Antoine *et al.* (2013), Böhme *et al.* (2013) and Kapur *et al.* (2019).

limited to the Indian sub-continent, blurs its palaeobiogeographical history. Furthermore, Asian records of *Elomeryx* cf. *borbonicus* are scarce (Ducrocq & Lihoreau, 2006), and there is a large gap with the record of *Bakalovia orientalis* from the late Eocene (Böhme *et al.*, 2013), which contributes to the uncertainty of the geographical origin of *Parabrachyodus* (Fig. 11). *Arretotherium* and especially *A. meridionale* from Central America must be included in further phylogenetic analyses, since the phylogenetic position of this genus is unclear, either in an *Elomeryx* clade (Kostopoulos *et al.*, 2012) or in polytomy with *E. borbonicus* and Merycopotamini (Lihoreau & Ducrocq, 2007; Böhme *et al.*, 2013; Rincon *et al.*, 2013). It is a critical point for biogeographical purposes regarding the concomitant origination of merycopotamines in Asia.

The identification of *Gonotelma* in the same stratigraphic level as *Parabrachyodus*, *Sivameryx*, probably *Telmatodon* (Antoine *et al.*, 2013) and *Hemimeryx* (Lihoreau *et al.*, 2016), implies that the Bugti Hills faunas simultaneously comprised at least five phylogenetically related bothriodontines. Such diversity is not surprising for the megafaunas of the region, as nine distinct species of rhinocerotids are known to co-occur from Kumbi 4 (Antoine *et al.*, 2010), the lateral equivalent of SAM 4. The diversity of merycopotamines from the Early Miocene of the Bugti Hills is unique in that no homotaxic assemblages are known elsewhere. The available cranio-mandibular material for *Par. hyopotamoides* did neither allow us to define a sexual dimorphism in the studied populations, nor a semi-aquatic lifestyle, as for *Sivameryx* (Rowan *et al.*, 2015) and contrary to what is observed in certain bothriodontines with a proven semi-aquatic lifestyle (Orliac *et al.*, 2013; Lihoreau *et al.*, 2014). Yet, the predominance of the remains of *Par. hyopotamoides* over other Bugti anthracotheres (Pickford, 1987: tab. 6) and the proportion of unicuspidate P4/ for *Par. hyopotamoides*, show that these megaherbivores must have lived in sufficiently isolated and

small populations for such dental variations to become common (Ducrocq *et al.*, 1995; Lihoreau *et al.*, 2006).

CONCLUSION

Parabrachyodus is a monospecific genus restricted to Lower Miocene deposits of the Indian sub-continent and mostly known in the Bugti Hills faunas. Despite its recent age compared to the late Oligocene selenodont *Hemimeryx* (Lihoreau *et al.*, 2016), the addition of this enigmatic taxon in our phylogenetic analysis sheds light on the ancestral morphotype of the Merycopotamini: additional styles and cristae providing the jugal teeth with a very thick enamel with a unique anthracotheriine cachet among bothriodontines, derived premolars and deciduous premolars and an enamel microstructure reminiscent of all merycopotamines. We here document the deep origination of this tribe in the Indian sub-continent (where it occurs all over its evolutionary history), preceding two major punctual dispersal events from Asia to Africa following the same pathways (e.g. Lihoreau *et al.*, 2019). All these features distinguish *Parabrachyodus* and Merycopotamini from *Brachyodus*, at the origin of a dispersal event from Africa to Asia, which is far less understood (e.g. Grossman *et al.*, 2019). In this context, a systematic revision of the small *Gonotelma shahbazi* together with an analysis of its enamel microstructure would be relevant for clarifying the phylogenetic relationships between the Bugti bothriodontines and the similar *Afromeryx zelteni* from Africa, since this approach bears phylogenetic interest (Alloing-Séguier *et al.*, 2014, 2016; Lihoreau *et al.*, 2016; this study). In particular, the question of a closer proximity of *Gonotelma* with the endemic *Telmatodon* (Kumar & Kad, 2003), or with *Afromeryx* (Pickford, 1987; this study) needs to be reassessed.

We also bridge the gap of the merycopotamine fossil record from the Late Oligocene between the evolutionary history of this Indian lineage and the Eocene-Oligocene *Elomeryx* from Eurasia. This new well-resolved phylogenetic framework demonstrates the relevance of

the revision of *Parabrychodus hyopotamoides* for understanding the evolution of the ‘Anthracotheriidae’ and implies a redefinition of the tribe Merycopotamini *sensu* [Lihoreau et al., 2016](#), including *Par. hyopotamoides*. This extended clade includes at least 14 bothriodontine species (mostly from the Indian subcontinent) sharing a lack of connection between the lingual cusps of upper molars and between the mesialmost cristids of lower molars, a duplication of the anterior crest and the presence of at least two accessory cusps on the distal crest of the first three upper premolars, two main mandibular foramina, an important development of radial outer enamel, and dP3/ with four main cusps and three accessory cusps. Since our study pointed out the position of the enigmatic Late Eocene *Bakalovia* near the bothriodontine origin, a revision of this early-diverging Eurasian merycopotamine genus must be conducted, especially when considering the very procumbent lower premolars of *Ba. palaeopontica* ([Nikolov, 1967](#); [Hellmund, 1991](#)) compared to the derived morphology exhibited by *Bakalovia orientalis* ([Böhme et al., 2013](#)), and in view of the confirmed phylogenetic interest of this dental locus in Merycopotamini ([Lihoreau et al., 2019](#); this study). In this sense, further research could focus on the origin of bothriodontines and the clarification of the phylogenetic relationships between the major bothriodontine lineages.

ACKNOWLEDGEMENTS

This article is dedicated to the memory of Jean-Loup Welcomme, who passed away on May 18th, 2021. As a long-time colleague and friend, he was a key figure in the palaeontological project in the Bugti Hills area of Pakistan, notably as head of the ‘*Mission Paléontologique Française au Baloutchistan*’ (MPFB). None of the fossil discoveries in the Bugti Hills between 1995 and 2004 could have been made without his courage, determination, humanity and friendship.

We are also particularly grateful to the late Nawab Akbar Shahbaz Khan Bugti, Lord of the Bugti Tribes, for his constant support and interest in our work in the Bugti Hills, as well as Zulficar, Brahumdagh Khan Bugti, and Shaheed Hassan Bugti for their invitations and help. The fossils from the Bugti Hills studied in this paper were collected during the 1998-2000 field seasons, as part of a collaborative palaeontological programme with the University of Balochistan (Quetta, Pakistan). We would like to thank J. Barry (Peabody Museum of Harvard University, Cambridge, USA) for its pictures and precise data related to the specimens from localities Z114 and Z154 in the Zinda Pir. We are grateful to S. Ramin (wpd offshore solutions GmbH) and M. Kollmann for their helpful clarification of the geological and geographical contexts of the Safed Nala (Zinda Pir Dome) fossils collected during a fieldwork supervised by the late Prof. Dr. D. Helmcke (Universität Göttingen). Many thanks to A.-L. Charruault (ISE-M) for the preparation of some fossil specimens from the Bugti Hills, and to M. Orliac for the lending of artiodactyl specimens used for coding. We thank our friends and colleagues, members of the MPFB, J.-Y. Crochet (ISE-M), D. de Franceschi (Muséum national d'Histoire naturelle, Paris), as well as J.-J. Jaeger, M. Benammi and Y. Chaimanee (PALEVOPRIM, Université de Poitiers) for their contributions in the field. Many thanks to the Shawani family (Quetta, Pakistan) as well as our Bugti bodyguards and Bugti local people for their efficient help during the numerous field seasons in the Bugti Hills. We are also thankful to Kamal Madjidulah (Karachi, Pakistan) for his tireless assistance and enthusiasm. Many thanks to Marc de Grossouvre (French Embassy, Islamabad) for his great interest in our French/Pakistani collaborative programme. The Ministry of Foreign Affairs (MAE) via the French Embassy in Islamabad, the CNRS (Eclipse-Programme), the Fondation de France, the Department of Anthropology and Peabody Museum (Harvard University), the Leakey, Fyssen, Bleustein-Blanchet and Singer-Polignac foundations, the Gédéon Programmes, and the Institut des Sciences de l'Evolution de Montpellier (ISE-M) have

financially supported the fieldwork and post-field studies of the 1998-2004 project. The work in the framework of this paper was supported by the Agence Nationale de la Recherche: Splash programme (ANR-15-CE32-0010-01). We thank the two anonymous reviewers, and the editors James Hansford and Maarten Christenhusz, for their constructive comments on the manuscript. This is ISE-M publication n° 2023-011 SUD.

CONFLICT OF INTEREST

The authors declare that there are no conflicts of interest.

DATA AVAILABILITY

Data used in this article is presented in the Supporting Information section at the end of the paper and is freely available to download from the publisher's website.

REFERENCES

- Alloing-Séguier L, Lihoreau F, Boisserie JR, Charruault AL, Orliac M, Tabuce R. 2014.** Enamel microstructure evolution in anthracotheres (Mammalia, Cetartiodactyla) and new insights on hippopotamoid phylogeny. *Zoological Journal of the Linnean Society* **171**: 668–695.
- Alloing-Séguier L, Martinand-Mari C, Barczy JF, Lihoreau F. 2016.** Linking 2D Observations to 3D Modeling of Enamel Microstructure – a New Integrative Framework Applied to Hippopotamoidea Evolutionary History. *Journal of Mammalian Evolution* **24**: 221–231.
- Andrews CW. 1899.** Fossil Mammalia from Egypt, Part I. *Geological Magazine* **6**: 481–484.
- Andrews CW, Beadnell HJL. 1902.** *A preliminary note on some new mammals from the Upper Eocene of Egypt.* Survey Department of Public Works Ministry, Cairo: 1–9.
- Antoine PO, Welcomme, JL. 2000.** A new rhinoceros from the Bugti Hills, Baluchistan, Pakistan: The earliest Elasmotheriinae. *Palaeontology* **43**: 795-816.
- Antoine PO, Shah SMI, Cheema IU, Crochet JY, de Franceschi D, Marivaux L, Métais G, Welcomme JL. 2004.** New remains of the baluchitherid *Paraceratherium bugtiense*

(Pilgrim, 1910) from the Late/latest Oligocene of the Bugti hills, Balochistan, Pakistan. *Journal of Asian Earth Sciences* **24**: 71–77.

Antoine PO, Downing KF, Crochet JY, Duranthon F, Flynn LJ, Marivaux L, Métais G, Rajpar AR, Roohi G. 2010. A revision of *Aceratherium blanfordi* Lydekker, 1884 (Mammalia: Rhinocerotidae) from the Early Miocene of Pakistan: postcranials as a key. *Zoological Journal of the Linnean Society* **160**: 139–194.

Antoine PO, Métais G, Orliac MJ, Crochet JY, Flynn LJ, Marivaux L, Rajpar AR, Roohi G, Welcomme JL. 2013. Mammalian Neogene Biostratigraphy of the Sulaiman Province, Pakistan. In: Xiaoming W, Flynn LJ, Fortelius M, eds. *Fossil Mammals of Asia*. New York: Columbia University Press, 400–422.

Antunes MT, Ginsburg L. 2003. The last Anthracothere *Brachyodus onoideus* (Mammalia, Artiodactyla) from westernmost Europe and its extinction. *Ciências da Terra* **15**: 161–172.

Arnason U, Gullberg A, Solweig G, Ursing B, Janke A. 2000. The mitochondrial genome of the sperm whale and a new molecular reference for estimating eutherian divergence rate. *Journal of Molecular Evolution* **50**: 569–578.

Barrier E, Vrielynck B, Brouillet JF, Brunet MF. 2018. Paleotectonic Reconstruction of the Central Tethyan Realm. Tectono-Sedimentary-Palinspastic maps from Late Permian to Pliocene. *Paris: Commission for the Geological Map of the World (CGMW/CCGM)*.

Bhandari A, Mohabey DM, Bajpai S, Tiwari BN, Pickford M. 2010. Early Miocene mammals from central Kutch (Gujarat), Western India: Implications for geochronology, biogeography, eustasy and intercontinental dispersals. *Neues Jahrbuch für Geologie und Palaontologie - Abhandlungen* **256**: 69–97.

Bhandari A, Bajpai S, Flynn LJ, Tiwari BN, Mandal N. 2021. First Miocene rodents from Kutch, western India. *Historical Biology* **33**: 3471–3479.

Böhme M, Aiglstorfer M, Antoine PO, Appel E, Havlik P, Métais G, Phuc LT, Schneider S, Setzer F, Tappert R, Tran DN, Uhl D, Prieto J. 2013. Na Duong (northern Vietnam) - An exceptional window into Eocene ecosystems from Southeast Asia. *Zitteliana Reihe A: Mitteilungen der Bayerischen Staatssammlung für Palaontologie und Geologie* **53**: 121–167.

Boisserie JR. 2005. The phylogeny and taxonomy of Hippopotamidae (Mammalia: Artiodactyla): A review based on morphology and cladistic analysis. *Zoological Journal of the Linnean Society* **143**: 1–26.

Boisserie JR, Lihoreau F, Orliac M, Fisher RE, Weston EM, Ducrocq S. 2010. Morphology and phylogenetic relationships of the earliest known hippopotamids (Cetartiodactyla, Hippopotamidae, Kenyapotaminae). *Zoological Journal of the Linnean Society* **158**: 325–366.

Crochet JY, Antoine PO, Benammi M, Iqbal N, Marivaux L, Métais G, Welcomme JL. 2007. A herpetotheriid marsupial from the Oligocene of Bugti Hills, Balochistan, Pakistan. *Acta Palaeontologica Polonica* **52**: 633–637.

Depéret C. 1895. Über die Fauna von miozänen Wilberthieren aus der ersten Mediterranstufe von Eggenburg. *Sitzungsberichten Kaiserliche Akademie Wissenschaften Wien* **104**: 395–416.

- Dineur H. 1981.** Le genre *Brachyodus*, Anthracotheriidae (Artiodactyla, Mammalia) du Miocène inférieur d'Europe et d'Afrique. Unpublished thesis, Université Pierre et Marie Curie - Paris VI.
- Ducrocq S. 1995.** The contribution of Paleogene anthracotheriid artiodactyls in the paleobiogeographical history of southern Europe. *Neues Jahrbuch für Geologie und Paläontologie* **6**: 355–362.
- Ducrocq S. 1997.** The anthracotheriid genus *Bothriogenys* (Mammalia, Artiodactyla) in Africa and Asia during the Paleogene: phylogenetical and paleobiogeographical relationships. *Stuttgarter Beiträge Naturkunde* **250**: 1–44.
- Ducrocq S. 2020.** Taxonomic revision of *Anthracokeryx thailandicus* Ducrocq, 1999 (Anthracotheriidae, Microbunodontinae) from the Upper Eocene of Thailand. *Vertebrata Palasiatica* **58**: 293–304.
- Ducrocq S, Lihoreau F. 2006.** The occurrence of bothriodontines (Artiodactyla, Mammalia) in the Paleogene of Asia with special reference to *Elomeryx*: Paleobiogeographical implications. *Journal of Asian Earth Sciences* **27**: 885–891.
- Ducrocq S, Chaimanee Y, Suteethorn V, Jaeger JJ. 1995.** Dental anomalies in Upper Eocene Anthracotheriidae: a possible case of inbreeding. *Lethaia* **28**: 355–360.
- Ducrocq S, Chaimanee Y, Suteethorn V, Jaeger JJ. 2003.** Présence de l'anthracothère *Brachyodus* (Artiodactyla, Mammalia) dans le Miocène moyen de Thaïlande. *Comptes Rendus - Palevol* **2**: 261–268.
- Falconer H, Cautley PT. 1836.** Note on the fossil hippopotamus of the Siwalik Hills. *Asiatic Research Calcutta* **19**: 39–53.
- Falconer H, Cautley PT. 1847.** *Fauna Antiqua Sivalensis*. London: Smith, Elder and Co.
- Forster-Cooper C. 1913.** New anthracotheres and allied forms from Baluchistan – Preliminary notice. *Annals and Magazine of Natural History* **12**: 514–522.
- Forster-Cooper C. 1915.** New genera and species of mammals from the Miocene deposits of Baluchistan - Preliminary notice. *Annual Magazine of Natural History* **16**: 404–410.
- Forster-Cooper C. 1924.** The Anthracotheriidae of the Dera Bugti deposits in Baluchistan. *Memoirs of the Geological survey of India. Palaeontologica Indica* **4**: 1–59.
- Gabounia L. 1966.** Sur les mammifères oligocènes du Caucase. *Bulletin de la Société Géologique de France* **8**: 857–869.
- Geais G. 1934.** Le *Brachyodus borbonicus* des argiles de St-Henri (près Marseille). *Travaux du Laboratoire de Géologie de la Faculté de Lyon* **25**: 1–54.
- Gentry AW, Hooker JJ. 1988.** The phylogeny of the Artiodactyla. In: Benton MJ, ed. *The phylogeny and classification of the Tetrapods. Volume 2: Mammals, vol 35B Systematics Association Special Volume*. Oxford: Clarendon Press, 235–272.
- Gervais P. 1859.** *Zoologie et Paléontologie françaises (animaux vertébrés). Nouvelles recherches sur les animaux vertébrés dont on trouve les ossements enfouis dans le sol de la*

France et sur leur comparaison avec les espèces propres aux autres régions du globe. Paris: Arthur Bertrand.

Ginsburg L, Morales J, Soria D. 2001. Les Ruminantia (Artiodactyla, Mammalia) du Miocène des Bugti (Balouchistan, Pakistan). *Estudios Geologicos* **57**: 155–170.

Gomes Rodrigues H, Lihoreau F, Orliac M, Boisserie JR. 2020. Characters from the deciduous dentition and its interest for phylogenetic reconstruction in Hippopotamoidea (Cetartiodactyla: Mammalia). *Zoological Journal of the Linnean Society* **20**: 1–19.

Gradstein FM, Ogg JG, Schmitz MD. 2012. *The Geologic Time Scale 2012*. Amsterdam: Elsevier, 1144.

Gray JE. 1821. On the natural arrangement of vertebrate animals. *London Medical Repository* **15**: 296–310.

Grossman A, Calvo R, López-Antoñanzas R, Knoll F, Hartman G, Rabinovich R. 2019. First record of *Sivameryx* (Cetartiodactyla, Anthracotheriidae) from the lower Miocene of Israel highlights the importance of the Levantine Corridor as a dispersal route between Eurasia and Africa. *Journal of Vertebrate Paleontology* **39**: e1599901.

Hellmund M. 1991. Revision der europäischen Species der Gattung *Elomeryx* Marsh, 1894 (Anthracotheriidae, Artiodactyla, Mammalia) - odontologische Untersuchungen. *Palaeontographica* **220**: 1–101.

Holroyd PA, Lihoreau F, Gunnell GF, Miller ER. 2010. Anthracotheriidae. In: Werdelin L, Sanders WJ, eds. *Cenozoic mammals of Africa*. Berkeley: University of California Press, 843–851.

Kapur VV, Pickford M, Chauhan G, Thakkar MG. 2019. A Middle Miocene (~14 Ma) vertebrate assemblage from Palasava, Rapar Taluka, Kutch (Kachchh) District, Gujarat State, western India. *Historical Biology* **33**: 595–615.

Kostopoulos DS, Koufos GD, Christanis K. 2012. On some anthracotheriid (Artiodactyla, Mammalia) remains from northern Greece: comments on the palaeozoogeography and phylogeny of *Elomeryx*. *Swiss Journal of Palaeontology* **131**: 303–315.

Kumar K, Kad S. 2003. Early Miocene vertebrates from the Murree Group, northwest Himalaya, India: affinities and age implications. *Himalayan Geology* **24**: 29–53.

Leidy J. 1869. The extinct mammalian fauna of Dakota and Nebraska. *Journal of the Philadelphia Academy of Natural Sciences* **7**: 1–472.

Li ZC, Li YX, Zhang YX, Li WH, Xie K. 2016. Nanpoting fauna of the Lanzhou Basin and its environmental significance. *Science China Earth Sciences* **59**: 1258–1266.

Li C, Wang SQ, Yang Q. 2022. Discovery of a primitive *Gomphotherium* from the Early Miocene of northern China and its biochronology and palaeobiogeography significance. *Historical Biology*, 1–9.

Lihoreau F. 2003. *Systématique et paléoécologie des Anthracotheriidae [Artiodactyla; Suiformes] du Mio-Pliocène de l'Ancien Monde: implications paléobiogéographiques*. Unpublished Ph.D. thesis, Université de Poitiers, France.

- Lihoreau F, Ducrocq S. 2007.** Family Anthracotheriidae. In: Protero DR, Foss SE, eds. *The evolution of artiodactyls*. Baltimore: The John Hopkins University Press, 89–105.
- Lihoreau F, Blondel C, Barry J, Brunet M. 2004a.** A new species of the genus *Microbunodon* (Anthracotheriidae, Artiodactyla) from the Miocene of Pakistan: genus revision, phylogenetic relationships and palaeobiogeography. *Zoologica Scripta* **33**: 97–115.
- Lihoreau F, Barry J, Blondel C, Brunet M. 2004b.** A new species of Anthracotheriidae, *Merycopotamus medioximus* nov. sp. from the Late Miocene of the Potwar Plateau, Pakistan. *Comptes Rendus Palevol* **3**: 653–662.
- Lihoreau F, Boisserie JR, Viriot L, Coppens Y, Likius A, Mackaye HT, Tafforeau P, Vignaud P, Brunet M. 2006.** Anthracothere dental anatomy reveals a late Miocene Chad-Libyan bioprovince. *Proceedings of the National Academy of Sciences of the USA* **103**: 8763–8767.
- Lihoreau F, Barry J, Blondel C, Chaimanee Y, Jaeger JJ, Brunet M. 2007.** Anatomical revision of the genus *Merycopotamus* (Artiodactyla; Anthracotheriidae): its significance for late Miocene mammal dispersal in Asia. *Palaeontology* **50**: 503–524.
- Lihoreau F, Ducrocq S, Antoine PO, Vianey-Liaud M, Rafay S, Garcia G, Valentin X. 2009.** First complete skulls of *Elomeryx crispus* (Gervais, 1849) and of *Protaceratherium albigense* (Roman, 1912) from a new Oligocene locality near Moissac (SW France). *Journal of Vertebrate Paleontology* **29**: 242–253.
- Lihoreau F, Boisserie JR, Blondel C, Jacques L, Likius A, Mackaye HT, Vignaud P, Brunet M. 2014.** Description and palaeobiology of a new species of *Libycosaurus* (Cetartiodactyla, Anthracotheriidae) from the Late Miocene of Toros-Menalla, northern Chad. *Journal of Systematic Palaeontology* **12**: 761–798.
- Lihoreau F, Boisserie JR, Manthi FK, Ducrocq S. 2015.** Hippos stem from the longest sequence of terrestrial cetartiodactyl evolution in Africa. *Nature Communications* **6**: 6264.
- Lihoreau F, Alloing-Séguier L, Antoine PO, Boisserie JR, Marivaux L, Métais G, Welcomme JL. 2016.** Enamel microstructure defines a major Paleogene hippopotamoid clade: the Merycopotamini (Cetartiodactyla, Hippopotamoidea). *Historical Biology* **29**: 947–957.
- Lihoreau F, Essid EM, Khayati Ammar H, Marivaux L, Marzougui W, Tabuce R, Temani R, Vianey-Liaud M, Merzeraud G. 2019.** The *Libycosaurus* (Hippopotamoidea, Artiodactyla) intercontinental dispersal event at the early late Miocene revealed by new fossil remains from Kasserine area, Tunisia. *Historical Biology* **33**: 146–158.
- Lindsay EH, Flynn LJ, Cheema IU, Barry JC, Downing K, Rajpar AR, Raza SM. 2005.** Will Downs and the Zinda Pir Dome. *Palaeontologia Electronica* **8**: 1–19.
- Lydekker R. 1877.** Notices of new or rare mammals from the Siwaliks. *Records of the Geological Survey of India* **10**: 76–83.
- Lydekker R. 1878.** Notices of Siwalik mammals. *Records of the Geological Survey of India* **11**: 64–104.

- Lydekker R. 1882.** Note on some Siwalik and Narbada fossils. 7. Gigantic *Hyopotamus*. *Records of the Geological Survey of India* **15**: 107.
- Lydekker R. 1883.** Siwalik selenodont suina. *Memoirs of the Geological survey of India. Palaeontologica Indica* **10**: 143–177.
- Macdonald JR. 1956.** The North American Anthracotheres. *Journal of Paleontology* **30**: 615–645.
- MacInnes DG. 1951.** Miocene Anthracotheriidae from East Africa. *Fossil Mammals of Africa* **4**: 1–24.
- van der Made J. 1999.** Intercontinental relationship Europe-Africa and the Indian Subcontinent. In: Rösner GE, Heissig K, eds. *The Miocene land mammals of Europe*. Munich: Friedrich Pfeil, 457–472.
- Marivaux L, Welcomme JL, Antoine PO, Métais G, Baloch IM, Benammi M, Chaimanee Y, Ducrocq S, Jaeger JJ. 2001.** A fossil lemur from the Oligocene of Pakistan. *Science* **294**: 587–591.
- Marivaux L, Vianey-Liaud M, Welcomme JL, Jaeger JJ. 2002.** The role of Asia in the origin and diversification of hystricognathous rodents. *Zoologica Scripta* **31**: 225–239.
- Marivaux L, Antoine PO, Baqri SRH, Benammi M, Chaimanee Y, Crochet JY, De Franceschi D, Iqbal N, Jaeger JJ, Métais G, Roohi G, Welcomme JL. 2005.** Anthropoid primates from the Oligocene of Pakistan (Bugti Hills): Data on early anthropoid evolution and biogeography. *Proceedings of the National Academy of Sciences of the USA* **102**: 8436–8441.
- Marsh OC. 1872.** Preliminary description of new tertiary mammals, Parts I-IV. *American Journal of Science* **4**: 1–35.
- Marsh OC. 1894.** Miocene artiodactyls from the eastern *Miohippus* beds. *Journal of Science* **48**: 175–178.
- Métais G, Antoine PO, Baqri SRH, Crochet JY, De Franceschi D, Marivaux L, Welcomme JL. 2009.** Lithofacies, depositional environments, regional biostratigraphy and age of the Chitarwata Formation in the Bugti Hills, Balochistan, Pakistan. *Journal of Asian Earth Sciences* **34**: 154–167.
- Miller ER, Gunnell GF, Gawad MA, Hamdan M, El-Barkooky AN, Clementz MT, Hassan SM. 2014.** Anthracotheres from Wadi Moghra, early Miocene, Egypt. *Journal of Paleontology* **88**: 967–981.
- Montgelard C, Catzeflis FM, Douzery E. 1997.** Phylogenetic relationships of artiodactyls and cetaceans as deduced from the comparison of cytochrome b and 12S rRNA mitochondrial sequences. *Molecular Biology and Evolution* **14**: 550–559
- Nanda AC, Sehgal RK, Chauhan PR. 2017.** Siwalik-age faunas from the Himalayan Foreland Basin of South Asia. *Journal of Asian Earth Sciences* **162**: 54–68.
- Nikolov J. 1967.** Neue obereozäne Arten der Gattung *Elomeryx*. *Neues Jahrbuch für Geologie und Paläontologie Abhandlungen* **128**: 205–214.

- Orliac MJ, Antoine PO, Métais G, Marivaux L, Crochet JY, Welcomme JL, Baqri SRH, Roohi G. 2009.** *Listriodon guptai* Pilgrim, 1926 (Mammalia, Suidae) from the early Miocene of the Bugti Hills, Balochistan, Pakistan: New insights into early Listriodontinae evolution and biogeography. *Naturwissenschaften* **96**: 911–920.
- Orliac MJ, Antoine PO, Roohi G, Welcomme JL. 2010.** Suoidea (Mammalia, Cetartiodactyla) from the early Oligocene of the Bugti Hills, Balochistan, Pakistan. *Journal of Vertebrate Paleontology* **30**: 1300–1305.
- Orliac MJ, Antoine PO, Charruault AL, Hervet S, Prodeo F, Duranthon F. 2013.** Specialization for amphibiosis in *Brachyodus onoideus* (Artiodactyla, Hippopotamoidea) from the Early Miocene of France. *Swiss Journal of Geosciences* **106**: 265–278.
- Patnaik R, Prasad V. 2016.** Neogene climate, terrestrial mammals and flora of the Indian subcontinent. *Proceedings of the Indian National Science Academy* **82**: 605–615.
- Pickford M. 1987.** Révision des suiformes (Artiodactyla, Mammalia) de Bugti (Pakistan). *Annales de Paléontologie* **73**: 289–350.
- Pickford M. 1991.** Revision of the Neogene Anthracotheriidae of Africa. *The Geology of Libya* **4**: 1491–1525.
- Pickford M. 2009.** Metric variation in *Afromeryx* and *Libycosaurus* (Anthracotheriidae: Mammalia) and its utility for biochronology. *Revista Española de paleontología* **24**: 107–120.
- Pilgrim GE. 1907.** Description of some new Suidae from the Bugti Hills, Baluchistan. *Records of the Geological Survey of India* **36**: 45–56.
- Pilgrim GE. 1908.** The Tertiary and Post-tertiary Freshwater Deposits of Baluchistan and Sind: With Notices of New Vertebrate. *Records of the Geological Survey of India* **37**: 139–166.
- Pilgrim GE. 1912.** The vertebrate fauna of the Gaj series in the Bugti Hills and the Punjab. *Memoirs of the Geological Survey of India. Paleontologia Indica* **4**: 1–83.
- Prasad KN. 1964.** Miocene vertebrates from Cutch District, Gujrat, India. *Bulletin of the Geological Society of India* **1**: 9–12.
- Prasad KN. 1967.** Fossil mammals from Cutch District, Gujarat, India. *Quarterly Journal of the Geological, Mining and Metallurgical Society of India* **39**: 187–192.
- R Core Team. 2020.** *R: a language and environment for statistical computing*. Vienna: R Foundation for Statistical Computing. Available at: <https://www.R-project.org>. Accessed 8 September 2020.
- Rasmussen DT, Bown TM, Simons EL. 1992.** The Eocene-Oligocene transition in continental Africa. In: Prothero DR, Berggren WA, eds. *Eocene–Oligocene Climatic and Biotic Evolution*. Princeton: Princeton University Press, 548–567.
- Raza SM, Meyer GE. 1984.** Early Miocene geology and paleontology of the Bugti Hills. *Geological Survey of Pakistan* **11**: 43–63.

- Raza SM, Barry JC, Meyer GE, Martin L. 1984.** Preliminary report on the geology and vertebrate fauna of the Miocene Manchar Formation, Sind, Pakistan. *Journal of Vertebrate Paleontology*, **4**: 584-589
- Rincon AF, Bloch JI, MacFadden BJ, Jaramillo CA. 2013.** First Central American record of Anthracotheriidae (Mammalia, Bothriodontinae) from the early Miocene of Panama. *Journal of Vertebrate Paleontology* **33**: 421–433.
- Roddaz M, Said A, Guillot S, Antoine PO, Montel JM, Martin F, Darrozes J. 2011.** Provenance of Cenozoic sedimentary rocks from the Sulaiman fold and thrust belt, Pakistan: Implications for the palaeogeography of the Indus drainage system. *Journal of the Geological Society* **168**: 499–516.
- Rowan J, Adrian B, Grossman A. 2015.** The first skull of *Sivameryx africanus* (Anthracotheriidae, Bothriodontinae) from the early Miocene of East Africa. *Journal of Vertebrate Paleontology* **35**: e92830537–e92830541.
- Russell DE, Zhai RJ. 1987.** The Paleogene of Asia: mammals and stratigraphy. *Memoires du Museum National d'Histoire Naturelle* **52**: 1–490.
- Scherler L, Lihoreau F, Becker D. 2018.** To split or not to split *Anthracotherium*? A phylogeny of Anthracotheriinae (Cetartiodactyla: Hippopotamoidea) and its palaeobiogeographical implications. *Zoological Journal of the Linnean Society* **185**: 487–510.
- Scott WB. 1940.** The mammalian fauna of the White River Oligocene: part IV. Artiodactyla. *Transactions of the American Philosophical Society* **28**: 363–746.
- Sehgal RK, Bhandari A. 2014.** Miocene mammals from India: present status and future prospects. In: Tiwari, RP, ed. Indian Miocene: a geodynamic and chronological framework for palaeobiota, sedimentary environments and palaeoclimates. *Palaeontological Society of India Special Publication* **5**: 199–212.
- Speijer RP, Pälke H, Hollis CJ, Hooker JJ, Ogg JG. 2020.** The Paleogene Period. In: Gradstein FM, Ogg JG, Schmitz M, Ogg GM, eds. *Geologic Time Scale 2020*. Amsterdam: Elsevier, 1087–1140.
- Swofford DL. 2002.** *PAUP* Phylogenetic analysis using parsimony (* and other methods)* v.4. Sunderland: Sinauer.
- Thewissen JGM, Russell DE, Gingerich PD, Hussain ST. 1983.** A new dichobunid artiodactyl (Mammalia) from the Eocene of north-west Pakistan. *Proceedings of the Koninklijke Nederlandse Akademie van Wetenschappen* **86**: 153–180.
- Tsubamoto T, Zing-Maung MT, Egi N, Nishimura T, Taung-Htike, Takai M. 2011.** A new anthracotheriid artiodactyl from the Eocene Pondaung formation of Myanmar. *Vertebrata Palasiatica* **49**: 85–113.
- Viret J. 1961.** Artiodactyla. In: Piveteau J, ed. *Traité de Paléontologie VI*. Paris : Masson, 887–1021.
- Wang SQ. 2020.** The anthracotheres from northern Junggar Basin and their palaeoclimatic significance in relation to the Tibetan Plateau. *Palaeobiodiversity and Palaeoenvironments* **101**: 839–852.

Wang BY, Qiu ZX. 2004. Discovery of Early Oligocene Mammalian Fossils from Danghe Area, Gansu, China. *Vertebrata Palasiatica* **42**: 130–143.

Welcomme JL, Ginsburg L. 1997. Mise en évidence de l'Oligocène sur le territoire des Bugti (Balouchistan, Pakistan). *Comptes rendus de l'Académie des Sciences, Paris* **325**: 999–1004.

Welcomme JL, Antoine PO, Duranthon F, Mein P, Ginsburg L. 1997. Nouvelles découvertes de Vertébrés miocènes dans le synclinal de Dera Bugti (Balouchistan, Pakistan). *Comptes rendus de l'Académie des Sciences, Paris* **325**: 531–536.

Welcomme JL, Benammi M, Crochet JY, Marivaux L, Métais G, Antoine PO, Baloch I. 2001. Himalayan Forelands: Palaeontological evidence for Oligocene detrital deposits in the Bugti Hills (Balochistan, Pakistan). *Geological Magazine* **138**: 397–405.

SUPPORTING INFORMATION

Appendix S1. Synonymy list of *Parabrachyodus hyopotamoides* emended from Pickford (1987).

Signs: * designation of the type specimen; **v** material seen by the authors; **p** only part of the material in the reference can be attributed to the species, the rest being either not identified or belonging to another taxa; ? uncertain attribution due to the lack of description or the unavailability of the specimens; **no** assignment to the revised taxon is not valid but is indicated to support the exclusion of the concerned material; *date* in italics indicates that the taxon is only mentioned in the reference.

1882 « Upper and lower molars of a gigantic species of *Hyopotamus* »; Lydekker: 107.

* 1883a *Anthracotherium hyopotamoides* nov. sp.; Lydekker: 152-154, pl. 24, fig. 2; pl. 25, figs. 1, 3.

1883a *Hyopotamus giganteus* nov. sp.; Lydekker: 160-164, fig. 1; pl. 24, fig. 3; pl. 25, fig. 2.

? 1883a *Anthracotherium* sp.; Lydekker: 176, fig. 3.

1883b *Hyopotamus giganteus* Lydekker; Lydekker: 74.

1883b *Anthracotherium hyopotamoides* Lydekker; Lydekker: 74, 89.

1884 *Anthracotherium hyopotamoides* Lydekker; Teller: 61.

1885 *Anthracotherium hyopotamoides* Lydekker; Lydekker: 41.

1885 *Hyopotamus giganteus* Lydekker; Lydekker: 41.

? 1885 *Anthracotherium* sp.; Lydekker: 41.

1895 *Brachyodus giganteus* (Lydekker); Depéret: 407-408.

1899 *Brachyodus giganteus* (Lydekker); Andrews: 484.

1899 *Brachyodus hyopotamoides* (Lydekker); Andrews: 484.

1900 *Brachyodus giganteus* (Lydekker); Pavlow: 21.

1904 *Anthracotherium hyopotamoides* Lydekker; Trouessart: 650.

1904 *Brachyodus giganteus* (Lydekker); Trouessart: 651.

1907 *Anthracotherium hyopotamoides* Lydekker; Pilgrim: 46.

1907 *Brachyodus giganteus* (Lydekker); Pilgrim: 46.

no 1907 *Telmatodon bugtiensis* nov. sp.; Pilgrim: 45, pl. 12, figs. 4-5.

no 1908 *Brachyodus bugtiensis* (Pilgrim); Pilgrim: 151.

1908 *Brachyodus giganteus* (Lydekker); Pilgrim: 150.
1908 *Brachyodus hyopotamoides* (Lydekker); Pilgrim: 150-151.
1908 *Brachyodus giganteus* (Lydekker); Depéret: 161.
no 1910a *Brachyodus africanus* Andrews; Pilgrim: 68.
1910b *Brachyodus hyopotamoides* (Lydekker); Pilgrim: 201.
1910b *Brachyodus giganteus* (Lydekker); Pilgrim: 201.
no 1910b *Brachyodus africanus* Andrews; Pilgrim: 202.
1912 *Brachyodus giganteus* (Lydekker); Pilgrim: 49-57, pls. 15-18.
1912 *Brachyodus hyopotamoides* (Lydekker); Pilgrim: 57-59, pls. 19-21.
p 1912 *Brachyodus africanus* Andrews; Pilgrim: 59-62, pl. 22, figs. 2-3 (no figs. 1,5).
p 1912 *Telmatodon bugtiensis* Pilgrim; Pilgrim: pl. 24, figs. 2, 3b (no pl. 24, fig. 4), pl. 25, fig. 6.
1913 *Brachyodus giganteus* (Lydekker); Pilgrim: pl. 26.
? 1913 *Brachyodus* sp.; Pilgrim: 317.
p 1913 *Brachyodus africanus* Andrews; Pilgrim: 317, pl. 26.
p 1913 *Telmatodon bugtiensis* Pilgrim; Pilgrim: 317.
v 1913 *Brachyodus pilgrimi* nov. sp.; Forster-Cooper: 516-517, fig. 3.
v 1913 *Brachyodus* (?) *obtusus* nov. sp.; Forster-Cooper: 520-521, fig. 7.
v 1915 *Parabrachyodus obtusus* (Forster-Cooper); Forster-Cooper: 404-406, figs. 1-2.
v 1924 *Brachyodus pilgrimi* Forster-Cooper; Forster-Cooper: 27, pl. 1, fig. 2.
v 1924 *Brachyodus gandoiensis* nov. sp.; Forster-Cooper: 27-28, pl. 1, figs. 3-6.
1924 *Brachyodus giganteus* (Lydekker); Forster-Cooper: 28-29, pl. 2, fig. 1.
1924 *Brachyodus hyopotamoides* (Lydekker); Forster-Cooper: 29.
v 1924 *Brachyodus platydens* nov. sp.; Forster-Cooper: 29-31, pl. 2, figs. 2-3.
p 1924 *Brachyodus africanus* Andrews; Forster-Cooper: 31, pl. 3, fig. 2 (no pl. 3, fig. 1).
v 1924 *Brachyodus orientalis* nov. sp.; Forster-Cooper: 32, pl. 3, figs. 3-4.
v 1924 *Brachyodus indicus* nov. sp.; Forster-Cooper: 32, pl. 4, fig. 1.
v 1924 *Parabrachyodus obtusus* (Forster-Cooper); Forster-Cooper: 33-34, fig. 22.
v 1924 *Brachyodus* cf. *gandoiensis*; Forster-Cooper: 35-37, figs. 24-26.
v 1924 *Brachyodus* sp.; Forster-Cooper: 35-37, figs. 27-33: 39-40, figs. 36-39, fig. 41.
v 1924 *Brachyodus* cf. *indicus*; Forster-Cooper: 40, fig. 40.
v 1924 *Gonotelma major* sp. nov.; Forster-Cooper: 49-50, pl. 5, fig. 1.

p 1929 *Brachyodus* « *africanus* » Andrews; Matthew: 463.
1929 *Brachyodus hyopotamoides* (Lydekker); Matthew: 463.
1929 *Brachyodus giganteus* (Lydekker); Matthew: 463.
p 1929 *Telmatodon* Pilgrim; Matthew: 463.
p 1945 *Brachyodus* Depéret; Simpson: 147.
p 1945 *Telmatodon* Pilgrim; Simpson: 147.
v 1945 *Parabrachyodus* Forster-Cooper; Simpson: 148;
1961 *Parabrachyodus* Forster-Cooper; Viret: 948-949;
p 1961 *Telmatodon* Pilgrim; Viret: 949;
p 1961 *Brachyodus* Depéret; Takai: 255.
v 1961 *Parabrachyodus* Forster-Cooper; Takai: 255.
p 1961 *Telmatodon* Pilgrim; Takai: 255.
1964 *Brachyodus manchharensis* nov. sp.; Prasad: 9-12;
no 1966 *Elomeryx* cf. *borbonicoideus*; Gabounia: 860, 864, figs. 9d-e;
1967 *Brachyodus manchharensis* Prasad; Prasad: 188-190, figs. 1-2;
1981 *Parabrachyodus* Forster-Cooper; Dineur: 161;
v 1984 *Brachyodus pilgrimi* Forster-Cooper; Raza & Meyer: 52;
1984 *Brachyodus giganteus* (Lydekker); Raza & Meyer: 52;
v 1984 *Brachyodus gandoiensis* Forster-Cooper; Raza & Meyer: 52;
1984 *Brachyodus hyopotamoides* (Lydekker); Raza & Meyer: 52;
v 1984 *Brachyodus platydens* Forster-Cooper; Raza & Meyer: 52;
p 1984 *Brachyodus africanus* Andrews; Raza & Meyer: 52;
v 1984 *Brachyodus indicus* Forster-Cooper; Raza & Meyer: 52;
v 1984 *Brachyodus orientalis* Forster-Cooper; Raza & Meyer: 52;
v 1984 *Parabrachyodus obtusus* (Forster-Cooper); Raza & Meyer: 52;
pv 1984 *Telmatodon bugtiensis* Pilgrim; Raza & Meyer: 52;
v 1984 *Gonotelma major* Forster-Cooper; Raza & Meyer: 53.
1984 *Brachyodus giganteus* (Lydekker); Raza *et al.*, tab.2.
v 1984 *Parabrachyodus obtusus* (Forster-Cooper); Raza *et al.*, tab.2.
? 1984 cf. *Brachyodus* sp.; Raza *et al.*, tab.2, fig. 4.
pv 1987 *Anthracotherium bugtiense* Pilgrim; Pickford: 309-311.

p 1987 *Parabrachyodus hyopotamoides* (Lydekker); Pickford: 316-319.
pv 1987 *Telmatodon bugtiensis* Pilgrim; Pickford: 320-321.
pv 1987 *Telmatodon orientale* Forster-Cooper; Pickford: 322-323.
no 1987 *Parabrachyodus cf. borbonicoides*; Russell & Zhai: 392.
1997 *Parabrachyodus hyopotamoides* (Lydekker); Welcomme & Ginsburg, tab.1 (no p.1002).
1997 *Parabrachyodus hyopotamoides* (Lydekker); Welcomme *et al.*: 533, 535.
no 1999 *Parabrachyodus* Forster-Cooper; Lucas & Emry: 164.
p 2001 *Parabrachyodus hyopotamoides* (Lydekker); Welcomme *et al.*, fig. 4.
2003 *Parabrachyodus hyopotamoides* (Lydekker); Antunes & Ginsburg: 162.
no 2004 *Parabrachyodus* sp.; Wang & Qiu: 137-138, 142, fig. 5A.
? 2005 *Parabrachyodus* sp.; Lindsay *et al.*: tab.1.
pv 2005 *Parabrachyodus hyopotamoides* (Lydekker); Lindsay *et al.*: 16, tab.1.
no 2006 *Parabrachyodus* Forster-Cooper; Ducrocq & Lihoreau: 886.
2007 *Parabrachyodus* Forster-Cooper; Lihoreau & Ducrocq: 97.
no 2008 *Parabrachyodus* sp.; Wang *et al.*: fig. 8.
? 2009 *Parabrachyodus hyopotamoides* (Lydekker); Métais *et al.*: 162, fig. 5.
? 2009 *Parabrachyodus cf. hyopotamoides*; Métais *et al.*: 163, fig. 5.
2010 *Parabrachyodus hyopotamoides* (Lydekker); Bhandari *et al.*: 76, fig. 7A.
? 2010 *Parabrachyodus* sp.; Bhandari *et al.*: 91-92, tab.2.
v 2010 *Brachyodus pilgrimi* Forster-Cooper; Malkani: tab.2.
2010 *Brachyodus giganteus* (Lydekker); Malkani: 52, tab.2.
v 2010 *Brachyodus gandoiensis* Forster-Cooper; Malkani: tab.2.
2010 *Brachyodus hyopotamoides* (Lydekker); Malkani: tab.2.
v 2010 *Brachyodus platydens* Forster-Cooper; Malkani: tab.2.
p 2010 *Brachyodus africanus* Andrews; Malkani: 52, tab.2.
v 2010 *Brachyodus indicus* Forster-Cooper; Malkani: tab.2.
v 2010 *Brachyodus orientalis* Forster-Cooper; Malkani: tab.2.
v 2010 *Parabrachyodus obtusus* (Forster-Cooper); Malkani: tab.2.
pv 2010 *Telmatodon bugtiensis* Pilgrim; Malkani: tab.2.
v 2010 *Gonotelma major* Forster-Cooper; Malkani: tab.2.
no 2011 *Parabrachyodus* sp.; Xie & Zhao: 598.

no 2011 *Parabrachyodus* Forster-Cooper; Xie & Zhao: 599.
? 2013 *Parabrachyodus* Forster-Cooper; Antoine *et al.*: fig. 3.
? 2013 *Parabrachyodus* sp.; Antoine *et al.*: tab.1, fig. 4.
pv 2013 *Parabrachyodus hyopotamoides* (Lydekker); Antoine *et al.*: tabs.1-2, fig. 4.
? 2013 *Parabrachyodus* cf. *hyopotamoides*; Antoine *et al.*: 413.
2014 *Parabrachyodus hyopotamoides* (Lydekker); Sehgal & Bhandari: 201.
2016 *Parabrachyodus hyopotamoides* (Lydekker); Patnaik & Prasad: 607.
no 2016 *Parabrachyodus* sp.; Li *et al.*: tab.1.
p 2016 *Parabrachyodus hyopotamoides* (Lydekker); Lihoreau *et al.*: fig. 1.
p 2017 *Parabrachyodus hyopotamoides* (Lydekker); Nanda *et al.*: tabs. 5,7.
? 2020 *Parabrachyodus* Forster-Cooper; Wang: 12, fig. 6B-C.
no 2020 *Parabrachyodus* sp.; Wang: 10.
2021 *Parabrachyodus hyopotamoides* (Lydekker); Bhandari *et al.*: 1.
no 2022 *Parabrachyodus* Forster-Cooper; Li *et al.*: 7.

Supplementary references for Appendix S1:

Andrews, C. W. (1899). Fossil Mammalia from Egypt, Part I. *Geol. Mag.*, 6, 481-484.

Antoine, P. O., Metais, G., Orliac, M. J., Crochet, J. Y., Flynn, L. J., Marivaux, L., ... & Welcomme, J. L. (2013). Mammalian Neogene biostratigraphy of the Sulaiman province, Pakistan. In *Fossil mammals of Asia* (pp. 400-422). Columbia University Press.

Antunes, M. T., & Ginsburg, L. (2003). The last Anthracothere *Brachyodus onoideus* (Mammalia, Artiodactyla) from westernmost Europe and its extinction. *Ciências da Terra/Earth Sciences Journal*, 15, 161-172.

Bhandari, A., Mohabey, D. M., Bajpai, S., Tiwari, B. N., & Pickford, M. (2010). Early Miocene mammals from central Kutch (Gujarat), Western India: Implications for geochronology, biogeography, eustacy and intercontinental dispersals. *Neues Jahrbuch für Geologie und Paläontologie-Abhandlungen*, 256(1), 69-97.

Bhandari, A., Bajpai, S., Flynn, L. J., Tiwari, B. N., & Mandal, N. (2021). First Miocene rodents from Kutch, western India. *Historical Biology*, 33(12), 3471-3479.

- Depéret, C. (1895) - Über die Fauna von miozänen Wilberthieren aus der ersten Mediterranstufe von Eggenburg. *Sitzungsberichten Kaiserliche Akademie Wissenschaften Wien*, 104(1), 395-416.
- Depéret, C. (1908). L'histoire géologique et phylogénie des Anthracothéridés. *C.R. Acad. Sci. Paris*, Séanc. 27 janv., 158-162.
- Dineur, H. (1981). Le genre *Brachyodus*, Anthracotheriidae (Artiodactyla, Mammalia) du Miocène inférieur d'Europe et d'Afrique. Thèse 3ème Cycle, Université Pierre et Marie Curie, Paris VI.
- Ducrocq, S., & Lihoreau, F. (2006). The occurrence of bothriodontines (Artiodactyla, Mammalia) in the Paleogene of Asia with special reference to Elomeryx: paleobiogeographical implications. *Journal of Asian Earth Sciences*, 27(6), 885-891.
- Forster-Cooper, C. (1913). LXIV.—New anthracotheres and allied forms from Baluchistan.—Preliminary notice. *Annals and Magazine of Natural History*, 12, 514-522.
- Forster-Cooper, C. (1915). XLIX.—New genera and species of mammals from the Miocene deposits of Baluchistan.—Preliminary notice. *Journal of Natural History*, 16, 404-419.
- Forster-Cooper, C. (1924). The Anthracotheriidae of the Dera Bugti Deposits in Baluchistan. *Mem. Geol. Surv. India Palaeontol. Indica*, 8(2), 1-59.
- Gabounia, L. (1966). Sur les mammifères oligocènes du Caucase. *Bulletin de la Société géologique de France*, 7, 857-869
- Li, Z. C., Li, Y. X., Zhang, Y. X., Li, W. H., & Xie, K. (2016). Nanpoping fauna of the Lanzhou Basin and its environmental significance. *Science China Earth Sciences*, 59(6), 1258-1266.
- Li, C., Wang, S. Q., & Yang, Q. (2022). Discovery of a primitive *Gomphotherium* from the Early Miocene of northern China and its biochronology and palaeobiogeography significance. *Historical Biology*, 1-9.
- Lihoreau, F., & Ducrocq, S. (2007). Family Anthracotheriidae. In D. R. Prothero & S. E. Foss (Eds.) *The evolution of artiodactyls* (p. 89– 105). Baltimore: The Johns Hopkins University Press.
- Lihoreau, F., Alloing-Séguier, L., Antoine, P. O., Boisserie, J. R., Marivaux, L., Métais, G., & Welcomme, J. L. (2016). Enamel microstructure defines a major Paleogene hippopotamoid clade: the Merycopotamini (Cetartiodactyla, Hippopotamoidea). *Historical Biology*, 29(7), 947-957.
- Lindsay, E. H., L. J. Flynn, I. U. Cheema, J. C. Barry, K. F. Downing, A. R. Rajpar, and S. M. Raza. 2005. Will Downs and the Zinda Pir Dome. *Paleontologia Electronica*, 8, 1-19.
- Lucas, S. G., & Emry, R. J. (1999). Taxonomy and biochronological significance of *Paraentelodon*, a giant entelodont (Mammalia, Artiodactyla) from the Late Oligocene of Eurasia. *Journal of Vertebrate Paleontology*, 19, 160-168.
- Lydekker, R. (1883). Siwalik Selenodont Suina. *Mem. Geol. Surv. India Paleontol. Indica*, 10

- Lydekker, R. (1883). Synopsis of the fossil Vertebrata of India. *Rec. Geol. Surv. India*, 16, 61-93.
- Lydekker, R. (1885). *Catalogue of Siwalik Vertebrates in the Indian Museum*, Calcutta, Calcutta.
- Malkani, M. S. (2010). Updated stratigraphy and mineral potential of Sulaiman basin, Pakistan. *Sindh University Research Journal (Science Series)*, 42(2), 39-66.
- Métais, G., Antoine, P. O., Baqri, S. H., Crochet, J. Y., De Franceschi, D., Marivaux, L., & Welcomme, J. L. (2009). Lithofacies, depositional environments, regional biostratigraphy and age of the Chitarwata Formation in the Bugti Hills, Balochistan, Pakistan. *Journal of Asian Earth Sciences*, 34(2), 154-167.
- Matthew, W. D. (1929). Critical observations upon Siwalik Mammals. *B. Am. Mus. Nat. Hist.*, 56(7), 435–560.
- Nanda, A. C., Sehgal, R. K., & Chauhan, P. R. (2017). Siwalik-age faunas from the Himalayan foreland Basin of South Asia. *Journal of Asian Earth Sciences*, 162, 54-68.
- Patnaik, R., & Prasad, V. (2016). Neogene climate, terrestrial mammals and flora of the Indian Subcontinent. In *Proc. Indian Nat. Sci. Acad*, 82, 605-615.
- Pavlow, M. (1900). Etudes sur l'histoire paléontologique des ongulés : VII. Artiodactyles anciens. *Bull. Soc. Natur. Moscou*, 13, 1-62.
- Pickford, M. (1987). Révision des suiformes (Artiodactyla, Mammalia) de Bugti (Pakistan). *Annales de Paléontologie*, 73, 289– 350.
- Pilgrim, G. E. (1907). Description of some new Suidae from the Bugti Hills, Baluchistan. *Rec. Geol. Surv. India*, 36, 45-56.
- Pilgrim, G. E. (1908). The Tertiary and Post-tertiary Freshwater Deposits of Baluchistan and Sind: With Notices of New Vertebrate. *Rec. Geol. Surv. India*, 37, 139-166
- Pilgrim, G. E. (1910a). Notices of new mammalian genera and species from the Tertiaries of India. *Rec. Geol. Surv. India*, 40, 63-71.
- Pilgrim, G. E. (1910b). Preliminary note on a revised classification of the Tertiary freshwater deposits of India. *Rec. Geol. Surv. India*, 40, 185-205.
- Pilgrim, G. E. (1912). The vertebrate fauna of the Gaj Series in the Bugti Hills and Punjab. *Mem. Geol. Surv. India Palaeont. Indica*, 4(2), 1-83.
- Pilgrim, G. E. (1913). The correlation of the Siwalik with mammal horizons of Europe. *Rec. Geol. Surv. India*, 43, 264-326.
- Prasad, K. N. (1964). Miocene vertebrates from Cutch District, Gujrat, India. *Bull. Geol. Soc. India*, 1(2), 9-12.

- Prasad, K. N. (1967). Fossil Mammals of Cutch District Gujarat. *India. Quarterly Journal of the Geological, Mineralogical and Metallurgical Society of India*, 39(3), 187-192.
- Raza, S. M., & Meyer, G. E. (1984). Early Miocene geology and paleontology of the Bugti Hills. *Geological Survey of Pakistan*, 11, 43-63.
- Raza, S. M., Barry, J. C., Meyer, G. E., & Martin, L. (1984). Preliminary report on the geology and vertebrate fauna of the Miocene Manchar Formation, Sind, Pakistan. *Journal of Vertebrate Paleontology*, 4(4), 584-599.
- Russell, D.E., Zhai, R. (1987). The Paleogene of Asia: mammals and stratigraphy. *Mémoires du Muséum National d'Histoire Naturelle, Ser. C, Sciences de la Terre*, 52, 1–488
- Sehgal, R., & Bhandari, A. (2014). Miocene mammals from India: present status and prospects. *Palaeontological Society of India Special Publication*, 5, 199-212.
- Simpson, G. G. (1945). The principles of classification and a classification of mammals. *Bull. Amer. Museum Nat. History*, 85.
- Takai, F. (1961). A new anthracothere from the Shiramizu Group in the Joban Coal-Field, Japan, with notes on its geological age. *Proceedings of the Japan Academy*, 37(5), 255-260.
- Teller, F. (1884). Neue Anthracotherienreste aus Sudsteiermark und Dalmatien. *Beitr. Palaeontol. Osterr-Ungarns u.d. orientis*, 4(1), 45-133.
- Trouessart, E. (1904). *Catalogus mammalium tam viventium quam fossilium Quinquennale supplementum*. Friedlander, Berlin.
- Viret, J. (1961). Artiodactyla. In *Traité de Palaeontologie VI* (ed. J. Piveteau), pp. 887–1084. Masson, Paris.
- Wang, B., & Qiu, Z. (2004). Discovery of early Oligocene mammalian fossils from Danghe area, Gansu, China. *Vertebrata Pal Asiatica*, 42(2), 130-143.
- Wang, S. Q. (2020). The anthracotheres from northern Junggar Basin and their palaeoclimatic significance in relation to the Tibetan Plateau. *Palaeobiodiversity and Palaeoenvironments*, 1-14.
- Wang, X., Wang B.-Y., Qiu Z.-X. (2008). Early explorations of Tabenbuluk region (western Gansu Province) by Birger Bohlin – reconciling classic vertebrate fossil localities with modern stratigraphy. *Vertebrata PalAsiatica*, 46: 1–19.
- Welcomme, J. L., & Ginsburg, L. (1997). Mise en évidence de l'Oligocène sur le territoire des Bugti (Balouchistan, Pakistan). *Comptes Rendus de l'Académie des Sciences-Series IIA-Earth and Planetary Science*, 325(12), 999-1004.

Welcomme, J. L., Antoine, P. O., Duranthon, F., Mein, P., & Ginsburg, L. (1997). Nouvelles découvertes de Vertébrés miocènes dans le synclinal de Dera Bugti (Balouchistan, Pakistan). *Comptes Rendus de l'Académie des Sciences-Series IIA-Earth and Planetary Science*, 325(7), 531-536.

Welcomme, J. L., Benammi, M., Crochet, J. Y., Marivaux, L., Métais, G., Antoine, P. O., & Baloch, I. (2001). Himalayan Forelands: palaeontological evidence for Oligocene detrital deposits in the Bugti Hills (Balochistan, Pakistan). *Geological Magazine*, 138(4), 397-405.

Xi, G., & Zhao, D. (2011). Cenozoic climate and environmental change with evolution of mammalian fauna in Gansu Province. *Quaternary Sciences*, 31(4), 597-607.

Appendix S2. Descriptions of the taxa added to the matrix of Gomes Rodrigues *et al.* (2020).

Bothriodontinae Scott, 1940

Parabrachyodus hyopotamoides (Lydekker), 1883

Temporal and geographical distribution : early Miocene, Indian sub-continent.

Origin and nature of the coded material : Samane Nala 4 and 5, and Tobah, Bugti Hills, Pakistan (housed in the University of Montpellier), and hypodigm (this work) from Lundo Chur, Dera Bugti, Kumbi and Bugti, Bugti Hills (housed in the Natural History Museum, London).

References : Pickford (1987), this work.

Telmatodon bugtiensis Pilgrim, 1907

Temporal and geographical distribution : early Miocene, Indian sub-continent.

Origin and nature of the coded material : Kumbi and Lundo Chur, Bugti Hills, Pakistan. M9570 (left M3/), M9571 (left M/3), and M12728 (left M/3) (housed in the Natural History Museum, London).

Reference : Pickford (1987).

Telmatodon orientalis Forster-Cooper, 1924

Temporal and geographical distribution : early Miocene, Indian sub-continent.

Origin and nature of the coded material : Dera Bugti and Lundo Chur, Bugti Hills, Pakistan. M12040 (left M3/), M12041 (right P4/-M3/), M12747 (right M/3) (housed in the Natural History Museum, London).

Reference : Pickford (1987).

Gonotelma shahbazi Pilgrim, 1908

Temporal and geographical distribution : early Miocene, Indian sub-continent.

Origin and nature of the coded material : Samane Nala 4, Bugti Hills, Pakistan. UM-SAM4-010 (right M3/) (housed in the University of Montpellier). Kumbi and Lundo Chur, Bugti Hills, Pakistan. M11078 (left M/2-M/3), M12737 (left M/2-M/3), M12745 (cranium with right M3/ and left M1/-M3/) (housed in the Natural History Museum, London).

Reference : Pickford (1987).

Elomeryx armatus Marsh, 1894

Temporal and geographical distribution : early Oligocene, North America.

Origin and nature of the coded material : coding based on the illustrations of references.

References : Macdonald (1956), Scott (1940).

Bakalovia spp.

Temporal and geographical distribution : late Eocene, Europe and Asia (Vietnam).

Origin and nature of the coded material : include *Bakalovia orientalis* Böhme *et al.*, 2013 ; *B. palaeopontica* (Nikolov), 1967 ; and *B. astica* (Nikolov), 1967. Coding based on the illustrations of references.

References : Böhme *et al.* (2013), Hellmund (1991).

Supplementary references for Appendix S2:

Böhme, M., Aiglstorfer, M., Antoine, P. O., Appel, E., Havlik, P., Métais, G., Phuc, L. T., Schneider, S., Setzer, F., Tappert, R., Tran, D. N., Uhl, D., & Prieto, J. (2013). Na Duong (northern Vietnam) - An exceptional window into Eocene ecosystems from Southeast Asia. *Zitteliana Reihe A: Mitteilungen Der Bayerischen Staatssammlung Fur Palaontologie Und Geologie*, 53, 121–167.

Ducrocq, S., & Lihoreau, F. (2006). The occurrence of bothriodontines (Artiodactyla, Mammalia) in the Paleogene of Asia with special reference to *Elomeryx*: Paleobiogeographical implications. *Journal of Asian Earth Sciences*, 27(6), 885–891.

Ducrocq, S. (2020). Taxonomic revision of *Anthracokeryx thailandicus* Ducrocq, 1999 (Anthracotheriidae, Microbunodontinae) from the Upper Eocene of Thailand. *Vertebrata Palasiatica*, 1930.

Forster-Cooper, C. (1924). The Anthracotheriidae of the Dera Bugti Deposits in Baluchistan. *Mem. Geol. Surv. India Palaeontol. Indica*, 8(2), 1-59.

Gomes Rodrigues, H., Lihoreau, F., Orliac, M., & Boisserie, J.-R. (2020). Characters from the deciduous dentition and its interest for phylogenetic reconstruction in Hippopotamoidea (Cetartiodactyla: Mammalia). *Zoological Journal of the Linnean Society*, 1–19.

Hellmund, M. (1991). Revision der europäischen Species der Gattung *Elomeryx* Marsh, 1894 (Anthracotheriidae, Artiodactyla, Mammalia) - odontologische Untersuchungen. *Palaeontographica*, 220, 1–101.

Lydekker, R. (1883). Siwalik Selenodont Suina. *Mem. Geol. Surv. India Paleontol. Indica*, 10, 143-177.

Macdonald, J. R. (1956). The North American Anthracotheres. *Journal of Paleontology*, 30(3), 615–645.

Marsh, O. C. (1894). Miocene artiodactyls from the eastern Miohippus beds. *Journal of Science*, 48, 175–178.

Nikolov, I. (1967). Neue obereozäne Arten der Gattung *Elomeryx*. *Neues Jahrbuch Für Geologie Und Paläontologie Abhandlung*, 128, 205–214.

Pickford, M. (1987). Révision des suiformes (Artiodactyla, Mammalia) de Bugti (Pakistan). *Annales de Paléontologie*, 73, 289– 350.

Pilgrim, G. E. (1907). Description of some new Suidae from the Bugti Hills, Baluchistan. *Rec. Geol. Surv. India*, 36, 45-56.

Pilgrim, G. E. (1908). The Tertiary and Post-tertiary Freshwater Deposits of Baluchistan and Sind: With Notices of New Vertebrate. *Rec. Geol. Surv. India*, 37, 139-166

Scott, W. B. (1940). The mammalian fauna of the White River Oligocene: part IV. Artiodactyla. *Transactions of the American Philosophical Society*, 28, 363–746.

Appendix S3. Definitions of the new characters (A) and list of the 224 characters used (B)

A. Definitions of the characters added to the matrix of Gomes Rodrigues *et al.* (2020):

83) M/3 hypoconulid in line with labial cuspids: yes (0), no (1).

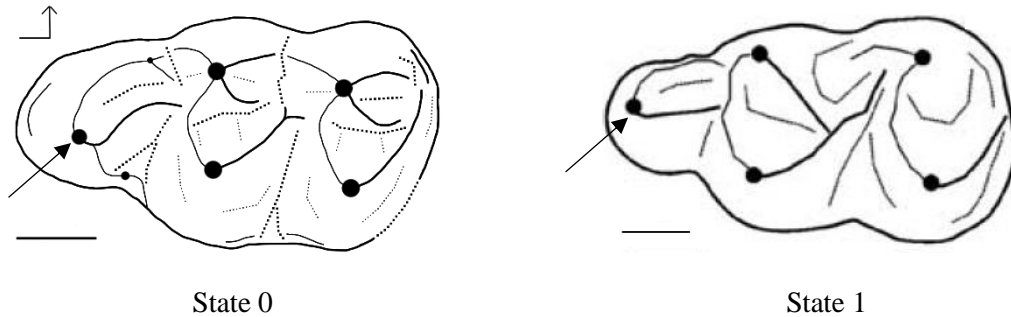


Figure 1. States 0 and 1 for the character 83, illustrated on the occlusal views of the right M/3 of *Parabrachyodus hyopotamoides* (0) and *Brachyodus onoideus* (1). Drawings of *B. onoideus* modified from Ducrocq & Lihoreau (2006). Scale bars equal 10 mm.

117) Postectoprotocrista reaching the lingual margin of the M3/: no (0), yes (1).

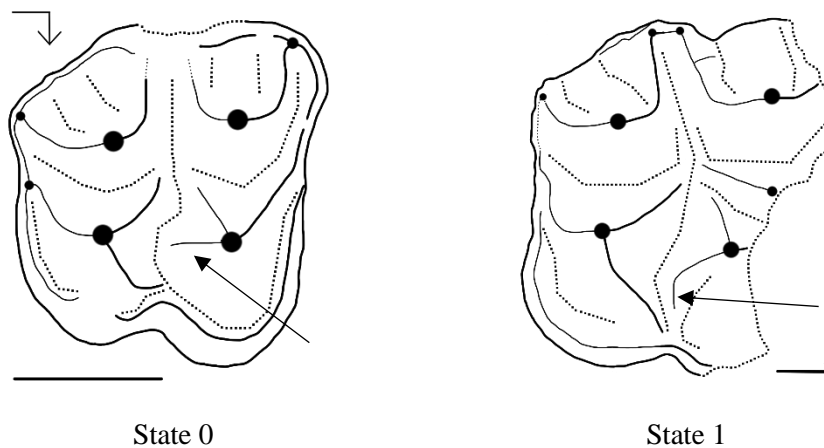


Figure 2. States 0 and 1 for the character 117, illustrated on the occlusal views of the right M3/ of *Gonotelma shahbazi* (0) and *P. hyopotamoides* (1). Scale bars equal 10 mm.

152) Angle between the slope of the metaconule and the dental collet of M3/: less than or equal to 40° (0), between 40 and 45° (1), greater than or equal to 45° (2).

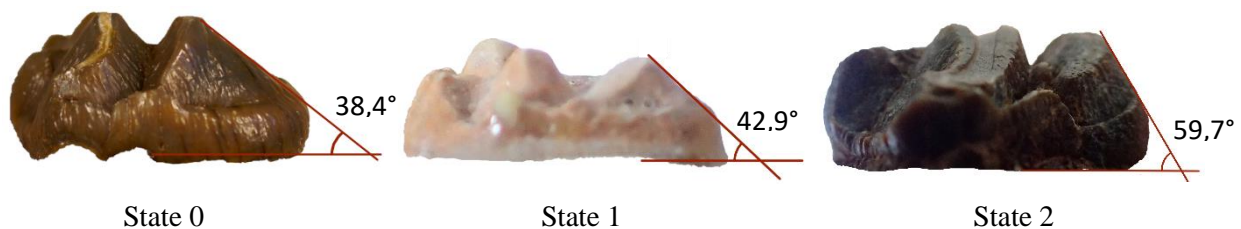


Figure 3. States 0 to 2 for the character 152, illustrated on distal views of M3/ (not to scale) of *Telmatodon orientalis* (0), *Microbunodon* (1) and *Sivameryx palaeindicus* (2).

B. List of the characters used in our phylogenetic analysis (modified from Gomes Rodrigues *et al.*, 2020)

- | | | |
|---|---|---|
| <p>1. Number of lower incisors:
 0. three
 1. two
 2. one</p> | <p>2. Lower incisor morphology:
 0. not caniniform
 1. at least one caniniform lower incisor</p> | <p>2. two, one mesial and one distal
 3. one mesial</p> |
| <p>3. Relative dimensions of lower incisors:
 0. all of equal size
 1. one or two more developed</p> | <p>4. Most developed incisor:
 0. i2
 1. i3
 2. i1</p> | <p>11. Wear on lower canine:
 0. distal wear facet contact with canine
 1. mesial wear facet contact with I3</p> |
| <p>5. Transverse section of lower incisors crowns:
 0. strongly irregular
 1. about rounded</p> | <p>6. Lower incisor cervix morphology :
 0. no deep indentation
 1. indented cervix, indentation as long as the root diameter on the cervix
 2. deep indentation longer than the root diameter at cervix</p> | <p>12. Groove on labial side of lower canine:
 0. no
 1. yes</p> |
| <p>7. Crown of lower i1:
 0. straight
 1. spatulate, with convex mesial and distal border</p> | <p>8. Presence of a median lingual pillar (lingual rib) on lower i1:
 0. yes
 1. no</p> | <p>13. Groove on lingual side of lower canine:
 0. no
 1. yes</p> |
| <p>9. Lower canine cross section at cervix:
 0. subcircular
 1. elliptical</p> | <p>10. Cristids on lower canine enamel caps:
 0. none
 1. one distal</p> | <p>14. Lower canine in male:
 0. fang-like
 1. premolariform
 2. incisiform</p> |
| | | <p>15. Crown of lower canine in male:
 0. small near premolar size
 1. at least twice the premolar size
 2. prolonged growth to ever-growing</p> |
| | | <p>16. P/1 roots:
 0. one
 1. two</p> |
| | | <p>17. P/1 caniniform :
 0. No
 1. Yes</p> |
| | | <p>18. Paraconid on lower premolars:
 0. no
 1. yes</p> |
| | | <p>19. Accessory cusp on the preprotocristid of all lower premolars:
 0. none
 1. at least one
 2. at least two</p> |
| | | <p>20. Elongated p3:
 0. no (shorter or equal than m1 length)
 1. yes (longer than m1 length)</p> |

21. **Three lobed p3:**
 0. no
 1. yes
22. **Orientation of postprotocrisid on p3:**
 0. distal
 1. distolingual
 2. distolabial
23. **High cingulid on labial face of p3:**
 0. no
 1. yes
24. **Endoprotocrisid on p3:**
 0. no
 1. yes
25. **Entoconid on p3:**
 0. never
 1. at least on some specimens
26. **p3 hypoconid:**
 0. no
 1. yes
27. **Preprotocrisid mesiolingually curved on p3:**
 0. no
 1. yes
28. **Mesial accessory cusp on preprotocrisid on p3:**
 0. simple slope
 1. Shoulder like structure on lateral view
 2. adorned with accessory cusp
29. **Lingual contour at cervix of p4 in occlusal view:**
 0. convex to straight
 1. concave
30. **Labial wall on p3 or p4:**
 0. convex
 1. concave
31. **Change in the orientation of the preprotocrisid mesially to the junction of accessory mesiolingual crest on lower premolars:**
 0. no
 1. yes
32. **Orientation of the endoprotocrisid on p4:**
 0. absent
1. separated from postprotocrisid at the protoconid apex and then strait and distolingual
 2. fused with postprotocrisid in part and then curved mesiolingually
33. **Distolingual cingulid on p4 in lingual view:**
 0. forming a continuous wall lingually until the distostylid
 1. reaching the level of the distal basin and keeping be shallow until the distostylid
 2. reaching the level of distal basin and then being high when joining the distostylid (distolingual notch of cingulid)
34. **Presence of a preentocrisid on p3 and/or on p4:**
 0. no
 1. yes
35. **Mesiolingual secondary cristid on p4 (cristid connecting lingual margin and preprotocrisid):**
 0. no
 1. yes
36. **Labial cingulid form a V (indentated) on p4 before to reach the distal cingulid:**
 0. no
 1. yes
37. **Marked postprotofossid on p4:**
 0. absent
 1. present
38. **Postectoprotocrisid on p4:**
 0. no
 1. yes
39. **Hypoconid on p4:**
 0. no
 1. yes (even incipient)
40. **Ectoprotofossid on p4:**
 0. absent
 1. frequent
41. **Postprotocrisid position on p4 (in regard of a mesiodistal midline):**
 0. median or labial
 1. lingual
42. **Endoprotofossid on p4:**

0. reaches lingual border
1. reaches lingual cingulid wall
- 43. Postentocristid on p4:**
0. no
1. short
2. long that reaches cingulid distally
- 44. Preprotocristid direction on p4:**
0. mesiolingual (but can be moderately curved)
1. lingual then mesial
2. mesial then lingual
- 45. Entostylid on p4:**
0. no
1. yes
2. continuous junction with cingulid without clear apice
- 46. Metaconid on p4:**
0. no
1. yes (indeed an entostylid surrounded by cingulid and not formed by cingulid)
- 47. Premetacristid on lower molars:**
0. strong
1. reduced or missing
- 48. Paraconid on lower molars, almost on unworn specimens:**
0. yes
1. no
- 49. Lower molar trigonid:**
0. equal in height with talonid
1. higher than talonid
- 50. Connection between premetacristid and preprotocristid on lower molars:**
0. yes
1. no
- 51. Postectoprotocristid on lower molars:**
0. absent
1. reduced in the valley to fully developed at least on m1
- 52. Postprotofossid on lower molars at least on m3:**
0. no
1. yes
- 53. Postmetacristid on m1-2:**
0. curving toward postprotocristid forming a transverse bridge with it orientated straight toward the centre of the tooth
1. forming a rounded postmetaconulid not preferentially orientated
2. joins prehypocristid
- 54. Ectoprotofossid on lower molars:**
0. absent
1. present
- 55. Ectometafossid on lower molars:**
0. yes
1. no
- 56. Endometacristid on lower molars:**
0. no or slightly expressed much more like an enamel fold
1. present
- 57. Postectometacristid on lower molars:**
0. lightly marked to absent
1. always present and well marked
- 58. Premetafossid on lower molars:**
0. present
1. absent
- 59. Preentocristid :**
0. absent
1. present
- 60. Preentocristid connects:**
0. endohypocristid
1. prehypocristid toward the cuspid apex
2. prehypocristid toward its mesial extremity
- 61. Postectoentocristid on lower molars:**
0. absent
1. present but more like a keel on cusp
2. present and well individualized from the cusp
- 62. Ectoentocristid:**
0. present
1. absent
- 63. Postentocristid on lower molars:**
0. absent
1. present
- 64. Postentocristid mesiodistally oriented and comprised between the posthypocristid**

- and the entoconid (=the entoconid fold):**
0. no
1. yes
- 65. Prehypocristid dividing in two mesial arms on lower molars:**
0. yes
1. no
- 66. Prehypocristid inflated (not salient when unworn) in transverse valley of lower molars:**
0. no
1. yes (even to form a conulid)
- 67. Prehypocristid reaches:**
0. median part of transverse valley
1. lingual part of transverse valley
2. labial part of the transverse valley
- 68. Main arm of prehypocristid connects:**
0. trigonid distal walls (junction between cristids from metaconid and protoconid)
1. postmetafossid
2. lingual margin of transverse valley
3. postmetacristid
- 69. Posthypocristid joins:**
0. nothing or distostylid
1. postentocristid
2. postectoentocristid
- 70. Endohypocristid on lower molars:**
0. absent
1. present
- 71. Posthypofossid on lower molars:**
0. absent
1. present
- 72. Entostylid on lower molars that could sometimes be linked to an entocristylid:**
0. never
1. frequently present
- 73. Ectostylid on lower molars:**
0. no cingulid
1. a shallow and constant cingulid in front of the transverse valley
2. frequently developed cingulid in a /some stylid at least on m1
- 74. Ectocrystilid on lower molars :**
0. no
1. yes even if variable
- 75. Cingulid surrounding m3 hypoconulid:**
0. no specimen exhibiting such extension
1. occasionally bordering the labial wall
- 76. Presence of one or many postentostylid on m3:**
0. no
1. yes
- 77. Ectohypocristulid on m3:**
0. absent
1. not complete
2. present joining the summit of hypoconulid
- 78. Distostylid on m1-m2:**
0. median
1. lingual
2. none
- 79. Mesial part of Loop-like hypoconulid:**
0. open
1. pinched
- 80. Posthypocristulid:**
0. complete
1. incomplete
- 81. Posthypocristulid incomplete due to:**
0. a groove separates the cristid in two part
1. It lacks a part or totality of the cristid
- 82. Entoconulid:**
0. no
1. yes
- 83. m3 hypoconulid in line with labial cusps:**
0. yes
1. no
- 84. Number of upper incisors:**
0. 3
1. 2
2. none
- 85. Central upper incisor:**
0. morphologically similar to I2/I3
1. peg-like, morphologically different from others
2. caniniform

- 86. I3/ reduced in size compared to I1:**
 0. no
 1. yes
- 87. Upper canine morphology:**
 0. strong with circular or elliptic cross section
 1. strong and laterally compressed (blade-like)
 2. premolariform
- 88. Canine size root:**
 0. equivalent to slightly longer than the crown
 1. at least twice the size of the crown
 2. prolonged to continuous growth of root
 3. prolonged and continuous growth of crown
- 89. Dimorphic upper canine:**
 0. no
 1. yes
- 90. Diastem C-P1 ou C-P:**
 0. yes
 1. no
- 91. Diastem P1-P2:**
 0. no
 1. yes
- 92. Number of upper premolar:**
 0. 4
 1. 5
 2. 3
- 93. Distolabial crests of upper premolars (postparacrista):**
 0. simple
 1. with a maximum of two accessory cusps
 2. with more than two accessory cusps at least on one premolar
- 94. Number of mesial crests on P1-3:**
 0. one
 1. two
- 95. Disto-lingual basin in P2:**
 0. yes
 1. no
- 96. Accessory cusp on disto-lingual cingulum of P3:**
 0. none
- 97. Metacone on P3:**
 0. no
 1. yes
- 98. P3 root pattern:**
 0. one mesial root, two distal root not fused
 1. one mesial root and fused distal ones
- 99. P4 paracone:**
 0. simple with crest
 1. complex with fossa
 2. very complex with more fossae
- 100. Orientation of preparacrista on P4:**
 0. mesial
 1. labial
- 101. Postprotocrista on P4:**
 0. absent
 1. present
- 102. Postprotocrista on P4 joins:**
 0. base of paracone
 1. distostyle
 2. metastyle
- 103. Preprotocrista on P4 joins α :**
 0. mesiostyle
 1. base of the paracone then mesiostyle
 2. parastyle
- 104. Postectoprotocrista on P4:**
 0. absent
 1. present
- 105. P4 protocone :**
 0. rounded
 1. crescentic
- 106. In lingual view protocone of P4 is:**
 0. displaced mesially
 1. median
- 107. P4 mesial margin:**
 0. concave
 1. convexe
- 108. Strong development of distostyle on P4:**
 0. no

1. yes
- 109. Mesial accessory cusp on P4 that can be linked to mesiostyle:**
 0. no
 1. yes
- 110. P4 metacone:**
 0. absence
 1. presence
- 111. P4 paracone higher than the protocone:**
 0. slightly higher than protocone
 1. much higher than protocone
- 112. P4 endoparacrista:**
 0. absence
 1. presence
- 113. Distal accessory cusp on postprotocrista of P4 that can be linked to distostyle:**
 0. no
 1. yes
- 114. Height of lingual cingulum compared to unworn protocone height on upper molars:**
 0. one third
 1. half
 2. no cingulum
- 115. Mesio-distal ribs development of labial cusps of upper molars:**
 0. almost half the molar length
 1. pinched (inferior to one third of molar length)
 2. enlarged (superior to half the molar length)
- 116. Postectoprotocrista:**
 0. absent
 1. present
- 117. Postectoprotocrista reaching the lingual margin of M3/:**
 0. no
 1. yes
- 118. Postprotocrista:**
 0. present
 1. absent
- 119. Protocone and metaconule junction on upper molars:**
 0. none
 1. premetacristule-postectoprotocrista
 2. premetacristule-postprotocrista
3. postprotocrista and lingual part of metaconule
- 120. Premetacristule divided in two mesial arms:**
 0. no
 1. yes
- 121. Ectometacristule on upper molars:**
 0. absent
 1. present at least on M1
 2. not frequent and only on M2 or M3
- 122. Postmetafossule:**
 0. absent
 1. present
- 123. Secondary cristule labial to metaconule eventually an endometacristule or enamel knob:**
 0. no
 1. yes
- 124. Distostyle on upper molar:**
 0. yes
 1. no
- 125. Distostyle position on upper molars levels:**
 0. metaconule
 1. metacone
- 126. Secondary ectometafossule lingual to ectometacristule:**
 0. absent or very light
 1. present mesially at least on M1 linked to ectometacristule
- 127. Paraconule on upper molars:**
 0. present
 1. absent
- 128. M2/ paraconule when present:**
 0. similar in size with protocone
 1. smaller than protocone
- 129. Postparacristule extend to connect:**
 0. none
 1. base of the paracone
 2. transverse valley
- 130. Preparacrista connects the parastyle:**
 0. no, separated by a groove
 1. yes linguallly
 2. yes labially
- 131. Endoparacrista on upper molars:**

0. absence
1. presence
- 132. Ectoparafossa on upper molars:**
0. no
1. yes
- 133. Ectocristyle:**
0. frequently present
1. absent
- 134. Premetacrista and postparacrista connect:**
0. no connection
1. direct connection centrocrista
2. connection to mesostyle (via ectocristyle or not)
- 135. Endometacrista and endometacristule forming a transverse crest:**
0. absence
1. presence
- 136. Parastyle development:**
0. enamel knob
1. smaller or equal than mesostyle
2. larger than mesostyle
- 137. Premetacristule invade labial part of the transverse valley:**
0. no
1. yes
- 138. Position of metaconule on upper molar:**
0. labial side of the protocone
1. distal side of the protocone
- 139. M2 metaconule:**
0. similar in size with protocone
1. smaller than protocone
- 140. Mesostyle on upper molars:**
0. no
1. yes
- 141. Mesostyle:**
0. enamel knob
1. half to the size of labial cusp
2. larger than labial cusp
- 142. Cingulum at the junction between postparacrista and premetacrista forming labial structure on mesostyle:**
0. high triangular cingulum
1. wing-like cingulum
2. low or absent cingulum
- 143. Division of the mesostyle on upper molar:**
0. no, one style or continuous cristae
1. two apices in unworn molars but still connect by cristae
2. fully isolated style apices
- 144. Metastyle:**
0. reduced to enamel knob or absent
1. fully developed
- 145. Root fusion on upper molars:**
0. four roots with occasional fusion close to cervix the apices always remaining free
1. fully fused lingual roots
2. three roots
- 146. Lingual cingulum on upper molars:**
0. no
1. yes
2. developed in entostyle
- 147. Hypocone on upper molars (at least M2):**
0. yes
1. no
- 148. Shape of M1:**
0. triangular
1. quadrate
- 149. Shape of M3:**
0. triangular
1. quadrate
- 150. M3 size:**
0. Larger than M2
1. equal in size with M2
2. reduced (less than 60%)
- 151. Mesiolingual style on upper molar mesial cingulum:**
0. no
1. yes
- 152. Angle between the slope of the metaconule and the dental collet of M3/:**
0. lower or equal to 40°
1. between 40° and 45°
2. upper or equal to 45°
- 153. Symphysis morphology in sagittal section, ventral border:**
0. convex
1. straight to almost straight
2. concave

154. **Symphysis morphology in sagittal section, dorsal border:**
 0. convex
 1. straight or almost straight
 2. markedly concave
155. **Diastem c-p1:**
 0. absent
 1. present
156. **Bone fusion at symphysis in adult specimens:**
 0. no
 1. yes
157. **Maximal thickness of the symphysis in sagittal section:**
 0. in the middle part
 1. in the rostral part
 2. in the nugal part
158. **Symphysis extension:**
 0. extends nuchally between c and p1
 1. extend nuchally between p1 and p3
 2. extends nuchally to p3
159. **Number and position of main external foramen:**
 0. numerous
 1. only one below the anterior part of the premolar row
 2. two, one below the anterior part and the other below the posterior
160. **Mandibular notch:**
 0. no
 1. yes, long extension behind coronoid process
 2. yes, short extension below m/3
161. **Transverse constriction of mandible at c-p1 diastema:**
 0. no
 1. yes
162. **Mandibular protuberance at the c/p1 level:**
 0. no
 1. yes
163. **p1-p2 diastema:**
 0. absent
 1. present
164. **p2-p3 diastema:**
 0. yes
 1. no
165. **Opening of internal choanes:**
 0. at M3
 1. nugal to M3
166. **Opening of main palatal foramen:**
 0. at palatin-maxillary jonction in front of molars to P3
 1. on maxillary in front of P2-P1
 2. on maxillary cranial to P1
167. **Enamel ornamentation:**
 0. no
 1. yes
168. **Schmelzmuster composed of:**
 0. two layers
 1. three layers
 2. one layer
169. **Inner radial enamel:**
 0. absent
 1. present
170. **HSB percent of Schmelzmuster:**
 0. absent
 1. less than 75%
 2. more than 76%
171. **Outer radial enamel :**
 0. less or equal to 20%
 1. more than 20%
172. **Hsb zone:**
 0. thin with bands always less than 100µm
 1. large (equal or more than 100µm)
173. **Regular aspect (constant width):**
 0. yes
 1. no
174. **HSB variable (SD>20):**
 0. no
 1. yes
175. **HSB angle with EDJ:**
 0. >70°
 1. <70 °
176. **Orientation of HSB:**
 0. straight
 1. bent

- 177. HSB definition (decussation angle and size of transition zone):**
 0. clear
 1. blurry
- 178. Division of HSB:**
 0. anastomosis
 1. bifurcation
 2. no division
- 179. HSB configuration:**
 0. curved
 1. transverse
- 180. Synchronous prism undulation on horizontal section:**
 0. no
 1. yes but few
 2. yes but more or equal to 4
- 181. IPM in inner portion:**
 0. closed sheath
 1. Inter row sheets
- 182. IPM in middle portion:**
 0. closed sheath
 1. Inter row sheets
 2. no IPM
- 183. IPM in outer portion:**
 0. closed sheath
 1. no IPM
- 184. Prism angle with EDJ:**
 0. equal or more than 60°
 1. less than 60°
 2. tend to diminish in the inner part
- 185. Prism diameter:**
 0. mean between 3 and 3.9 μm
 1. small diameter mean below 3 μm
 2. large diameter mean above or equal to 4
- 186. Eruption of M3 compared to permanent premolars:**
 0. Eruption of M3 before permanent premolars
 1. Eruption of M3 before or simultaneous to only P4
 2. Eruption of M3 after P4
- 187. dp2 Paraconid:**
 0. Absent
 1. Mesial
 2. Mesio-lingual
- 188. dp2 Hypoconid:**
 0. Absent
 1. Present
- 189. dp2 Division of the distalmost cristid:**
 0. Absent
 1. Present
- 190. dp3 Paraconid:**
 0. Absent
 1. Mesial
 2. Mesio-lingual
- 191. dp3 Postprotocristid:**
 0. Distally oriented
 1. Reaching the lingual side
- 192. dp3 cingulid on the lingual side of the protoconid:**
 0. Absent
 1. Present (or with entostylid)
- 193. dp3 Hypoconid:**
 0. Absent
 1. Incipient to marked
- 194. dp3 Prehypocristid:**
 0. Longitudinal and reaching the postprotocristid
 1. Lingually oriented and reaching the postprotocristid
 2. Reaching the lingual side
 3. Reduced to absent
- 195. dp3 Posthypocristid:**
 0. Distally oriented
 1. Labially oriented
 2. Lingually oriented
 3. Reaching the lingual side
- 196. dp3 Entoconid:**
 0. Absent
 1. Incipient to marked
- 197. dp3 Preentocristid:**
 0. Absent
 1. Labially oriented
 2. Mesially oriented
- 198. dp3 Postentocristid:**
 0. Absent
 1. Distally oriented
 2. Labially oriented
- 199. dp3 Distostylid:**
 0. Absent

1. Present
- 200. dp3 Post-entostylid:**
 0. Absent
 1. Small disto-lingual cingulid
 2. Present
- 201. dp4 root under protoconid:**
 0. Absent
 1. Coalescent with the mesial root
 2. Present
- 202. dp4 Position of paraconid (lingual) vs primoconid (labial):**
 0. Paraconid more mesial
 1. Same level
 2. Paraconid more distal
- 203. dp4 Preprimocristid:**
 0. Reduced to absent
 1. Enlarged toward the mesio-lingual side
 2. Connected to the preparacristid mesially
 3. Connected to the preparacristid lingually
- 204. dp4 Mesioconid:**
 0. Absent
 1. Stylar
 2. Marked
- 205. dp4 Postparacristid:**
 0. Enlarged and directed toward premetacristid
 1. Reduced to absent
- 206. dp4 Postectoparacristid:**
 0. Absent
 1. Present
- 207. dp4 Postprimocristid:**
 0. Directed distally
 1. Directed disto-lingually
 2. Reaching the lingual side
- 208. DP2 Metacone:**
 0. Absent
 1. Crested
 2. Marked
- 209. DP2 Parastyle:**
 0. Absent
 1. Present
- 210. DP2 Lingual basin:**
 0. Absent
1. Disto-lingual
- 211. DP2 Protocone:**
 0. Absent
 1. Present
- 212. DP2 Postparaconule:**
 0. Absent
 1. Present
- 213. DP3 Anterior lobe:**
 0. Presence of a mesial cingulum
 1. Developed with a parastyle
 2. With two cusps
- 214. DP3 Preparacrista:**
 0. Mesially oriented
 1. Mesio-labially oriented
 2. Mesio-lingually oriented
- 215. DP3 Endoparacrista:**
 0. Absent
 1. Present
- 216. DP3 Postparacrista:**
 0. Distally oriented
 1. Labio-distally oriented
- 217. DP3 Postparaconule:**
 0. Absent
 1. Present
- 218. DP3 Mesio-lingual basin:**
 0. Absent
 1. Present
- 219. DP3 Entostyle:**
 0. Absent
 1. Present
- 220. DP3 Position of the protocone:**
 0. At the level of the metacone
 1. Between the paracone and the metacone
- 221. DP3 Connection of preprotocrista:**
 0. No connection
 1. Connected to the lingual cingulum (or entostyle)
 2. Reaching the base of the paracone
- 222. DP3 Protocrista protruding mesio-lingually in the valley:**
 0. No
 1. Moderate
 2. Elongated

223. DP3 Connection Protocone-metacone:

- 0. Absent
- 1. Incomplete to complete

224. DP3 Postprotocrista:

- 0. Absent
- 1. Present

	?	?	?	?	?	?	?	?	?	?	?	?
	?	?	?	?	?	?	?	?	?	?	?	?
	?	?	?	?	?	?	?	?	?	?	?	?
<i>Dichobune</i>	0	0	0	-	0	0	?	?	1	2	?	?
	0	0	1	0	0	0	1	0	0	0	1	0
	0	0	0	0	2	0	0	0	0	0	0	0
	0	0	0	1	0	0	0	0	0	0	0	0
	0	1	0	0	0	0	0	0	0	0	1	0
	-	0	0	0	0	1	0	0	0	0	1	0
	0	2	0	0	0	0	0	0	0	-	0	1
	?	?	?	?	?	?	?	1	0	0	0	?
	1	?	0	0	0	0	-	0	0	0	1	1
	0	0	0	0	0	0	0	0	0	-	1	0
	0	0	0	0	0	0	0	0	1	0	1	0
	0	1	1	0	2	0	0	1	0	-	2	-
	0	2	0	0	1	0	2	0	-	0	0	0
	0	?	1	2	2	0	?	1	0	0	?	0
	0	1	2	0	0	1	1	0	0	1	0	?
	?	0	?	?	0	2	0	?	?	?	1	0
	0	1	0	1	0	0	0	0	0	1	0	2
	0	0&1	0	0	1	0	0	0	0	1	0	0
	0	0	0	0	0	0	0	0	0&1			
<i>Acotherulum</i>	?	?	?	?	?	?	?	?	?	?	?	?
	?	?	2	0	0	1	?	?	?	?	?	?
	?	?	?	?	?	?	?	?	?	?	?	?
	?	?	?	?	?	?	?	?	?	?	?	0
	0	0	0	0	1	0	0	0	?	1	0	0
	-	0	0	0	0	1	0	0	0	0	1	1
	0	2	0	?	?	?	0	?	?	?	?	?
	?	?	?	?	?	?	?	?	?	0	0	?
	2	0	?	1	0	1	1	2	0	1	0	1
	0	0	0	0	0	0	2	0	1	0	0	0
	0	0	1	0	1	-	0	0	1	0	1	0
	1	1	1	0	0	0	1	0	1	0	2	0
	0	0/1	2	1	1	1	2	0	?	?	?	1
	?	?	?	2	1	?	?	1	?	?	0	0
	?	?	?	?	?	?	?	?	?	?	?	?
	?	?	?	?	?	?	0	1	1	0	1	0
	0	1	0	-	0	0	0	0	0	1	1	2
	0	0&1	0&1	0	?	?	?	?	?	1	0	0
	0	0	0	0	0	0/1	0	1	1			
<i>Cebochoerus</i>	0	0	0	-	0	0	0	?	1	0	?	?
	0	0	2	0	1	1	0	0	0	0	0	0
	0	0	1	0	0	0	0	0	0	0	0	0
	0	0	0	1	0	0	0	0	0	0	1	0
	0	0	0	0	1	0	1	0	0	0	0	0
	-	1	0	0	0	1	0	0	0	0	0	1
	0	2	0	0	0	2	0	0	0	-	0	1
	?	?	?	2	0	0	0	1	0	0	0	0
	2	0	0	1	0	1	1	0	0	0	0	1
	0	0	0	0	0	0	0	2	0	-	0	2
	0	0	1	0	0	0	0	0	1	0	1	0
	0	0	1	0	2	0	1	0	0	-	2	-
	0	0	0	1	1	1	1	0	2	1	0	0
	1	2	1	2	2	0	0	1	1	0	0	0
	0	0	2	0	0	0	0	0	0	0	0	0
	0	0	0	0	0	1	0	?	?	?	1	0
	0	1	0	-	0	0	0	0	0	1	1	2
	0	0&1	0&1	0	2	0	0	0	0	1	0	0
	0	0	0	0	0	2	0	0	1			

<i>Gobiohyus</i>	?	?	?	?	?	?	?	?	?	1	1	?
	0	0	0	1	0	0	1	0	0	0	0	0
	0	0	0	1	0	0	0	0	1	2	0	0
	1	0	0	1	0	0	0	0	0	0/1	0/1	0
	0	1	0	0	0	0	0	0	0	1	1	1
	0	0	0	0	0	1	0	0	0	0	1	0
	0	1	0	0	0	1	0	0	0	-	0	1
	?	?	?	1	?	1	0	1	0	0	0	1
	2	0	0	1	0	1	1	0	0	1	0	1
	0	0	0	0	0	0	1	0	0	-	1	0
	0	0	0	0	1	-	0	0	1	0	1	0
	1	1	1	0	2	0	1	0	0	-	2	-
	0	2	1	1	1	1	1	0	2	?	?	1
	0	?	1	2	1	0	0	1	0	?	0	0
	?	?	?	?	?	?	?	?	?	?	?	?
	?	?	?	?	?	?	2	?	?	?	?	?
	?	?	?	?	?	?	?	?	?	?	?	?
	?	?	?	?	?	?	?	?	?	?	?	?
	?	?	?	?	?	?	?	?	?	?	?	?
	?	?	?	?	?	?	?	?	?	?	?	?
<i>Choeropotamus depereti</i>	0	0	0	0	-	?	?	?	?	?	?	?
	?	0	0	2	0	0	1	0	0	1	0	0
	0	0	0	0	0	1	0	0	0	1	0	0
	0	0	1	0	0	0	0	1	0	0	0	0
	0	1	0	0	0	0	1	0	0	0	0	0
	0	-	0	0	0	0	0	0	0	0	0	0
	0	1	2	0	0	1	0	0	0	0	-	0
	0	?	?	?	0	?	?	?	?	0	0	0
	1	0	0	?	0	0	1	1	0	0	1	0
	1	0	0	1	0	0	0	0	1	0	-	0
	2	0	1	1	1	0	0	0	0	1	1	0
	0	1	0	2	0	1	0	1	0	1	1	0
	0	1	?	1	1	1	1	1	0	0	0	0
	1	0	0	1	0	1	0	0	1	1	?	?
	1	0	0	1	1	1	1	1	0	0	0	0
	1	0	0	0	0	0	2	?	?	?	?	?
	?	?	?	?	?	?	?	?	?	?	?	?
	?	?	?	?	?	?	?	?	?	?	?	?
	?	?	?	?	?	?	?	?	?	?	?	?
<i>Choeropotamus parisiensis</i>				0	0	0	-	?	?	?	?	?
	?	?	?	?	2	?	0	1	0	0	0	0
	0	0	0	0	0	1	1	0	0	1	1	1
	0	1	0	1	0	1	0	0	1	0	0	0
	0	0&1	1	0	0	0	0	0	0	1	0	0
	1	1	2	0	0	0	0	0	1	0	0	0
	0	0	0	1	0	?	1	2	0	0	0	-
	1	0	?	?	?	?	?	?	?	?	0	1
	1	1	1	0	?	1	1	1	1	0	0	0
	1	0	0	0	1	0	0	0&1	1	0	0	-
	0	2	0	2	1	1	0	0	1	0	1	0
	1	0	1	0	2	0	1	0	1	0	1	1
	0	0	0	0	2	1	1	1	0	0	?	?
	?	0	?	?	?	2	1	?	?	1	1	0
	0	1	?	?	?	?	?	?	?	?	?	?
	?	?	?	?	?	?	?	?	2	?	?	?
	1	0	0	1	0	2	0	0	0	0	0	1
	?	?	?	?	?	?	?	?	?	?	?	0
	?	0	0	0	0	1	0	0	0	1	?	?
<i>Siamotherium</i>	0	?	?	?	?	0	0	?	?	0	0	0
	0	?	0	0	0	0	0	0	0	0	0	0
	0	0	0	0	0	0	0	0	1	0	0	0

0	1	0	0	1	0	1	0	0	0	0	0	0
1	0	0	0	0	0	0	0	0	0	0	0	1
0	1	0	0	0	1	0	0	0	0	0	1	1
0	0	0	0	0	2	0	0	0	0	-	0	0
0	0	0	0	1	?	0	?	0	0	0	0	1
0&1	0	1	1	0	0	-	0	0	0	0	0	1
0	0	0	0	0	0	1	0	0	0	-	0	2
1	0	0	0	0	1	0	0	1	1	1	1	0
1	0	1	0	0	0	1	0	1	0	2	0	0
0	0	1	1	1	1	0	0	2	0	0	0	0
0	2	1	2	1	0	0	0	1	0	?	?	1
0	0	2	0	0	0	0	0	0	0	0	0	1
0	0	0	0	0	2	?	?	?	?	?	?	?
?	?	?	?	?	?	?	?	?	?	?	?	?
?	?	?	?	1	0	0	0	0	0	0	0	0
1	0	0	0	0	0	0	1	0				
<i>Anthracokeryx tenuis</i>		0	0	0	-	0	0	0	0	0	1	?
1	0	0	0	0	0	0	0	0	0	1	0	0
0	0	0	0	0	0	0	0	0	0	1	1	0
0	0	0	0	0	0	0	0	0	0	0	0	0
0	1	0	1	0	0	0	0	0	0	1	1	0
1	0	1	0	0	0	1	0	0	0	0	0	1
0	0	0	0	0	0	2	0	0	0	0	-	0
0	0	0	0	1	2/3	?	0	1	0	0	0	0
1	0	0	?	0	0	?	?	?	?	?	1	0
?	?	?	0	0	0	0	0	0	0	1	0	0
1	1	1	0	0	0	1	0	0	1	1	1	1
0	1	0	2	0	2	0	1	0	1	1	1	2
0	0	?	1	1	1	1	0	0	?	0	0	0/1
1	0	2	1	1&2	1	1	0	1	0	0	0	0
1	?	?	?	?	?	?	?	?	?	?	?	?
?	?	?	?	?	?	?	?	?	?	?	?	?
0	0	1	0	0	0	0	0	0	0	2	1	0
2	0	0	1	1	?	?	?	?	?	?	1	0
0	1	1	0	0	1	2	0	1	1	1		
<i>Geniokeryx thailandicus</i>	?	?	?	?	?	?	?	?	?	?	?	?
?	?	?	?	?	0	0	0	0	0	0	0	0
0	0	0	0	0	0	0	0	0	0	1	1	0
0	0	1	0	0	0	0	0	0	0	0	0	0
0	1	0	0	0	0	0	0	0	0	1	1	0
1	2	1	0	0	0	1	0	0	0	0	0	0
0	0	1	0	0	0	2	0	0	0	0	-	0
0	?	?	?	?	?	?	?	?	?	?	0	0
?	0	0	0	1	0	1	1	0	0	0	1	0
0	0	0	0	0	0	0	2	1	0	0	-	0
2	0	0	0	0	0	1	0	0	1	2	2	1
0	1	0	2	0	1	0	1	0	1	0	0	0
0	1	0	1	1	1	1	0	1	1	1	0	0
1	0	0	1	2	?	1	0	1	1	1	0	0
1	?	?	?	?	?	?	?	?	?	?	?	?
?	?	?	?	?	?	?	?	?	?	?	?	?
?	?	?	?	?	?	?	?	?	?	?	?	?
?	?	?	?	?	?	?	?	?	?	?	?	?
?	?	?	?	?	?	?	?	?	?	?	?	?
<i>Microbunodon</i>	0	0	0	-	0	0	0	0	0	1	1	1
0	0	0	0	0	0	0	0	0	1	0	1	0
0	0	0	0	0	0	0	0	0	1	1	0	0
0	0	0	0	0	0	0	0	1	0	1	0	0
1	0	0	0	0	0	0	0	0	1	1	0	1
2	1	1	0	0	1	0	0	0	0	0	0	0

0	0	0	0	0	0	0	0	0	1	0	0
1	1	1	0	1	0	0&1	1	0	1	2	1
0	1	0	2	0	2	0	1	0	1	1	0
0	1	0	2	1	1	1	0	1	2	0	0
0	1	0	1	2	0	0	0	1	1	0	?
1	0	0	2	0	0	0	0	0	0	0	0
1	2	0	0	0	0	0	?	?	?	?	0
0	0	1	0	?	0	0	0	0	0	2	0
2	0	0	1	1	1	0	0	0	0	1	0
0	1	1	0	0	0	2	0	1	1	1	0
<i>Myaingtherium</i>	0	0	0	-	0	0	0	?	0	?	?
?	?	?	1	1	0	0	0	0	0	0	0
0	0	0	0	0	0	0	0	1	?	0	0
0	1	0	1	0	0	0	0	0	0	0	0
1	0	0	1	1	0	0	0	0	1	1	1
0	1	0	0	0	1	0	0	0	0	1	0
0	0	0	0	1	2	0	0	0	-	1	0
?	?	?	?	?	?	?	?	?	?	?	?
?	?	?	1	0	1	0	0	1	1	0	0
0	0	0	0	0	0	?	2	1	0	0	1
1	1	0	0	0	0	0	0	1	1	0	0
1	1	1	0	0	0	1	0	1	0	2	-
0	1	2	1	1	1	0	1	?	?	?	1
0	?	2	?	?	1	0	0	1	?	?	1
?	?	?	?	?	?	?	?	?	?	?	?
?	?	?	?	?	?	?	?	?	?	?	?
?	?	?	?	?	?	?	?	?	?	?	?
?	?	?	?	?	?	?	?	?	?	?	?
<i>Bothriogenys orientalis</i>	?	?	?	?	?	?	?	?	?	?	?
?	?	?	?	?	0	0	0	0	0	0	2
0	1	0	0	1	2	1	1	1	1	1	0
1	0	1	0	0	0	0	0	0	0	1	0
0	1	0	0	0	0	0	1	0	1	1	0
1	1	1	0	1	0	1	0	0	0	1	0
1	0	2	1	0	0	1	1	0	0	-	0
1	?	?	?	?	?	?	0	1	0	0	0&1
0	0	0	?	1	1	1	0	0	0	1	1
0	1	0	0	0	0	0	0	0	1	0	0
1	1	1	0	?	0	0	0	0	1	1	1
0	1	0	2	0	1	0	1	0	1	1	0
0	0	0	1	1	1	1	0	0	2	1	0
1	0	2	1	1	?	?	?	1	1	1	0
1	?	?	?	?	?	?	?	?	?	?	?
?	?	?	?	?	?	?	?	?	?	?	?
?	?	?	?	?	?	?	?	?	?	?	?
?	?	?	?	?	?	?	?	?	?	?	?
<i>Bothriogenys fraasi</i>	?	?	?	?	?	?	?	?	?	?	?
0	?	?	?	?	0	0	0	0	0	0	2
0	1	0	0	1	1	1	0	1	2	1	?
1	0	1	0	0	0	0	0	0	0	1	0
1	1	0	0	0	0	0	0	0	1	1	0
1	1	1	0	1	0	1	0	0	0	1	1
0	0	1	1	1	0	0	1	0	0	-	0
0	?	?	?	2	0	?	0	1	0	0	1
0	0	0	?	1	1	1	0	1	0	1	0
0	0	0	0	0	0	?	0	0	1	0	0
1	1	1	0	0	0	1	0	0	1	2	1
0	1	0	2	0	2	0	1	0	1	1	2

?	?	?	?	?	?	?	?	?	?	?	?	?
?	?	?	?	?	?	?	?	?	?	?	?	1
3	0	0	0/1	1	?	?	?	?	?	?	1	1
0	1	0	0	0	0	2	1	0/1	1			
<i>Brachyodus onoides</i>		1	1	1	1	0	0	1	1	1	1	2
0	0	0	1	0	0	0	0	0	0	0	0	0
0	1	0	0	1	1	0	1	0	2	1	0	0
1	0	1	0	0	0	0	0	0	0	0	2	0
1	1	0	1	0	0	0	0	1	0	1	1	1
1	1	2	1	0	0	1	0	1	1	1	2	0
0	0	0	1	1	0	0	1	0	0	0	-	0
1	1	2	1	2	0	0	0	0	0	0	0	1
0	0	0	?	1	1	1	0	1	0	1	0	0
0	0	0	0	0	0	1	0	1	1	1	0	1
0	0	0	0	0	0	1	0	0	1	2	1	1
0	1	0	2	0	2	0	1	0	1	1	1	2
0	1	0	1	1	1	1	0/1	0	2	0	1	1
1	1	2	0	1	1	1	0	0	1	1	1	2
1	2	0	2	0	0	0	0	1	1	0	0	0
1	2	0	1	0	1	0	2	0	0	0	0	2
1	1	1	3	2	1	2	2	0	1	2	1	1
2	0	0	0	2	1	0	1	0	0	1	1	1
0	1	0	0	0	0	2	0	1	1			
<i>Brachyodus depereti</i>		2	1	1	1	0	?	-	-	?	?	?
?	?	?	1	0	0	0	0	0	0	0	0	0
0	1	0	0	1	1	0	0	0	2	1	1	1
0	0	1	0	0	0	0	0	0	0	2	0	0
1	1	0	1	0	0	0	0	1	0	1	1	1
1	2	2	0	0	0	1	0	1	1	2	0	0
0	0	0	1	1	0	0	1	0	0	-	0	0
1	?	?	?	?	?	?	?	0	0	?	?	?
?	?	0	?	1	1	1	1	0	0	1	0	0
0	0	0	0	0	0	0	0	1	0	-	0	0
0	0	0	0/1	0	0	1	0	0	1	2	1	1
0	1	0	2	0	2	0	1	0	1	1	1	2
0	1	?	1	1	?	1	?	0	?	0	1	1
1	1	?	0	?	?	1	0	0	1	?	?	?
1	?	?	?	?	?	?	?	?	?	?	?	?
?	?	?	?	?	?	?	?	?	?	?	?	?
?	?	?	?	?	?	?	?	?	?	?	?	?
<i>Bothriodon</i>		0	0	1	0	0	0	1	0	1	2	0
0	0	0&1	0&1	0	0	0	0	0	0	0	0	0
0	0	0	1	2	1	0	0	1	0	0	0	0
0	1	0	0	0	0	0	0	0	1	0	0	1
1	0	0	0	0	0	0	0	1	1	0	1	1
2	2	0	0	0	1	0	0	1	2	0	0	0
0	1	?	0	0	0	1	1	0	-	0	0	0
0	0	0	2	0	0	0	1	0	0	0	0	1
0	0	?	1	1	1	1	0	0	1	0	1	1
0	0	0	0	0	0	0	1	1	0	0	0	0
1	1	0	0	0	0	0	0	0	2	2	0	0
1	1	2	0	1	0	1	0	1	2	2	1	1
0	0	1	1	1	1	0	0	2	0	1/2	1	1
1	2	1	1	1	1	0	1	0	0	0	0	1
1	1	1	0	0	0	0	1	1	0	0	1	1
0	0	1	0	1	0	2	?	?	?	2	1	1
0	1	1	2	1	1	0	0	0	2	0	0	3

	0	0	0&1	2	2	?	1	0	0	1	1	0
	1	1	0	0	0	1	0/1	1	1			
<i>Aepinacodon</i>	0	?	1	0	?	?	0	?	?	?	?	?
	?	0	0	1	0	0	0	0	0	0	0	0
	1	0	0	1	1	1	0	0	1	2	0	0
	1	1	0	0	1	0	0	0	2	1	0	1
	1	0	1	0	0	0	0	1	1	1	0	1
	2	2	0	0	0	1	0	1	1	2	0	0
	0	1	1	?	?	?	1	?	?	?	?	?
	0	0	0	2	0	0	0	1	0	0	0	1
	0	0	?	1	1	1	0	0	0	1	1	1
	0	0	0	0	0	0	0	1	1	0	0	0
	0	0	0	0	0	0	0	0	0	2	2	0
	1	1	2	0	1	0	1	0	1	1	2	1
0&1	?	1	1	1	1	1	0	0	?	0	1/2	1
1	2	1	1	?	?	?	?	?	?	?	?	?
?	?	?	?	?	?	?	?	?	?	?	?	?
?	?	?	?	?	?	?	?	?	?	?	?	?
?	?	?	?	?	?	?	?	?	?	?	?	?
?	?	?	?	?	?	?	?	?	?	?	?	?
<i>Bakalovia</i>	0	0	?	?	?	?	?	?	?	1	?	?
1	?	?	?	0	0	0	0	0	0	0	?	0
0	0	0	?	0	?	?	0	?	1	1	0	?
?	1	?	?	0	?	?	0	0	?	0	0	0
1	0	0	0	0	0	0	0	0	1	1	0	1
0	2	0	0	0	1	0	1	1	1	0	1	0
0	2	1	1	0	0	0	1	0	-	0	0	0
0	0	0	?	?	1	0	1	0	0	0	0	0
0	0	?	1	1	1	0	0	0	1	0	0	0
0	0	0	0	0	0	0	1	1	0	0	0	1
0	1	1	1	0	1	0	0	1	1	2	2	0
1	1	2	0	2	0	1	0	0	1	1	1	0
1	?	1	1	1	1	1	0	0	?	1/2	0	0
0	0/1	1	1	?	?	?	0	0	1	?	?	1
?	?	?	?	?	?	?	?	?	?	?	?	?
?	?	?	?	?	?	?	?	?	?	?	?	?
?	?	?	?	?	?	?	?	?	?	?	?	?
?	?	?	?	?	?	?	?	?	?	?	?	?
<i>Elomeryx crispus</i>	0	0	1	0	0	0	0	1	0	1	2	0
0	0	1	0	0	0	0	0	0&1	0	0	1	0
0	0	0	1	0&2	1	0	0	0	1	1	1	1
0	1	0	0	0	0	0	0	1	0	1	0	0
1	0	0	0	0	0	0	0	0	1	1	0	1
0&2	2	0	0	0	1	0	1	1	1	2	0&1	0
0	1	1	1	0	0	1	0/1	0	-	0	0&1	0
0	0	0	1	1	1	1	0	0	0	0	0	0
0	0	?	1	1	1	1	0	0	1	0	0	1
1	1	1	0	0	1	0	0	0	1	2	2	0
1	1	2	0	2	0	1	0	1	1	1	0	0
1	0	1	1	1	1	1	0	0	1	1	0	1
0	1	?	1	?	1	0	1	1	1	1	0	1
?	?	?	?	?	?	?	?	?	?	?	?	?
?	?	?	?	?	?	?	?	?	?	?	?	?
?	?	?	?	?	?	?	?	?	?	?	?	?
?	?	?	?	?	?	?	?	?	?	?	?	?
?	?	?	?	?	?	?	1	0	0	1	1	0
1	1	0	0	0	2	1	1	1	1			

?	?	?	?	?	?	?	?	?	?	?	?	?
0	1	0	1	0	0	?	0	0	1	1	0	0
1	2	2	0	1	0&1	0	0	0	0	0	0	0
0	0	2	1	1	0	0	?	1	0	-	0	0
1	?	?	?	?	?	?	?	?	?	?	?	?
?	?	?	?	?	?	?	?	?	?	?	?	?
?	?	?	?	?	?	?	?	0	1	1	1	0
0	0	2	1	0	0	1	0	1	1	-	-	2
0	1	1	2	0	2	0	1	0	1	1	1	1
0/1	1	0	2	1	1	1	0	0	0	?	?	?
?	?	?	?	?	?	?	?	?	?	?	?	?
1	?	?	?	?	?	?	?	?	?	?	?	?
?	?	?	?	?	?	?	?	?	?	?	?	?
?	?	?	?	?	?	?	?	?	?	?	?	?
?	?	?	?	?	?	?	?	?	?	?	?	?
?	?	?	?	?	?	?	?	?	?	?	?	?
<i>Telmatodon orientalis</i>	?	?	?	?	?	?	?	?	?	?	?	?
?	?	?	?	?	?	?	?	?	?	?	?	?
?	?	?	?	?	?	?	?	?	?	?	?	?
?	?	?	?	?	?	?	?	?	?	?	?	?
0	1	0	1	0	0	?	0	0	1	1	0	0
1	2	2	0	1	0	1	0	1	1	0	0	0
0	0	2	1	1	0	0	?	1	0	-	0	0
0	?	?	?	?	?	?	?	?	?	?	?	?
?	?	?	?	1	1	1	1	0	0	1	0	0
0	1	0	0	0	0	1	0	1	1	0	0	0
0	0	2	1	0	0	1	0	1	-	-	2	2
0	1	1	2	0	2	0	1	0	1	1	1	1
1	1	0	2	1	1	1	0	0	0	?	?	?
?	?	?	?	?	?	?	?	?	?	?	?	?
1	?	?	?	?	?	?	?	?	?	?	?	?
?	?	?	?	?	?	?	?	?	?	?	?	?
?	?	?	?	?	?	?	?	?	?	?	?	?
?	?	?	?	?	?	?	?	?	?	?	?	?
?	?	?	?	?	?	?	?	?	?	?	?	?
<i>Gonotelma shahbazi</i>	?	?	?	?	?	?	?	?	?	?	?	?
?	?	?	?	?	?	?	?	?	?	?	?	?
?	?	?	?	?	?	?	?	?	?	?	?	?
?	?	?	?	?	?	?	?	?	?	?	?	?
0	1	0	1	0	0	0	0	0	1	1	0	0
1	2	2	0	0	0	1	0	0	0	0	0	0
0	0	2	1	1	1	0	1	1	1	1	0	0
1	?	?	?	?	?	?	?	?	?	?	?	?
?	?	?	?	?	?	?	?	?	?	?	?	?
?	?	?	?	?	?	?	0	1	1	0	0	0
0	0	2	0	0	0	1	0	1	-	-	2	2
0	1	1	2	0	2	0	1	0	1	1	1	1
0	1	0	2	1	1	1	0	0	2	?	?	?
?	?	?	?	?	0/1	?	?	?	?	1	?	?
1	?	?	?	?	?	?	?	?	?	?	?	?
?	?	?	?	?	?	?	?	?	?	?	?	?
?	?	?	?	?	?	?	?	?	?	?	?	?
?	?	?	?	?	?	?	?	?	?	?	?	?
?	?	?	?	?	?	?	?	?	?	?	?	?
<i>Afromeryx</i>	0	?	1	?	?	?	1	?	1	?	?	?
?	?	0	1	0	0	0	1	0	0	1	0	0
0	0	0	1	2	1	0	0	1	1	0	0	0
1	1	0	0	0	1	1	0	2	1	0	1	1
1	0	1	0	0	0	0	0	1	1	0	1	1
2	2	0	0	0	1	0	0	0	0	0	0	0

0	1	1	1	1	0	1	1	1	1	0	1
0	?	0	?	1	1	0	0	0	1	1	0
0	0	?	1	1	1	1	0	0	1	0	0
0	0	0	0	0	0	0	1	1	0	0	0
0	0	0	0	0	1	0	1	-	-	2	0
1	1	2	0	2	0	1	0	1	1	1	0
1	0	2	1	1	1	0	0	2	1	0	1
0	2	1	2	0	1	0	0	1	1	1	1
0	0	1	1	0	0	0	1	1	0	1	1
1	0	1	1	1	1	2	?	?	?	1	1
0	1	2	3	1	1	0	0	0	2	0	3
0	0	0	2	?	?	?	?	?	?	?	?
?	?	?	?	?	?	?	?	?	?	?	?
<i>Sivameryx palaeindicus</i>	?	?	?	?	?	?	?	?	?	?	?
?	?	?	?	?	1	0	0	1	0	0	1
0	1	0	0	1	2	1	0	0	2	1	0
0	0	1	0	1	0	1	1	1	2	1	0
0	1	0	0&1	0	0&1	0	0	0	1	1	0
1	2	2	0	0	0	1	0	1	2	0&2	0
0	0	1	1	1	0	0	1	1	0	-	0
0	?	?	?	?	?	?	?	?	?	1	1
0	0	0	1	1	1	1	0&1	0	0	1	0
0	0	0	0	0	0	0	0	1	1	0&1	0
0	0	0	0	0	0	1	0	0	1	1	2
0	1	1	2	0	1	0	1	0	1	1	1
0	1	0	2	1	1	1	0	0	2	?	?
1	0	2	0	2	?	1	1	0	1	?	?
1	?	?	?	?	?	?	?	?	?	?	?
?	?	?	?	?	?	?	?	?	?	?	1
1	1	1	2	3	1	1	0	0	?	?	?
?	?	?	?	?	?	?	?	?	?	?	?
?	?	?	?	?	?	?	?	?	?	?	?
<i>Sivameryx africanus</i>	0	?	?	0	-	?	?	?	?	1	1
0	0	0	0	?	1	0	0	1	0	0	1
0	1	0	0	1	2	1	0	0	2	1	0
0	0	1	0	1	0	1	0	0	2	1	0
1	1	0	1	0	0&1	0	0	1	1	1	0
1	2	2	0	1	1	1	0	1	2	0	0
0	0	2	1	1	0	0	1	1	0	-	0
0	?	?	?	0	?	?	0	0	0	1	1
?	0	0	?	1	1	1	?	?	?	1	?
1	?	?	0	0	?	?	0	1	1	0	0
0	0	0	1	0	0	1	0	0	1	2	2
0	1	1	2	0	1	0	1	0	1	1	?
0	1	?	2	1	1	1	0	0	2	2	1
1	0	2	0	2	0	1	1	0	1	1	1/2
1	2	1	0	-	-	-	-	-	-	-	-
-	1	1	2	1	1	0	?	?	?	?	?
?	?	?	?	?	?	?	?	?	?	?	1
3	0	0	0	2	?	?	?	?	?	?	?
?	?	?	?	?	?	?	?	?	?	?	?
<i>Hemimeryx blanfordi</i>	?	?	?	?	?	?	?	?	?	1	2
?	?	0	?	?	1	0	0	1	0	0	1
0	1	0	0	1	2	1	0	0	2	1	0
0	0	1	0	1	0	1	0	0	2	1	0
0	1	0	0	0	0	0	0	0	0&1	1	0
1	2	2	0&1	0	0	1	0	1	2	0	0
0	0	2	1	0	0	0	1	1	0	-	0
0	?	?	?	?	?	?	?	?	?	?	?
?	?	?	?	1	1	0	-	0	0	1	0

0	0	0	0	0	0	0	0	1	1	0	0&1
0	0	0	0	0	0	1	0	1	-	-	2
0	1	1	2	0	1	0	1	0	1	1	2
0	1	1	2	1	1	1	0	0	2	2	1
1	0	2	0	2	1	0	1	0	1	?	?
1	2	1	0	-	-	-	-	-	-	-	-
-	1	1	2	1	1	0	?	?	?	?	?
?	?	?	?	?	?	?	?	?	?	?	?
?	?	?	?	?	?	?	?	?	?	?	?
?	?	?	?	?	?	?	?	?	?	?	?
<i>Merycopotamus nanus</i>	0	0	0	-	0	?	?	?	?	1	1
0	1	0	0	1	1	0	0	1	0	0	1
0	0	0	0	1	2	1	0	0	2	1	0
0	0	1	0	1	0	1	0	0	2	1	0
1	1	0	1	0	0	0	0	1	0	1	1
1	2	1	0&1	0	0	1	0	1	2	0	0
0	0	1	1	1	0/1	0	1	1	0	-	0
0	0	0	0	0	1	?	0	0	0	1	1
0	0	0	1	1	1	1	1	0	0	1	0
1	0	0	0	0	0	0	0	1	0	-	0
0	0	0	0	0	0	1	0	1	-	-	2
0	1	1	2	0	1	0	1	0	1	1	1
0	1	1	2	1	1	1	0	0	2	1&2	0
1	0	0	1	2	2	1	0	0	1	1	1
1	0	0	1	1	1	1	1	1	1	1	2
1	1	1	1	1	?	2	2	2	0	0	1
1	0	1	2	3	1	1	0	0	0	2	1
3	0	0	0	2	?	?	?	?	?	2	1
0	1	1	0	1	0	0&1	1	0	1		
<i>Merycopotamus medioximus</i>	0	0	0	-	?	?	?	?	?	?	1
1	0	?	?	0	2	1	0	0	1	0	0
1	0	0	0	0	1	2	1	0	0	2	1
0	0	0	1	0	1	0	1	0	1	2	1
0	1	1	0	1	0	0	0	0	1	0	1
1	1	2	1	1	0	0	1	0	1	2	0
0	0	0	1	1	1	1	1	1	1	0	-
0	0	?	?	?	0	2	?	0	0	0	1
1	0	0	0	1	1	1	1	1	0	0	1
0	1	0	0	0	0	0	0	0	1	0	-
0	0	0	0	0/1	0	0	1	0	1	-	-
2	0	1	1	2	0	1	0	1	0	1	1
1	1	1	1	1	1	1	1	1	0	0	2
0	1	1	0	1	0	2	1	0	0	1	1
1	1	1	1	1	1	1	1	1	1	1	1
2	1	1	1	2	1	1	2	?	?	?	?
?	?	?	?	?	?	?	?	?	?	?	2
?	?	?	?	?	?	2	0	0	0	1	2
1	0	1	1	0	1	0	1	1	0	1	
<i>Merycopotamus dissimilis</i>	0	0	0	-	0	?	?	?	?	1	1
0	1	0	0	2	1	0	0	1	0	0	1
0	0	0	0	1	2	1	0	0	2	1	0
0	0	1	0	1	0	1	0	1	2	1	0
1	1	0	1	0	0	0	0	1	0	1	1
1	2	1	0	1	1	1	0	1	2	0	0
0	0	2	1	1	1	0	1	1	1	1	0
0	?	?	?	0	2/3	1	0	0	0	1	1
0	0	0	1	1	1	1	0	0	0	1	0
1	0	0	0	0	0	0	0	1	0	-	0
0	0	2	0	0	0	1	0	1	-	-	2
0	1	1	2	0	1	0	1	0	1	1	1

<i>Archaeopotamus qeshta</i>	0	0	1	0	1	2	0	1	1	?	
0	0	1	0	2	0	0	0	0	?	0	2
1	?	1	1	1	0	1	1	-	1	2	1
0	1	1	0	1	1	0	0	?	0	?	?
1	1	0	1	1	1	3	1	1	?	0	0
1	2	0	1	1	?	1	1	0	3	0	?
1	1	2	1	1	1	?	0	0	?	?	0
1	0	0	1	0	3	?	?	?	0	?	0
?	2	0	1	?	?	1	1	0	0	1	1
?	1	?	0	?	?	1	0	2	0	-	0
2	0	0	1	0	0	0&1	0	0	1	0	0
0	1	1	0	0	0	0	1	0	0&1	0	?
0	0	?	2	1	?	1	?	0	2	?	?
1	1	0&1	2	0	?	0	0	?	0	?	?
1	?	?	?	?	?	?	?	?	?	?	?
?	?	?	?	?	?	?	?	?	?	?	?
?	?	?	?	?	?	?	?	?	?	?	?
?	?	?	?	?	?	?	?	?	?	?	?
<i>Archaeopotamus harvardi</i>	0	0	1	2	1	2	0	1	1	?	
0	0	1	0	2	0	0	0	0	0	0	2
1	0&1	1	1	1	0	1	1	-	1	2	1
0	1	1	0	1	1	0	0	?	0	?	?
1	1	0	1	1	1	3	1	1	1	0	0
1	2	0	1	0&1	0	1	1	0	3	0	0
1	1	2	1	1	1	2	0	0	0	-	0
1	0	0	0	0	3	1	0	1	0	1&2	0
0	2	0	1	2	0	1	1	0	0	1	1
0	1	1	0	0	1	1	0	2	0	-	0
2	0	0	1	0	0	0&1	0	0&1	-	-	0
0/1	1	0	0&1&2	0	0	0	1	0	1	0	2
0	0	0	2	1	1	1	1	0	2	0	1
1	1	0	2	0	0	0	0	1	0&1	1	2
1	?	?	?	?	?	?	?	?	?	?	?
?	?	?	?	?	?	?	1	0	0	1	2
0	1	1	3	2	1	2	1	0	0	0	1
2	0	1	1	1	1	0	1	0	0	1	0
0	1	0	0	0	0	0	1	0	1		
<i>Hexaprotodon</i>	0	0	1	2	1	2	0	1	1	?	0
0	1	0	2	0	0	0	0	0	0	2	1
0&1	1	1	1	0	1	1	-	1	2	1	0
1	1	0	1	1	0	0	?	0	?	?	1
1	0	1	1	1	3	1	1	1	0	0	1
1&2	0	1	0&1	0	1	1	0	3	0	0&1	1
1	2	1	1	1	2	0	0	0	-	0	1
0	0	0	0	3	1	0	0&1	0	1&2	0	0
2	0	1	2	0	1	1	0	0	1	1	0
1	1	0	0	1	1	0	2	0	-	0	2
0	0	1	0	0	0&1	0	0&1	-	-	0	0/1
1	0	0&1&2	0	0	0	1	0	1	0	2	0
0	0	2	1	1	1	1	0	2	0/2	1	1
1	0	2	0	0	0	0	1	0&1	1	?	1
1	1	1	1	1	1	1	1	1	1	2	1
2	1	2	1	1	1	1	0	?	1	2	1
1	1	3	2	1	0&2	2	1	0	0	1	2
0	1	1	1	0	0	1	0	0	1	0	0
1	0	0	0	0	0	1	0	1			
<i>Hippopotamus</i>	1	0	1	2	1	2	0	1	1	2	0
0	1	0	2	0	0	0	0	0	0	0	1
0	1	1	1	0	1	1	-	0	2	1	0

	1	1	0	0&1	1	0	0	?	0	?	?	1
	1	0	1	0	1	3	1	1	1	0	0	1
	1&2	0	1	0&1	0	1	1	0	3	0	0	1
	1	2	1	1	1	0/2	0	0	0	-	0	1
	1	0	-	0	3	1	0	1	0/2	1	0	1
	0&1&2	0	1	1&2	0	1	1	0	0	1	1	0
	1	1	0&1	1	1	1	0	2	0	-	0	2
	0	0	1	0	0	0&1	0	1	-	-	0	0/1
	1	1	0&1&2	0	0	0	1	0	1	0	2	0
	0	0	2	1	1	1	1	0	2	0	2	1
	1	0	2	0	0	0	0	1	0&1	1	2	1
	1	1	1	1	1	0	0	1	1	1	2	1
	2	1	1	1	2	2	1	0	0	1	2	0&1
	0	1	3	2	1	0&2	2	1	0	0	1	0
	1	1	1	1	0	0	0	0	0	1	0	0
	0/1	0&1	0	0&1	0	0	1	0&1	1			
<i>Choeropsis</i>	2	0	-	-	-	1	2	0	1	1	2	0
	0	1	0	2	0	0	0	0	0	0	2	0
	0	0	1	1	0	0	1	-	1	2	1	0
	1	1	0	1	1	0	0	?	0	?	?	1
	1	0	1	1	1	1&3	1	1	1	0	0	1
	2	0	1	1	0	1	1	0	3	0	0	1
	1	2	0	1	1	0	0	0	0	-	0	1
	1	0	-	0	3	1	0	1	0	1&2	0	0
	1&2	0	1	2	0	1	1	0	0	1	1	0&1
	0	0	0	0&1	1	0	0	2	0	-	0	2
	0	0	1	0	0	0&1	0	1	-	-	0	1
	1	1	0&2	0	0	0	1	0	1	0	2	0
	0	0	2	1	1	1	1	0	2	2	1	1
	1	2	2	0	0	0	0	1	0	1	2	1
	?	?	?	?	?	?	?	?	?	?	?	?
	?	?	?	?	?	?	?	?	?	?	?	?
	1	1	3	2	1	0&2	2	1	0	0	1	0
	1	1	1	1	0	0	0	0	0	1	0	0
<i>Egatochoerus</i>	?	?	?	?	?	?	?	?	?	?	?	?
	?	?	?	?	?	?	?	?	?	?	?	?
	?	?	?	?	?	?	?	?	?	?	?	?
	?	?	?	?	?	?	?	?	?	?	?	1
	0	1	1	1	1	0	0	1	1	1	0	1
	0	0	0	0	0	0	1	0	0	0	1	0
	0	1/2	0	?	?	?	0	?	?	?	?	?
	?	?	?	?	?	?	?	?	?	?	?	?
	?	?	?	?	?	0	-	?	0	1	1	1
	0	0	?	?	?	0	0	2	0	-	1	0
	0	1	0	1	0	0	0	0	1	0	1	1
	0	1	1	1	0	0	1	0	0	-	2	-
	0	?	0	1	1	1	0	0	?	?	?	?
	?	?	?	?	?	?	?	?	?	?	?	1
	?	?	?	?	?	?	?	?	?	?	?	?
	?	?	?	?	?	?	?	?	?	?	0	0
	0	?	3	-	0	0	0	0	?	0	1	2
	2	0	0	0	?	?	?	?	?	?	?	?
	?	?	?	?	?	?	?	?	?	?	?	?
<i>Palaeochoerus</i>	0	0	1	0&2	0	1	0	0	0	1	3	0
	1	1	0	2	0	0	0	0	0	0	0	0
	0	0	0	0	0	0	0	-	0	-	0	0
	0	0	0	1	0	0	1	1	0	0	1	1
	1	0	0	1	1	0	0	0	0	1	1	0
	-	1	0	0	0	1	1	0	1	0	0	0

	0	1	0	0	0	0	0	0	0	0	0	1
	0	?	1	0	2	1	0&1	0	0	0	0	0
	1	0	1	0	0	0	-	0	0	0	1	1
	0	1	1	0	0	0	2	2	0	-	1	0
	0	1	1	1	0	0	0	0	1	0	0	0
	0	1	0	1	0	0	1	0	0	-	2	-
	0	1	0	1	1	1	1	0	?	1	0	1
	1	?	1	?	2	0	0	0	1	?	0	0
	0	0	2	0	0	0	0	0	0	0	0&1	0
	0	0	0	0	0	0	2	0	0	0	0	0
	0	0	3	0	0	0	0	0	0	0	1	1
	2	0&1	0&1	0	0	0	1	0	0	0	2	0
	0	0	0	1	0	2	0	1	1			
<i>Kenyasus</i>	0	0	1	0&2	0	1	0	0	1	3	0	0
	1	0	0	2	1	0	0	0	0	0	0	0
	0	0	0	0	0	0	0	-	0	-	0	0
	0	0	0	1	0	0	0	?	?	?	?	1
	1	0	0	0	1	2	0	0	1	0	0	0
	-	1	1	1	0	1	0	0	1	0	1	0
	0	1	0	0	1	0	0	0	0	0	0	1
	0	1	1	0	2	?	0	1	0	0	0	?
	0	0	?	1	0	1	1	0	0	1	0	1
	0	0	1	0	0	0	2	2	0	-	1	0
	0	1	1	0	0	0	1	0	1	0	0	1
	0	1	0	1	0	0	1	0	0	-	2	-
	0	1	0	1	1	1	0	0	?	1	0	0
	1	?	1	?	2	0	0	0	1	0	?	0
	1	1	2	0	0	0	0	0	0	0	0	1
	0	0	1	0	0	0	?	?	?	?	?	?
	?	?	?	?	?	?	?	?	?	?	?	?
	?	?	?	?	?	?	?	?	?	?	?	?
<i>Perchoerus</i>	0	0	1	0&2	0	?	0	0	0	1	3	0
	1	1	0	2	0	0	0	0	0	0	?	0
	0	?	0	?	?	0	0	-	0	?	0	0
	0	0	0	1	0	0	0	?	?	?	?	1
	1	0	0	1	1	0	0	0	0	1	0	0
	-	?	1	?	0	1	0	0	1	0	1	0
	0	1	0	0	?	0	0	0	?	?	0	1
	0	?	?	0	2	?	0&1	1	0	0	0	?
	0	0	?	0	0	0	-	0	0	0	0	1
	0	0	1	0	0	0	2	2	0	-	1	0
	0	1	0	0	0	?	0	0	1	0	0	0
	0	1	1	0	0	0	1	0	0	-	2	-
	0	?	0	1	1	1	1	0	?	1	0	1
	1	?	?	2	2	?	0	1	1	?	0	0
	?	?	?	?	?	?	?	?	?	?	?	?
	?	?	?	?	?	?	2	?	?	?	0	0
	0	0	3	0	0	0	0	0	0	?	?	?
	?	?	?	?	?	?	?	?	?	0	2	0
	0	0	0	0/1	0	2	0	1	1			
<i>Amphimeryx</i>	0	0	1	1	0	0	0	0	1	1	0	?
	0	0	2	0	0	0	1	0	1	1	2	0
	0	0	1	0	0	1	0	0	0	-	0	0
	0	0	0	1	0	0	-	0	0	0	1	1
	1	0	1	0	0	3	0	1	0	0	1	1
	2	0	1	1	0	1	0	1	3	1	0	0
	0	0	0	0	0	0	1	1	1	1	0	?
	0	?	?	2	?	?	?	1	0	0	0	?
	2	1	0	0	0	1	2	2	0	1	1	1

	0	0	0	0	0	0	2	1	0	-	0	2
	0	0	0	0	1	-	0	0	0	2	2	0
	1	1	2	0	1	1	1	0	1	1	2	0
	0	2	0	1	1	1	1	0	2	1	0	0
	0	0	1	2	0	1	0	1	0	0	0	0
	2	1	0	-	-	-	-	-	-	-	-	-
	0	0	0	0	0	2	0	1	1	0	1	0
	0	1	0	2	1	1	0	0	0	0	0	2
	0	0	0	1	?	?	?	?	?	1	2	0
	1	0	0	0	1	0	1	0	1			
Khirtaria	?	?	?	?	?	?	?	?	?	?	?	?
	?	?	?	?	?	?	0	0	0	0	0	0
	0	0	0	0	0	0	0	0	1	0	0	0
	0	1	0	1	0	0	1	0	0	0	0	1
	1	1	0	0	1	-	0	1	1	1	1	1
	0	0	0	1	0	1	0	2	0	0	1	0
	0	0	0	0	0	1	0/2	0	1	0	0/1	1
	?	?	?	?	?	?	?	?	?	?	?	?
	?	?	?	?	?	?	?	?	?	?	?	?
	?	?	?	?	?	?	0	2	0	-	0	0
	0	1	0	1	0	0	0	0	1	1	0	1
	0	1	1	1	0	0	1	1	0	-	2	-
	0	2	1	1	0	0	2	1	0	?	?	?
	?	?	?	?	?	?	?	?	?	?	?	1
	?	?	?	?	?	?	?	?	?	?	?	?
	?	?	?	?	?	?	?	?	?	?	?	?
	?	?	?	?	?	?	?	?	?	?	?	?
	?	?	?	?	?	?	?	?	?	?	?	?
	?	?	?	?	?	?	?	?	?	?	?	?
Mixtotherium	?	?	?	?	?	?	?	?	?	1	2	0
	0	0	0	1	0	0	1	0	1	1	2	0
	?	1	1	0	0	0	0	0	1	-	?	0
	0	0	0	1	0	0	0	0	0	0	1	0
	0	1	0	0	0	0	1	1	0	1	1	0
	-	1	0	1	0	1	0	0	0	1	0	1
	0	2	0	0	0	0	1	0	1	0	0	1
	?	?	?	0	1	?	1	0	0	0	0	?
	2	1	0	1	1	1	1	0	0	1	0	0
	0	0	1	0	0	0	0	1	0	-	0	2
	0	0	0	0	1	-	0	0	1	0	2	0
	0	0	2	0	2	0	1	1	1	1	0	0
	1	2	2	1	1	1	1	0	2	?	?	1
	?	?	?	?	?	?	?	1	1	?	?	0
	1	1	1	0	0	0	0	0	0	0	0	?
	?	0	0	0	0	2	0	1	1	1	1	0
	0	1	1	2	1	1	1	0	0	0	2	1
	1	1	1	2	2	1	0	1	0	1	0	0&1
	1	0	1	1	0	1	0	1	0			
Xiphodon	?	?	?	?	?	?	?	?	?	?	?	?
	?	?	?	0	0	0	1	0	1	1	2	0
	0	1	1	0	0	1	0	0	2	0	1	0
	0	0	0	1	0	0	0	?	2	0	1	1
	1	0	1	0	0	0	0	1	0	1	1	0
	-	2	0	0	0	1	0	1	1	0	0	0
	0	1	0	0	0	0	1	1	0	-	0	1
	?	?	?	?	?	?	?	0	0	1	0	1
	0	1	1	1	1	1	1	2	0	1	0	1
	0	0	0	0	0	0	2	1	0	-	0	0
	0	0	0	0	1	-	0	0	0	2	2	0
	0	1	2	0	1	1	1	0	1	1	0	0

	0	2	2	1	1	1	1	1	?	?	?	0
	0	?	1	2	0	?	?	0	1	?	2	0
	1	1	1	1	0	0	0	1	0	0	0&1	1
	1	0	0	0	1	2	0	1	1	0	1	0
	0	1	1	2	1	1	1	0	0	0	1	2
	0	0	0	2	1	1	0	0	0	1	0	0
	1	0	1	0	0	1	1	0/1	1			
<i>Dacrytherium</i>	0	?	?	?	?	0	0	?	?	1	2	1
	0	0	2	0	0	0	0	0	1	0	0	0
	0	0	1	1	1	0	0	0	2	2	1	0
	0	1	0	1	0	0	0	1	0	0	1	0
	1	1	1	0	0	0	0	0	0	0	1	0
	-	1	1	0	0	1	0	1	2	0	0	0
	1	0	0	0	0	0	1	0	0	-	0	1
	0	?	?	2	0	?	1	0	0	0	0	0
	2	0	1	1	1	0	-	2	0	1	0	1
	1	0	0	0	0	1	0	1	0	-	0	0
	0	0	0	0	1	-	0	0	1	0	2	0
	1	1	2	0	2	1	1	0	1	1	0	0
	1	2	0	1	1	1	0	0	2	1	0	0
	0	?	1	1	?	0	0	0	1	?	?	0
	?	?	?	?	?	?	?	?	?	?	?	?
	?	?	?	?	?	?	0	?	?	?	1	0
	0	1	1	2	1	1	1	0	0	0/1	1	1
	1	1	1	1	?	?	?	?	?	1	0	0
	1	0	1	1	0	1	1	0	0			
<i>Diplobune</i>	0	0	1	0	0	0	0	0	1	1	2	1
	0	0	1	0	0	0	0	0	1	1	0	0
	0	1	1	1	1	0	0	0	2	0	1	0
	0	0	0	1	0	0	0	0	0	0	1	1
	0	0	1	0	0	0	0	1	0	1	1	0
	-	1	1	0	0	1	1	1	2	2	0	0
	0	0	0	0	0	0	1	0	0	-	0	1
	0	2	1	2	0	0	1	0	0	0	0	1
	2	0	1	1	1	1	2	2	0	1	0	1
	0	0	0	0	0	0	2	1	0	-	0	0
	0	0	0	0	1	-	0	0	1	0	2	0
	0	1	2	0	1	1	1	0	1	1	0	0
	1	2	0	1	1	1	0	0	?	1	0	0
	0	0	1	2	0	0	0	0	1	0	?	0
	1	1	1	1	0	0	0	0/1	0	0	0	1
	0	0	0	0	1	2	0	1	1	1	1	0
	0	1	1	2	1	1	1	0	0	0	2	3
	0	1	1	2	2	1	0	1	0	1	0	0&1
	1	0	1	0	0	1	0	0&1	0			
<i>Anoplotherium</i>	?	?	?	?	?	?	?	?	?	?	?	?
	?	?	?	?	?	0	1	0	0	0	2	0
	1	0	1	1	0	1	0	0	2	2	1	1
	0	1	0	1	1	0	1	2	2	1	1	0
	0	0	1	0	0	0	0	1	0	1	0	0
	-	1/2	1	1	0	1	0	1	1	1	0	0
	0	0	0	0	0	0	1	1	0	-	0	1
	0	?	?	2	?	?	?	?	0	0	1	0
	2	0	1	1	1	1	1	0	0	1	1	1
	1	0	0	0	0	1	0	1	0&1	0	1	0
	0	0	0	0	1	-	0	0	1	0	2	0
	0	1	1	0	1	0	0&1	1	1	1	0	0
	1	1	0	1	1	1	0	0	?	?	?	?
	?	?	?	?	0	?	?	?	?	?	?	0
	1	1	1	1	1	0	1	0	0	0	1	1

<i>Archaeomeryx</i>	0	0	0	-	?	0	?	?	1	?	?
0	0	2	0	0	1	1	0	1	1	2	0
0	0	1	0	0	1	0	0	1	0	0	0
0	0	0	1	0	0	0	0	0	0	0	1
1	0	0	0	0	3	0	1	0	0	0	1
2	0	1	0	0	1	0	1	3	0	0	0
0	0	0	0	0	0	1	1	?	?	0	1
0	0	0	1	0	?	0	1	2	0	0	1
2	0/1	?	0	1	1	0	2	0	1	0	0
0	0	0	0	0	0	0	1	0	-	1	2
0	0	0	0	1	-	0	1	-	-	1	0
1	0	2	0	2	1	1	1	1	1	0	0
1	?	1	1	1	1	0	0	2	?	?	1
?	?	1	?	?	0	0	1	1	?	?	0
?	?	?	?	?	?	?	?	?	?	?	?
?	?	?	?	?	?	?	?	?	?	?	?
?	?	?	?	?	?	?	?	?	?	?	?
?	?	?	?	?	?	?	?	?	?	?	?
<i>Lophiomeryx</i>	0	0	1	2	0	0	1	?	1	?	?
?	?	2	0	0	0	1	0	1	1	2	0
0	0	1	0	0	0	0	0	1	-	0	0
0	0	0	1	0	0	0	0	2	0	1	1
1	0	1	0	0	3	0	1	0	0	1	1
2	0	1	0	0	1	0	1	3	0	0	0
0	2	0	0	0	0	1	1	1	1	0	1
?	-	-	2	?	0	0	1	2	0	0	1
1	0	0	0	1	1	2	2	0	1	1	1
0	0	0	0	0	0	0	1	0	-	0	2
0	0	0	0	1	-	0	1	-	-	2	0
1	1	2	0	1	1	1	0	1	1	0	0
1	?	1	1	1	1	0	0	2	1	0	1
0	?	0	2	2	0	0	1	1	1	?	0
?	?	?	?	?	?	?	?	?	?	?	?
?	?	?	?	?	?	0	0	1	1	1	0
0	1	0	1	0	0	0	0	0	2	0	2
0	0	0	0	?	?	?	?	?	1	0	1
1	0	0	0	1	1	0	1	0&1			
<i>Prodremotherium</i>	?	?	?	?	?	?	?	1	?	?	?
?	?	?	2	?	-	-	1	0	0	1	0
0	1	0	1	0	0	0	0	0	1	-	1
0	0	1	0	1	0	0	0	0	0	0	1
0	1	0	0	0	0	0	0	0	0	0	1
1	2	0	0	1	0	1	0	0	0	1	0
0	1	2	0	0	0	0	1	1	0	-	0
1	2	-	-	1	3	?	1	-	2	0	0
0	1	0	0	1	1	1	2	2	0	1	0
1	0	0	0	0	1	0	1	1	0	-	0
2	0	1	0	0	1	-	1	1	-	-	2
0	1	0	2	0	1	1	1	0	1	1	0
0	1	1	1	1	1	1	0	0	?	0	0
1	0	0	1	1	0	0	0	-	1	0	?
0	1	1	1	1	0	0	1	0	0	0	2
1	0	1	1	1	1	2	0	1	1	1	1
1	0	1	0	1	0	0	0	0	0	2	0
2	0	0	0	0	1	1	0	1	0	1	0
1	1	0	0	0	1	1	2	0	1		
<i>Bachitherium</i>	0	0	0	?	?	?	1	?	?	?	?
?	?	2	?	0	1	1	0	0	1	2	0
1	1	1	0	0	0	0	0	1	-	1	0

0	1	0	1	0	0	1	0	0	0	0	0
1	0	0	0	0	0	0	0	0	0&1	1	1
2	0	0	1	0	1	0	0	0	1	0	0
1	2	0	0&1	1	0	1	1	0	-	0	1
2	-	-	1	3	?	1	-	2	0	0	0
1	0	0	1	1	1	2	2	0	1	0	1
0	0	0	0	1	0	0	1	0	-	0	2
0	0	0	0	1	-	0	1	-	-	2	0
1	0	2	0	1	1	1	0	1	1	0	0
1	2	2	1	1	1	0	0	?	0	0	0
0	0	1	1	0	0	0	1	1	?	?	0
1	1	1	1	0	0	0	0	0	0	0/1	1
1	0	1	0	1	2	0	1	1	1	1	1
0	1	1	2	1	1	1	0	0	2	0	2
0	0	0	0&2	?	?	?	?	?	1	0	1
1	0	0	0	1	1	2	0	1			

B. Modifications in the coding of some character states (for selected artiodactyls) from the matrix of Gomes Rodrigues *et al.* (2020), considering the position in the matrix of the additional characters of our work:

Archaeomeryx ; **79** : ? -> 1

Anthrakokeryx thailandicus -> *Geniokeryx thailandicus* (from Ducrocq, 2020) ; **93** : ? -> 0 ; **94** : ? -> 0 ; **98** : ? -> 0 ; **102** : 0 -> 1 ; **114** : ? -> 2 ; **115** : 0 -> 1 ; **120** : 1 -> 0 ; **121** : 0/1 -> 0 ; **141** : 1 -> 0 ; **151** : 0 -> 1 ; **157** : 2 -> 0

Anthrakokeryx tenuis ; **99** : 1 -> 0 ; **146** : ? -> 1 ; **153** : ? -> 0/1

Bothriogenys orientalis ; **90** : 0 -> 1

Bothriogenys fraasi ; **90** : 0 -> 1

Bothriogenys gorringei ; **1** : 0/1 -> 0 ; **4** : ? -> - ; **63** : 0 -> 0&1 ; **69** : 1&2 -> 0&1&2

Epirigenys ; **149** : 0 -> 1

Bothriodon ; **7** : 0 -> 1 ; **14** : 0 -> 0&1 ; **15** : 0 -> 0&1

Elomeryx crispus ; **28** : 0/2 -> 0&2 ; **60** : 0 -> 0&2 ; **70** : 1 -> 0&1 ; **159** : ? -> 0

Afromeryx ; **1** : 0/2 -> 0 ; **3** : ? -> 1 ; **7** : ? -> 1 ; **34** : ? -> 0 ; **75** : ? -> 1

Sivameryx africanus ; **63** : 0 -> 1

Sivameryx palaeindicus ; **52** : 0 -> 0&1

Merycoidodon ; **1** : ? -> 0 ; **2** : ? -> 0 ; **3** : ? -> 1 ; **4** : ? -> 1 ; **5** : ? -> 0 ; **76** : ? -> 0 ; **79** : ? -> 1 ; **80** : ? -> 0 ; **81** : ? -> - ; **82** : ? -> 0 ; **153** : ? -> 0

Table S1. Measurements (in mm) of the upper and lower jugal teeth of *Parabrachyodus hyopotamoides* from Samane Nala 4 and 5, Tobah, and Safed Nala. Lmd, mesio-distal length; Lll1-3, labio-lingual length 1-3 (see Material and Methods); *, measurement under-estimated of a broken specimen.

Specimen	Locus	Lmd	Lll1	Lll2	Lll3
UM-SAM4-001	M3/	39,9	42,2	40,9	
	M2/	36,6	38,3	37,5	
	P4/	18,2	21,2		
	P3/	19,9	16,8		
	P1/-P4/	79,9			
	M1/-M3/	97,2			
	P1/-M3/	177,3			
UM-SAM4-002	P4/	13,8	16,9*		
UM-SAM4-003	M3/	35,2	40,8	38,7	
	M2/	32	35,8	35,4	
	M2/-M3/	64,9			
UM-SAM4-004	M3/	36,3		42,9	
UM-SAM4-006	M3/	36,8	40,7	38,3	
UM-SAM4-007	M3/	38,8	46,8	45,4	
UM-SAM4-008	M3/	37,8	44,8	43,7	
UM-SAM4-009	M3/	37,5			
UM-SAM4-011	M3/			40,7*	
UM-SAM4-013	M/3	56,2	31	31,6	20,1
	M/2			27,3	
UM-SAM4-015	M/2	33,6	24,2	26,1	
UM-SAM4-016	M/2	36,5	27,9	30,1	
UM-SAM4-017	M/3		28,2	29,8	
UM-SAM4-020	M/3			31,4	23,3
UM-SAM4-025	P1/	18,4	12		
UM-SAM4-027	P/1	16,1	8,2		
UM-SAM5-001	M3/	38,1	45,1	40,7	
UM-TOB-001	M/3	50,7	27,7	29,3	18,9
	M/2	33	24	26,1	
	M/1	22,2			
	P/4	19,1	13,8		
	M/1-M/3	105,1			
	P/4-M/3	122,9			
UM-SFN-001	M/3		31,2	28,8	

Table S2. Measurements (in degree of arc) of the angle between the slope of the metaconule and the dental collet of the M3/ of (A) selected anthracotheres, n, number of specimens measured, with (B) detailed measurements for the M3/ of the specimens attributed to *Parabrachyodus hyopotamoides*.

A

Taxon	n	Mean	Min	Max	Sd
<i>Parabrachyodus hyopotamoides</i>	14	43,4	34,4	48	4,5
<i>Telmatodon [bugtiensis + orientale]</i>	3	38,3	34,9	41,7	3,4
<i>Gonotelma shahbazi</i>	1	49,2			
<i>Afromeryx zelteni</i>	1	60,4			
<i>Sivameryx [palaieindicus + africanus]</i>	4	56,7	54,4	58,5	1,7
<i>Libycosaurus anisae</i>	4	51,8	49,7	54	2,0
<i>Elomeryx [crispus + borbonicus]</i>	4	41,8	37,7	44,9	3,0
<i>Brachyodus onoideus</i>	3	55,3	52,3	57	2,6
<i>Bothriogenys fraasi</i>	2	47,2	46,6	47,8	

B

Specimen	Measurement
UM-SAM4-001	43,5
UM-SAM4-003	38,9
UM-SAM4-004	40,3
UM-SAM4-007	47
UM-SAM5-001	34,4
M12035	35,9
M12036	47,6
M12039	46,1
M12711	47,2
M12712	47,5
M12714	43,5
M12718	48
M12817	42
M43958	45